Fakultät Wissenschaftszentrum Weihenstephan für Ernährung, Landnutzung und Umwelt

Lehrstuhl für Entwicklungsgenetik

Molecular Characterisation of Neuroendocrine Tumours

Nikolai Fabian Ferdinand Falk

Vollständiger Abdruck der von der Fakultät Wissenschaftszentrum Weihenstephan für Ernährung, Landnutzung und Umwelt der Technischen Universität München zur Erlangung des akademischen Grades eines

Doktors der Naturwissenschaften

genehmigten Dissertation.

Vorsitzender:	Univ.-Prof. Dr. S. Scherer
Prüfer der Dissertation:	1. apl. Prof. Dr. J. Graw
	2. Univ.-Prof. Dr. G. Multhoff
	3. Priv.-Doz. Dr. N. S. Pellegata

Die Dissertation wurde am 09.04.2015 bei der Technischen Universität München eingereicht und durch die Fakultät Wissenschaftszentrum Weihenstephan für Ernährung, Landnutzung und Umwelt am 22.06.2015 angenommen.

“He who can no longer pause to wonder and stand rapt in awe, is as good as dead; his eyes are closed.”

-Albert Einstein

Für meine Eltern

Table of Contents

Abbreviations

Ago	Argonaute
AKT	Protein kinase B
Amp	Ampicillin
ARTN	Artenim
ATP	Adenosine triphosphate
BH	Benjamini-Hochberg
C. elegans	*Caenorhabditis elegans*
CDK	Cyclin-dependent kinase
cDNA	Complementary DNA
CIP	Calf-intestinal alkaline phosphate
CKI	Cyclin-dependent kinase inhibitor
DAB	Diaminobenzidine
dATP	Deoxyadenosine triphosphate
dCTP	Deoxycytidine triphosphate
DGCR8	DiGeorge syndrome critical region gene 8
dGTP	Deoxyguanosine triphosphate
Dicer	double-stranded RNA-specific endoribonuclease
DMEM	Dulbecco’s modified Eagle's medium
DMSO	Dimethyl sulfoxide
DNA	Deoxyribonucleic acid
dNTP	Desoxynucleoside triphosphate
DTT	Dithiothreitol
dTTP	Deoxythymidine triphosphate
E. coli	*Escherichia coli*
ECM	Extracellular matrix
EGFR	Epidermal growth factor receptor
eIF	Eukaryotic translational initiation factor
EMT	Epithelial-mesenchymal transition
ERK	Extracellular-signal-regulated kinases
FACS	Fluorescence-activated cell sorting
FDR	False discovery rate
FFPE	Formalin-fixed and paraffin embedded
FMTC	Familial medullary thyroid carcinoma
FTC	Follicular thyroid carcinoma

GDNF	Glial cell-derived neurotrophic factor
GFL	GDNF family ligands
H&E	Haematoxylin and eosin staining
HRP	Horseradish peroxidase
IPA	Ingenuity pathway analysis
LB	Lysogeny broth
MAPK	Mitogen-activated protein kinase
MEN	Multiple endocrine neoplasia syndrome
MEN1	Multiple endocrine neoplasia type 1
MEN2	Multiple endocrine neoplasia type 2
MEN2A	Multiple endocrine neoplasia type 2A
MEN2B	Multiple endocrine neoplasia type 2B
MEN4	Multiple endocrine neoplasia type 4
MENX	MEN-like syndrome
miR	microRNA
miRNA	microRNA
miRNP	miRNA ribonucleoprotein particles
mRNA	Messenger RNA
MTC	Medullary thyroid carcinoma
MTT	3-(4,5-dimethylthiazol-2-yl)-2,5-diphenyltetrazoliumbromide
mut/mut	Homozygous mutant
NTRN	Neurturin
P-Body	Processing body
p18	$p18^{INK4c}$
p27	$p27^{Kip1}$
p68	$p68^{DDX\ 5}$
p72	$p72^{DDX\ 17}$
PBS	Phosphate-buffered saline
PCR	Polymerase chain reaction
PI3K	Phosphatidylinositol-4,5-bisphosphate 3-kinase
pRb	Retinoblastoma protein
pre-miRNA	Precursor-miRNA
pri-miRNA	Primary miRNA
PSPN	Perserphin
PTC	Papillary thyroid carcinoma

RAB27A	Ras-related protein 27A
RAS	Rat sarcoma
RET	Rearranged during transfection
RISC	RNA induced silencing complex
RNA	Ribonucleic acid
RNAi	RNA interference
RNase	Ribonuclease
RT-PCR	Real time polymerase chain reaction
RTK	Receptor tyrosine kinase
SPHK1	Sphingosine kinase 1
T3	L-triiodothyronine
T4	L-thyroxine
TBE	Tris/Borate/EDTA
TBP	TATA box binding protein
TBS	Tris buffered saline
TEMED	Tetramethylethylenediamine
TGFβ	Transforming growth factor β
TKI	Tyrosine kinase inhibitor
TMB	3,3',5,5'-Tetramethylbenzidine
TRBP	Transactivation response RNA-binding protein
TRH	Thyroid releasing hormone
TSH	Thyroid stimulating hormone
UTR	Untranslated region
VEGF	Vascular endothelial growth factor
VEGFR	Vascular endothelial growth factor receptor
wt	Wild-type
wt/mut	Heterozygous mutant
wt/wt	Wild-type

Abstract

Medullary thyroid carcinoma (MTC) is a rare thyroid cancer subtype with rising incidence making up 2-3% of the thyroid malignancies. Interestingly, MTC accounts for 15% of deaths related to all thyroid cancer types because it has high tendency to metastasise. MTC can present itself sporadically or through hereditary predisposition. Hereditary MTC occurs in patients affected by the multiple endocrine neoplasia (MEN) type 2 syndrome, which is caused by germline mutations in the rearranged during transfection (*RET*) proto-oncogene.

We identified a variant of the MEN syndrome that spontaneously developed in a Sprague-Dawley rat colony. Affected animals show phenotypic overlap with the MEN type 1 and MEN type 2 syndromes in humans. Affected rats develop bilateral pheochromocytomas, parathyroid adenomas, pituitary adenomas and multifocal thyroid C-cell tumours. Due to the unique combination of affected organs, this multi-tumour spectrum was named MEN-like syndrome (MENX). MENX is caused by a frameshift mutation in *Cdkn1b*, encoding the cyclin-dependent kinase inhibitor $p27^{Kip1}$ (p27). Rats homozygous and heterozygous for this mutation develop C-cell tumours with a clear progression from hyperplasia to tumour with time.

The discovery of microRNAs (miRNAs) has revealed a new level of gene expression regulation, since these short, non-coding RNAs regulate the expression of target genes through an RNA interference-like repression mechanism. In the last years, increasing experimental evidence clearly indicates an important role of miRNAs in oncogenic processes of cancers.

We thus decided to investigate the miRNA expression of MTC in homozygous and age-matched heterozygous mutant rats to determine the influence of p27 gene levels on the miRNA expression. The prolonged life-span of heterozygous mutant rats allows the study of the progression of MTC tumours with equal p27 gene levels. In addition, the miRNA expression signature of human hereditary and sporadic MTC was determined to establish whether MENX rats might represent an animal model of the human disease.

The comparison of the miRNA expression profiles between human and MENX rat MTCs showed that over 35% of the differentially expressed miRNAs in human MTC were also identified as deregulated in tumours of MENX rats. Among the differentially expressed miRNAs, members of the miR-29 family of miRNAs and miR-124-3p were chosen for further studies as they showed a strong downregulation in both rat and human MTCs. The biological relevance of the downregulation of miR-29 family members and of miR-124-3p was investigated by transfecting the MTC cell lines TT and 6-23 MTC with specific miRNA

inhibitors. After downregulating the expression of the miR-29 family and miR-124-3p, an increase in cell migration and invasion was observed in both MTC cell lines. In addition, the miR-29 family members participate in the regulation of cell proliferation in MTC.

As miR-124-3p showed the highest differential expression between hereditary and sporadic MTC in humans, we identified the putative target genes in order to further understand the pathomechanisms of MTC. Specifically, the target genes of miR-124-3p were determined *in silico* by employing four different prediction algorithms. The genes *RAB27A*, coding for a small GTPase, and *SPHK1*, coding for a kinase, were experimentally validated by luciferase reporter assay as direct targets of miR-124-3p.

Zusammenfassung

Das medulläre Schilddrüsenkarzinom (MTC) ist eine seltene Form von Schilddrüsenkrebs, welches eine steigende Inzidenz verzeichnet und für 2-3% aller malignen Schilddrüsentumore verantwortlich ist. Interessanterweise wird in 15% aller durch Schilddrüsenkrebs verursachten Todesfälle ein MTC diagnostiziert, was auf dessen hohe Metastasierungsrate zurückzuführen ist. Das Auftreten kann sporadisch oder die Folge einer hereditären Prädisposition sein. Patienten, bei denen das hereditäre MTC auftritt, sind von dem multiplen endokrinen Neoplasie (MEN) Typ 2 Syndrom betroffen, welches durch Keimbahnmutationen im rearranged during transfection (*RET*) Protoonkogen verursacht wird.

Innerhalb einer Zucht von Sprague-Dawley-Ratten wurde das spontane Auftreten einer Variante des MEN Syndroms identifiziert. Der Phänotyp der betroffenen Tiere überlappt mit den im Menschen auftretenden Syndromen, MEN Typ 1 und MEN Typ 2. Diese Tiere sind von bilateralen Phäochromocytomen, Nebenschilddrüsenadenomen, Hypophysenadenomen sowie multifokalen C-Zelltumoren betroffen. Aufgrund der charakteristischen Kombination betroffener Organe wurde dieses Rattenmodell als MEN-ähnliches Syndrom (MENX) bezeichnet. Das MENX-Syndrom wird durch eine Leserasterverschiebung im *Cdkn1b* Gen, welches für den Cyclin-abhängigen Kinaseinhibitor $p27^{Kip1}$ (p27) kodiert, verursacht. Bei homo- als auch bei heterozygoten MENX-Ratten treten C-Zelltumore auf. Beide Genotypen weisen einen sequenziellen Verlauf auf, wobei es zu einer Progression von Hyperplasien zu Tumoren kommt.

Die microRNAs (miRNAs) stellen eine neuartige Regulierungsebene der Genexpression dar. Diese kurzen, nicht-kodierenden RNAs regulieren die Expression entsprechender Zielgene durch einen RNA-Interferenz-ähnlichen Inhibierungsmechanismus. In den letzten Jahren haben sich die Erkenntnisse gehäuft, dass miRNAs eine wichtige Rolle in der Karzinogenese verschiedener Krebsarten spielen.

Um die molekularen Vorgänge der Pathogenese des MTCs zu verstehen, haben wir die miRNA Expression in homozygoten mit der in gleichaltrigen heterozygoten MENX-Ratten verglichen. Somit konnte der Einfluss der p27 Gendosis auf die miRNA Expression ermittelt werden. Die längere Lebensdauer heterozygoter MENX-Ratten ermöglicht die Untersuchung der Progression von MTC Tumoren bei gleicher p27 Gendosis. Zusätzlich haben wir die Unterschiede zwischen der miRNA Expression in humanen hereditären und der in humanen sporadisch auftretenden MTCs ermittelt. Diese haben wir schließlich mit den im Tiermodell

generierten Ergebnissen verglichen, um festzustellen, ob sich die MENX-Ratte als Tiermodell zur Untersuchung von humanen MTCs eignet.

Der Vergleich der miRNA Expressionsmuster humaner MTCs mit denen der MENX-Ratten zeigte, dass über 35% der unterschiedlich exprimierten miRNAs im Menschen ebenfalls eine veränderte Expression im Tiermodell aufweisen. Eine besonders starke Deregulierung, sowohl im Menschen als auch im Tiermodell, wurde bei den miRNAs der miR-29 Familie sowie bei miR-124-3p festgestellt. Um die biologische Rolle dieser herunterregulierten miRNAs in der Entstehung des MTCs genauer zu verstehen, wurden die MTC Zelllinien TT und 6-23 MTC mit spezifischen miRNA Inhibitoren transfiziert. Aufgrund der Herunterregulierung der Expression der miR-29 Familie sowie von miR-124-3p, wurde ein Anstieg der Zellmigration und der Zellinvasion in beiden MTC Zelllinien beobachtet. Zudem sind die Mitglieder der miR-29 Familie an der Regulierung der Zellproliferation des MTCs beteiligt.

Bei dem Vergleich von humanen hereditären *versus* humanen sporadisch auftretenden MTCs wies miR-124-3p die größten Unterschiede in der Expression auf, woraufhin wir die möglichen miR-124-3p Zielgene ermittelten, um das Verständnis der Pathogenese des MTCs zu verbessern. Hierzu wurden eigens die Zielgene von miR-124-3p *in silico* durch Verwendung vier verschiedene Prognosealgorithmen ermittelt. Die aus der Suche hervorgegangenen Gene *RAB27A*, welches für eine kleine GTPase kodiert, und SPHK1, welches für eine Kinase kodiert, wurden experimentell durch Luziferase-Assay als Zielgene von miR-124-3p validiert.

1 Introduction

1.1 The morphology of the thyroid gland

The thyroid gland is located on the anterior surface of the trachea at the base of the neck. The gland is comprised of lobules of spherical follicles that are filled with colloid. Its main functions are the synthesis, storage and secretion of the thyroid hormones, L-triiodothyronine (T3), L-thyroxine (T4) as well as calcitonin. These hormones are produced in two distinct cell types, where the thyroid's follicular cells produce T3 as well as T4 and the parafollicular C-cells secrete calcitonin. Follicular epithelial cells line the follicles. The C-cells are situated in between follicles, in a location described as parafollicular (Kondo *et al.* 2006).

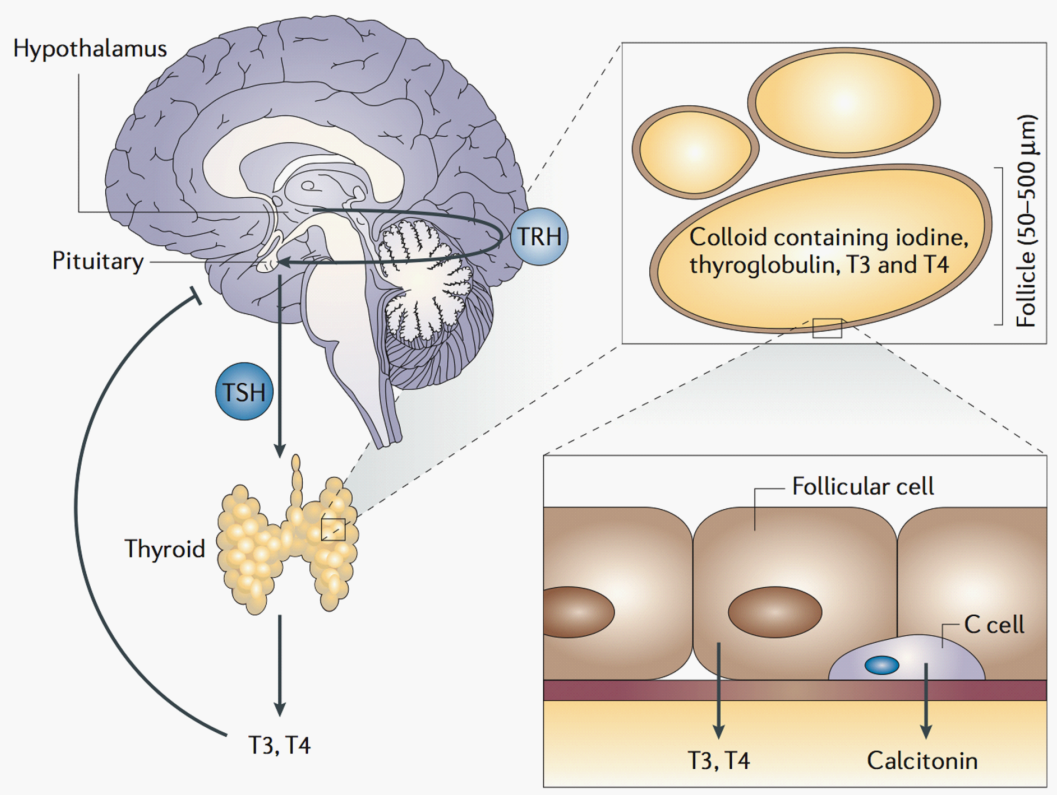

Figure 1: Morphology of the Thyroid Gland. The thyroid is a butterfly-shaped organ, which is located on the anterior surface of the trachea at the base of the neck. It is comprised of spherical follicles that are filled with colloid. The follicles are lined by follicular epithelial cells. C-cells, which produce calcitonin, are situated within follicles or in a parafollicular location. The main functions of the thyroid gland are synthesis, storage and secretion of thyroid hormones, T3 and T4, under the control of the hypothalamic–pituitary axis with negative feedback by the thyroid hormones. Thyrotropin-releasing hormone (TRH), which is secreted from the hypothalamus, stimulates the release of thyroid stimulating hormone (TSH) from the anterior pituitary gland. TSH stimulates the follicular cells to synthesise and secrete thyroid hormones (with permission from Kondo *et al.* 2006).

Regulation of the hormone secretion happens via the hypothalamic–pituitary axis with negative feedback by the thyroid hormones as depicted in Figure 1. In short, TRH is secreted by the hypothalamus, causing the release of TSH from the anterior pituitary gland. TSH induces the synthesis and secretion of thyroid hormones through the follicular cells (De Felice *et al.* 2004, Kondo *et al.* 2006).

1.2 Introducing thyroid cancer

Cancer research has received increased attention as more than 477,300 cases of cancer and 218,258 cancer related deaths were reported in Germany in 2010 (Kaatsch *et al.* 2013). Although many may be cured, cancer is still a major cause of death and is overshadowed only by cardiovascular diseases in the western world (David *et al.* 2010).

Thyroid cancer is one of the few malignancies with rising incidence and represents the most common endocrine neoplasia. Differentiated thyroid cancers originate from the thyroid follicular cells, where the most common subtype, papillary thyroid carcinoma (PTC; OMIM no. 188550), represents over 70% of all thyroid malignancies. Follicular thyroid carcinoma (FTC; OMIM no. 188470), a subgroup of PTC and its variants comprise the second largest group (Utiger 2005, Kaatsch *et al.* 2013).

Medullary thyroid carcinomas (MTC; OMIM no. 155240), arising from parafollicular calcitonin-producing C-cells, have a low prevalence and account for only 2–3% of all thyroid malignancies in Germany (Kaatsch *et al.* 2013). Interestingly, MTC is responsible for about 15% of all the deaths related to thyroid cancer worldwide and is known to metastasise. Distant metastases are observed in 7–23% of patients with MTC. The spreading of MTC often affects multiple organs including the lungs, bones and liver and more rarely the brain, skin and breasts (Ball 2007, Schlumberger *et al.* 2008). Although MTC presents itself sporadically in most cases, a hereditary pattern has been observed in about 25% of the cases. Hereditary cases of MTC are represented by patients affected by multiple endocrine neoplasia syndromes (MEN) type 2A (MEN2A; OMIM no. 171400), MEN type 2B (MEN2B; OMIM no 163200) or familial medullary thyroid carcinoma (FMTC; OMIM no. 155240), which are described more closely in section 1.3 (Vriens *et al.* 2009, Wells *et al.* 2009). The remaining 75% of all MTCs are sporadic. From the clinical point of view these patients neither have a family history of MTC nor do they have any other MEN type 2 (MEN2)-specific disease. Sporadic MTC can arise clinically at any age but its incidence peaks beginning with the fourth decade of life. Usually, a single unilateral thyroid tumour is found in the sporadic MTC cases (Leboulleux *et al.* 2004, Lodish *et al.* 2008).

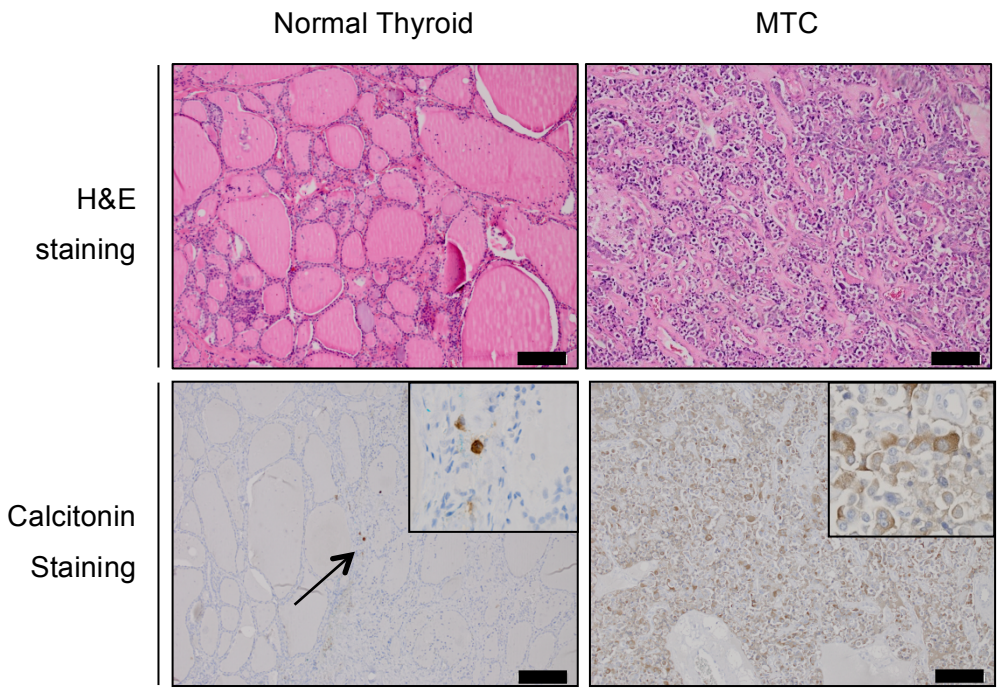

Figure 2: Normal Thyroid and MTC tissue. Haematoxylin and eosin (H&E) staining with the corresponding immunohistochemistry analysis of normal thyroid and MTC tissues. The specific antibody binding against calcitonin is visualised in brown with the haematoxylin counter-staining in blue. The arrow indicates individual calcitonin-positive C-cells in a parafollicular position in the normal thyroid. The scale bar indicates a length of 100 microns (Low power view: Magnification: 100x; High power view: Magnification 400x).

It is noteworthy that comparisons of normal C-cells and primary tumours are not possible, because of the low C-cell population (approximately 1%) in the thyroid cell mass (Maliszewska *et al.* 2013). Furthermore, there are no benign tumours arising from C-cells and even hyperplastic C-cell populations represent only a small percentage of thyroid tissue cells. For this reason a normal thyroid tissue cannot be used as a representative reference for normal C-cells (Ameur *et al.* 2009). As seen in Figure 2, the C-cells are situated in a position described as parafollicular and are scattered as individual cells around the thyroid gland and do not form a coherent tissue.

1.3 MEN Syndromes in humans

The MEN syndromes are autosomal dominantly inherited and characterised by tumours involving two or more neuroendocrine organs. Two such syndromes are clinically and genetically well characterised and described as MEN type 1 (MEN1; OMIM no. 131100) and MEN2. More recently, thanks to work done in our laboratory, a new syndrome was identified named type 4 (MEN4; OMIM no. 610755) (Marinoni *et al.* 2011, Lee *et al.* 2013).

MEN1 is caused by loss-of-function mutations in the tumour suppressor gene *MEN1* located on chromosome 11q13. The clinical manifestations of endocrine disease in patients with

MEN1 most often begin between the ages of 30 and 40 years, while an early onset at the age 10 years is rare (Marx *et al.* 1998, Machens *et al.* 2007). Affected patients typically develop multiple parathyroid adenomas, pancreatic islet cell neoplasia and anterior pituitary adenomas (Verges *et al.* 2002, Thakker *et al.* 2012). As it is typical for autosomal dominant inheritance pattern, males and females are affected equally. The MEN1 syndrome has been described in diverse geographic regions and ethnic groups and no racial predilection has been observed (Lairmore *et al.* 2004). The gene *MEN1* codes for the protein menin, a nuclear protein with tumour-suppressive function. More than 1,000 different *MEN1* germline mutations have been identified in several independent national studies based on a large series of MEN1 patients so far (Calender 2000, Lemos *et al.* 2008). Significant progress has been made in identifying menin as a regulator of gene transcription, cell proliferation, apoptosis and genome stability, thereby improving on understanding the tumour-suppressing function of the *MEN1* gene (Yang *et al.* 2007).

MEN2 is caused by activating germline mutations in the **re**arranged during **t**ransfection (*RET*) proto-oncogene localised on chromosome 10q11 (Ceccherini *et al.* 1993). Depending on the tumour spectrum, the subtypes MEN2A, MEN2B as well as FMTC are recognised (Eng *et al.* 1996). MEN2A patients are affected by MTC as well as pheochromocytoma and parathyroid hyperplasias in 50% and 15-30% of the cases, respectively (Eng *et al.* 1996, Brandi *et al.* 2001, Kloos *et al.* 2009). MEN2B patients are typically suffering from pheochromocytomas in approximately 50% of the cases and more seldom by ganglioneuromatosis of the intestine, thickening of the corneal nerves and *marfanoid habitus*. The only phenotype developed by FMTC is MTC (Brandi *et al.* 2001, Romei *et al.* 2012). Interestingly, over 98% of patients affected by MEN2 carry germline point mutations in *RET* (Santoro *et al.* 2004, Wells *et al.* 2013). A closer examination through genetic screening identified a finite number of *RET* mutations that cause more than 95% of hereditary MTC and were identified in 15-50% of patients with sporadic MTC (Mulligan *et al.* 1994, Elisei *et al.* 2008, Wells *et al.* 2013). The identified *RET* mutations have made it possible to develop simple and definitive tests to screen individuals at risk for this tumour syndrome (Cote *et al.* 1995). A correlation between specific *RET* mutations and the onset of tumour development provides the basis for personalised therapy in clinical management. In pre-symptomatic *RET* mutation carriers prophylactic surgery has to be performed prior to the development of cancer (Raue *et al.* 2009).

Patients have been identified that show clinical symptoms of MEN1, but are negative for mutations in the *MEN1* gene. This new group of patients suggests the involvement of another predisposing gene for multiple neuroendocrine tumours and this hypothesis was further affirmed, when in addition to the lack of *MEN1* mutations, no mutations in *RET* were

identified. Closer examination of the affected patients revealed mutations in the *CDKN1B* gene, coding for $p27^{Kip1}$ (p27). A total of six mutations have been identified so far and this new MEN syndrome was named MEN4. In MEN4 patients no occurrence of MTC has been so far reported (Marinoni *et al.* 2011, Lee *et al.* 2013).

1.4 Genetic alterations in hereditary and sporadic MTC

1.4.1 The RET receptor tyrosine kinase

RET codes for a receptor tyrosine kinase (RTK), thus belonging to a major family of disease genes, which represent promising therapeutic targets for many cancers (Gschwind *et al.* 2004).

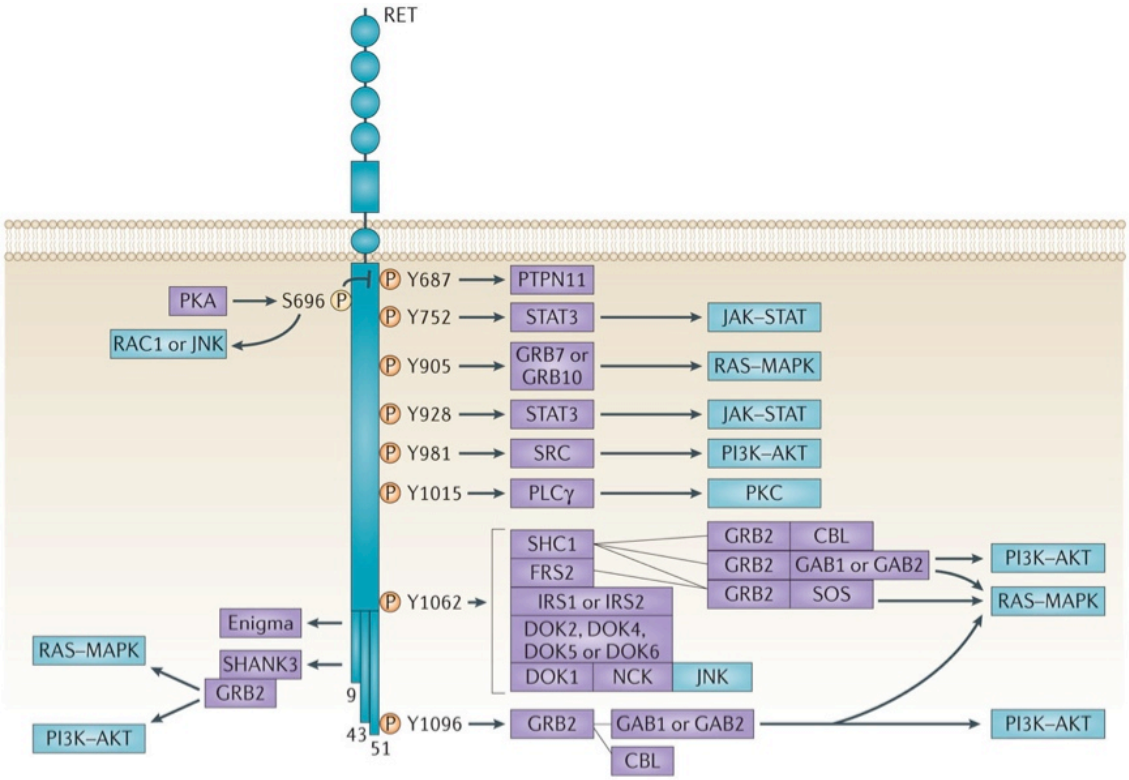

Figure 3: Signalling pathways associated with RET. A depiction of important signalling pathways in carcinogenesis upon activation of RET. Upon activation RET becomes phosphorylated on multiple intracellular tyrosine residues. These facilitate direct interactions with signalling molecules, which lead to the activation of multiple downstream signalling pathways that can promote cell growth, proliferation, survival or differentiation (with permission from Mulligan 2014).

The genes coding for RTKs are transmembrane-spanning receptors and ligand-binding induces dimerisation with a second RTK molecule. The consequent juxtaposition of the two catalytic domains allows the mutual transphosphorylation of specific tyrosine residues. The generated phosphotyrosines create a unique three dimensional surface and the signal is propagated by recruiting intracellular proteins that carry SRC homology 2 and

phosphotyrosine binding domains (Knowles *et al.* 2006, Ibanez 2013). Figure 3 shows how RTKs invoke intracellular signalling cascades that ultimately lead to gene expression modulations and biological responses (Schlessinger *et al.* 2003, Ibanez 2013, Mulligan 2014).

The extracellular portion of RET proto-oncogene consists of four cadherin–like repeats, a calcium binding site and a cysteine-rich domain. The intracellular domain contains the tyrosine kinase domain (Manie *et al.* 2001, Airaksinen *et al.* 2002, Santoro *et al.* 2004, Ibanez 2013).

The RET protein is expressed in neuroendocrine cells, neural cells, urogenital cells and germ cells of the testis. Under healthy conditions RET activation is closely regulated by the binding of one of the four glial cell-derived neurotrophic factor (GDNF) family ligands (GFL) (Wells *et al.* 2009). GLFs bind RET in conjunction with one of four GDNF-family-α-receptors (GRFα1, GRFα2, GRFα3, GRFα4) as depicted in Figure 4 (Airaksinen *et al.* 2002, Mulligan 2014). Ligand-induced activation of RET results in transduction of multiple signals that induce cell growth, cell motility, survival and differentiation through different downstream pathways. These include the rat sarcoma (RAS)- mitogen-activated protein kinases (MAPK) and phosphatidylinositol-3-kinase(PI3K)/Protein kinase B (AKT) pathways as depicted in Figure 3 (Cerrato *et al.* 2009).

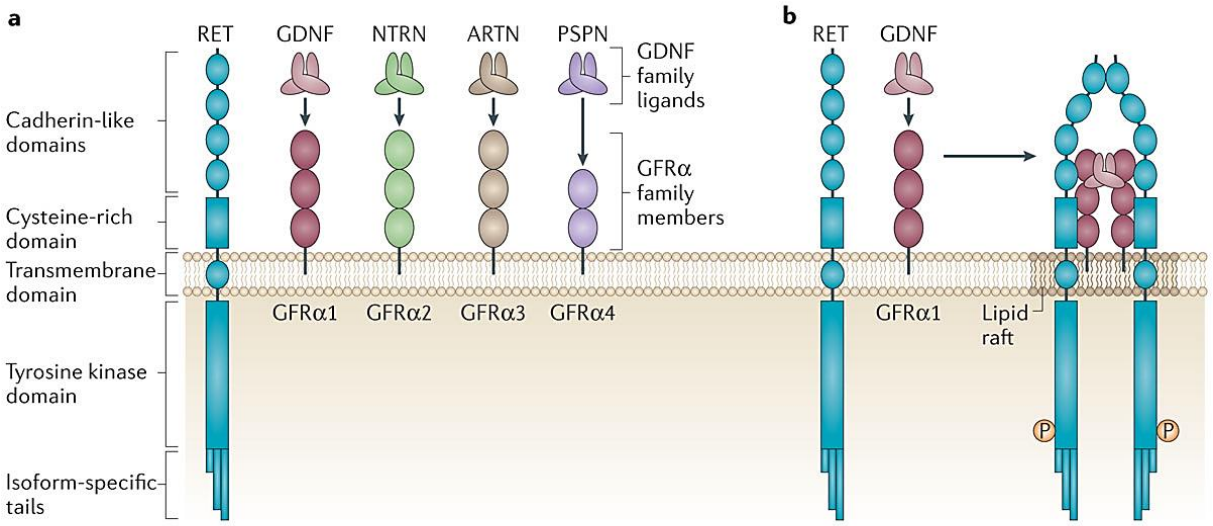

Figure 4: RET and its Co-Receptors. A: RET is the receptor for a family of soluble GDNF ligands, which include GDNF, neurturin (NTRN), artemin (ARTN) and persephin (PSPN). Each of these ligands interacts with RET via a cell surface co-receptor of the GFRα family members. **B:** GFLs do not directly interact with RET, but they bind with the GFRα co-receptors to form a heterodimeric complex. Once bound to the ligand–co-receptor complex, conformational changes facilitate RET monomer association and lead to receptor dimerisation and autophosphorylation (with permission from Mulligan 2014).

Between 95-98% of the mutations in *RET* observed in MEN2-associated MTC are gain-of-function mutations that are categorised into two major groups. In both cases, the receptor is constitutively activated in the absence of natural ligands (Calender 2000, Zbuk *et al.* 2007, Mulligan 2014). The first group involves mutations within the cysteine-rich domain, where the most frequently mutated residues in MEN2A patients are cysteine residues substituted for any other amino acid in codons 609, 611, 618, 620 and 634 as shown in Figure 5 (Mulligan 2014). These mutations lead to the loss of intramolecular disulphide bridge patterns and thereby allowing mutant RET proteins to form intermolecular disulphide bridges. Intermolecular bonding leads to constitutive receptor dimerisation and consequent aberrant signalling (Asai *et al.* 1995, Ibanez 2013). The second group of *RET* gain-of-function mutations are localised in the kinase domain and these activating mutations are more varied. Frequently occurring *RET* mutations are residues L790F, Y791F, S891A and R844L leading to relatively mild MTC and FMTC phenotypes as shown in Figure 5 (Geneste *et al.* 1999, Machens *et al.* 2008, Wells *et al.* 2013).

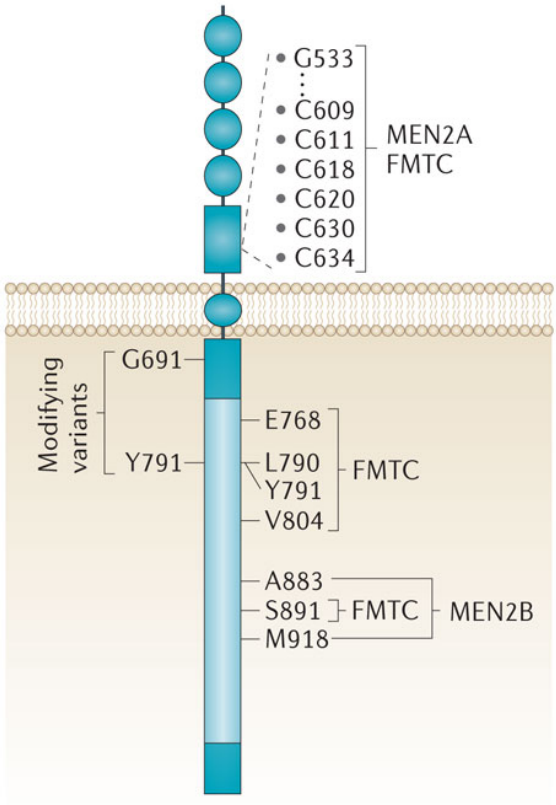

Figure 5: Mutated *RET* Codons. Germline *RET* mutations are present in 98% of families with MEN2A, 85% of families with FMTC and >98% of cases of MEN2B. *RET* point mutations lie at specific sites in the RET protein and lead to constitutive activation by either promoting dimerisation or by altering conformation and favouring kinase activity. In almost all MEN2A cases, missense mutations occur in one of five extracellular cysteine codons in exon 10 (Codon 609, Codon 611, Codon 618, and Codon 620) or exon 11 (Codon 634). Codon 634 mutations alone account for 85% of MEN2A cases. In MEN2B, a single mutation in exon 16, M918T, is responsible for 95% of cases (modified with permission from Mulligan 2014).

In contrast to the other *RET* mutations identified in the region coding for the tyrosine kinase domain, the *RET* mutation M918T has a very high transforming ability and is found in 95% of MEN2B patients. Contrary to the mutations found in MEN2A patients, the M918T mutation in *RET* causes signalling activation without dimerisation (Iwashita *et al.* 1996, Santoro *et al.* 1998, Kjaer *et al.* 2006, Wells *et al.* 2013). The MEN2B variant is an aggressive form of *RET* mutation-associated phenotypes, which is mainly due to the M918T mutation and only rarely caused by the A883F point mutation or the V804M/Y806C double mutation (Figure 5). Frame-shift mutations in *RET* caused by insertions or deletions affecting codons of non-cysteine residues are less frequent than point mutations in MEN2 patients (Santoro *et al.* 1998, Kjaer *et al.* 2006, Mulligan 2014).

1.4.2 Acquired mutations in hereditary MTC

In hereditary MTC patients, *RET* mutations are only the initiating step in the process of oncogenesis. Other mutations are to be accumulated in order for transformed C-cells to progress to MTC, where the sequence and identity of many gene mutations are still elusive. Loss-of-function mutations in *CDKN2C* and *CDKN1B* coding for $p18^{INK4c}$ (p18) and p27, respectively, were identified in MEN2A patients, allowing constitutively active RET to deregulate the cell cycle (Franklin *et al.* 2000, Ito *et al.* 2005, Joshi *et al.* 2007, van Veelen *et al.* 2008, van Veelen *et al.* 2009, Knight *et al.* 2011). Further studies reported interactions between RET and p27 suggesting the importance of a decreased p27 levels during MTC oncogenesis (Cerrato *et al.* 2009, Santarpia *et al.* 2009).

The mammalian cell cycle is highly regulated by a complex network of proteins and is restricted through cell cycle check points. This allows cells to react to mitogens, DNA damage or environmental stress and determine whether to complete mitosis. Passage through the cell cycle requires the successive activation of different cyclin-dependent kinases (CDKs) (Bartek *et al.* 2004, Lim *et al.* 2013). These enzymes are controlled by the oscillating expression of the Cyclin regulatory subunits, as well as binding of inhibitory polypeptides and reversible phosphorylation reactions (Nigg 1995, Malumbres *et al.* 2005, Pestell 2013). To promote progression through the cell cycle, the CDK-Cyclin complexes phosphorylate proteins required for the activation of genes involved in cell division, as well as components of the DNA replication machinery (Sherr 1994, Bartek *et al.* 2004, Lim *et al.* 2013).

CDK inhibitors (CKI) are divided into two families. The members of the INK4 family, comprising of $p16^{INK4a}$, $p15^{INK4b}$, p18 and $p19^{INK4d}$, block the progression of the cell cycle by binding to either CDK4 or CDK6 and inhibiting the action of Cyclin D as depicted in Figure 6 (Sherr *et al.* 1995, Malumbres *et al.* 2005). The four proteins of the INK4 family share a similar structure dominated by several ankyrin repeats. The INK4 proteins are commonly lost

or inactivated by mutations in diverse types of cancer and they represent established tumour suppressors for MTC (Canepa *et al.* 2007, van Veelen *et al.* 2009).

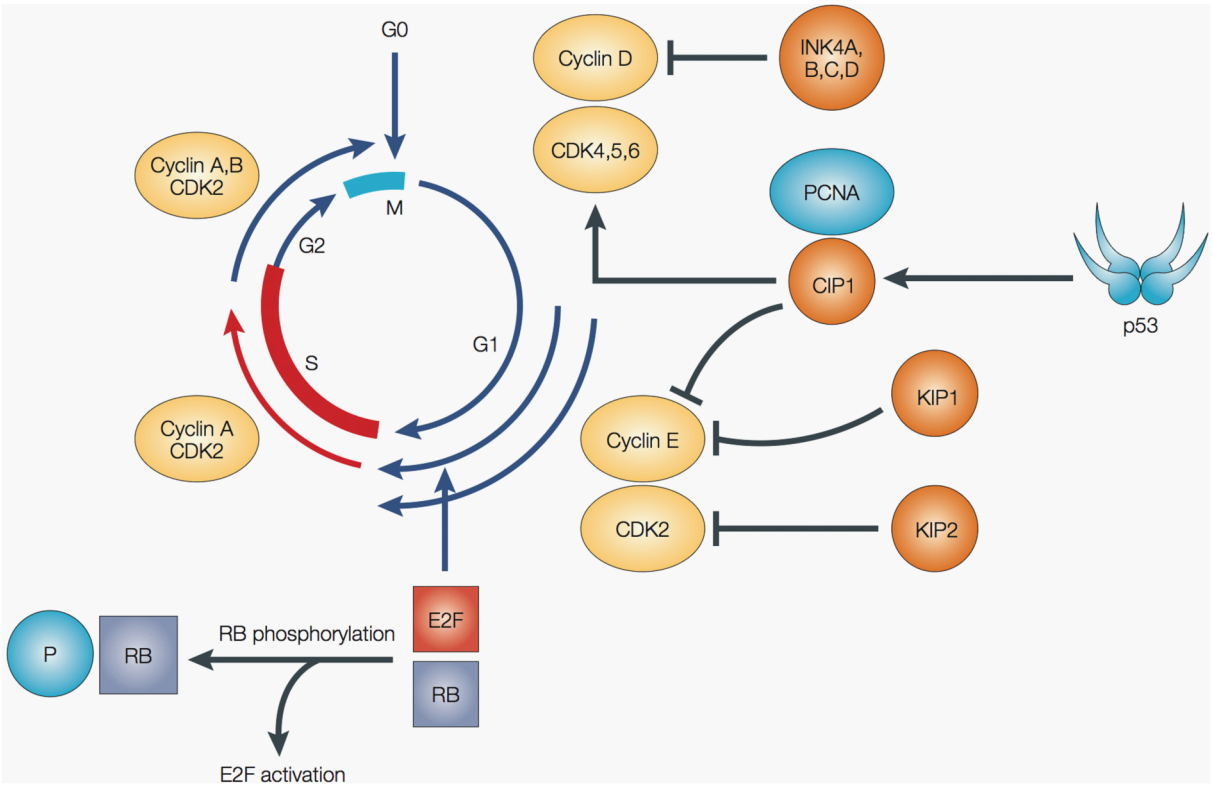

Figure 6: Regulatory effect of INK4 proteins on the cell cycle. Progression through G1 phase and initiation of S phase during the mammalian cell cycle are cooperatively regulated by the CDKs, the activities of which are controlled by CKIs. The activation of Cyclin E is regarded as a key event in the G1-S-phase transition. By phosphorylating the retinoblastoma protein (pRb) the E2F family transcription factors are release. By directly binding to CDK4 and CDK6, the INK4 proteins block the assembly of catalytically active Cyclin D–CDK complexes. The result is that the elevated expression of INK4 proteins causes a G1-phase cell-cycle arrest that is dependent on functional pRb (with permission from Nabel 2002).

The second family of CKIs is the Cip/Kip family, comprising $p21^{Cip1}$, p27 and $p57^{Kip2}$, which act as negative regulators of Cyclin E and Cyclin A-CDK2 as well as Cyclin B-CDK1 holoenzymes as shown in Figure 7. Paradoxically, CKIs of the Cip/Kip family act as positive regulators of the cyclin D-CDK4/6 complexes by mediating their assembly in the early G1 phase (Massague 2004, Malumbres *et al.* 2009).

The CKIs p18 and p27 are both regulated by RET and functionally collaborate in the oncogenesis of MTC. The loss of both alleles of p18 and p27 is critical in the development of neuroendocrine tumours, where the constitutively active MEN2A-specific *RET* mutation, coding for RET^{C634R}, correlates with reduced p18/p27 and elevated Cyclin D protein levels. This leads to an increased CDK activity, thereby increasing pRb phosphorylation and proliferation under growth arrest conditions. This indicates that p27 is a key regulator in the

development of MTC (Sheaff *et al.* 1997, Joshi *et al.* 2007, van Veelen *et al.* 2008, van Veelen *et al.* 2009, Knight *et al.* 2011).

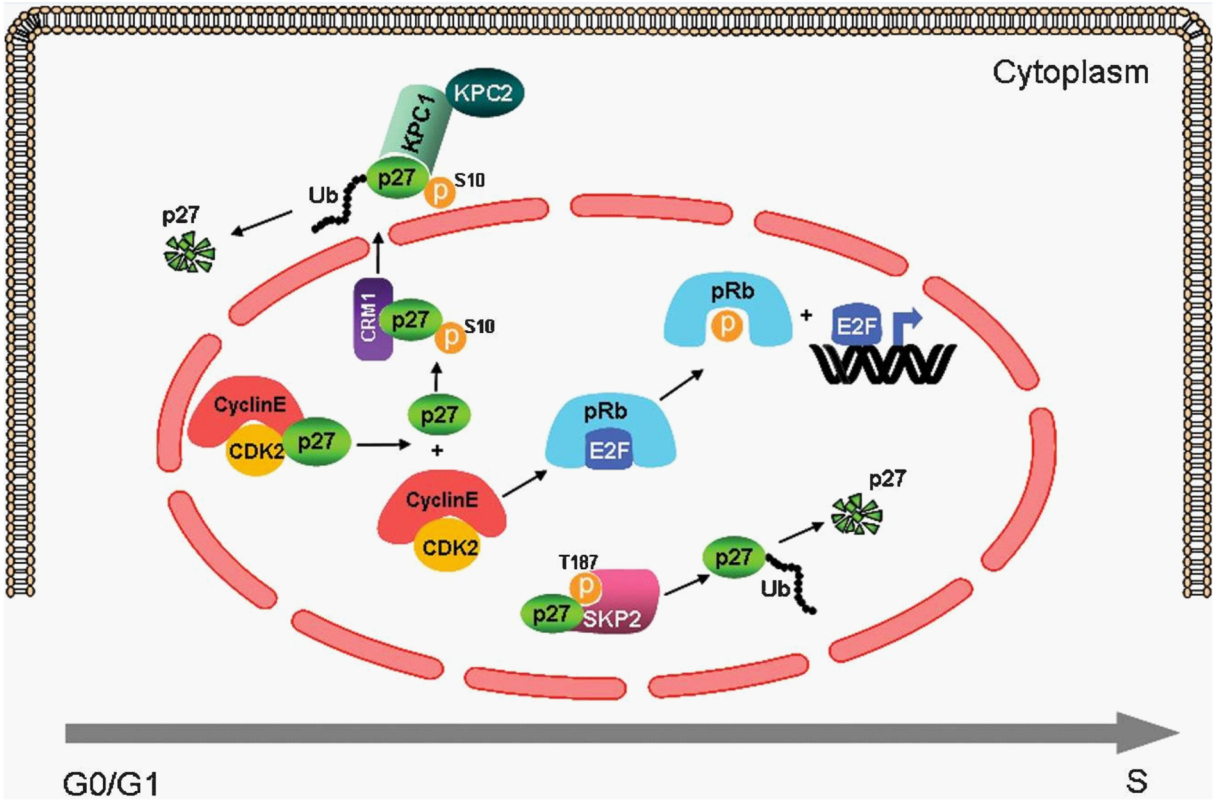

Figure 7: Regulation of the cell cycle by p27. Mitogenic stimulation releases p27 Cyclin E-CDK2 complexes and this dissociation from p27 activates CDK2, which, in turn, phosphorylates pRb. Phosphorylated pRb releases the transcription factor E2F, which is required for the G1-S-phase transition. After the dissociation of p27 from the Cyclin E-CDK2 complex in early G1 phase a portion of p27 is phosphorylated and exported into the cytoplasm. Once in the cytoplasm, p27 is ubiquitylated by the KPC1/KPC2 complex and degraded by the proteasome. Interestingly, mitogenic stimulation leads to the phosphorylation of p27 by the Cyclin E-CDK2 complex. A phosphorylation of p27 at the Thr187 residue creates a recognition site for the SKP2 ligase, which promotes ubiquitylation-mediated degradation of p27 by the proteasome in S phase (with permission from Pellegata 2012).

Interestingly, the MENX rats described in section 1.7 also develop C-cell tumours, indicating the importance of p27 during MTC oncogenesis. During the cell cycle, p27 regulates the G1-S-phase transition by the inactivation of the Cyclin E-CDK2 complex. As a consequence of the inhibition CDK2 cannot phosphorylate its substrate pRb and therefore prevents the release of the E2F transcription factor. This transcription factor is necessary for the expression of genes required for DNA replication and cell division (Marinoni *et al.* 2011, Lee *et al.* 2013).

1.4.3 Oncogenic alterations in sporadic MTC

In contrast to the better characterised acquired mutations in hereditary MTC, the nature of tumour progression in sporadic MTC is not well understood. At present only few somatic

mutations in MTC have been identified. In addition, sporadic mutations of the *RET* proto-oncogene have also been identified. Multiple studies, identified somatic *RET* mutations in approximately 15-50% of patients with sporadic MTCs, where the most frequent *RET* mutation was M918T and was associated with an aggressive form of MTC. The presence of somatic *RET* mutations correlates with the presence of lymph node metastases at diagnosis. Unfortunately, somatic *RET* mutations are not present in all tumour cells, making a targeted therapy difficult (Dvorakova *et al.* 2008, Elisei *et al.* 2008, Moura *et al.* 2009).

The three *RAS* genes, *HRAS*, *KRAS* and *NRAS* were among the first identified oncogenes in human cancers, where gain-of-function mutations were found in 20-25% of all human tumours (Downward 2003). The RAS proteins are small GTPases participating in many signalling transduction pathways (Wennerberg *et al.* 2005). *HRAS* and *KRAS* were first identified in cancer-promoting viruses, whereas *NRAS* was initially discovered in human neuroblastoma cells (Chang *et al.* 1982, Shimizu *et al.* 1983). A study in 2011 identified mutations in *HRAS* and *KRAS* in 17.6% cases of sporadic MTC. Interestingly, these mutations were not found in *RET* mutation positive MTC and therefore these two genetic events are mutually exclusive (Moura *et al.* 2011). The overall incidence of mutations in *HRAS* in MTC was found to be 8.1%, while mutations in *KRAS* were 6.5%. In contrast, the overall incidence of mutations in *NRAS* is 0.5% and constitutes a rare event in MTC. A slightly higher incidence of *RAS* mutations in *RET* mutation negative implies that *RAS* mutations are responsible for a tumoural transformation that leads to a less aggressive MTC phenotype (Ciampi *et al.* 2013).

In addition to point mutations, the overexpression of oncogenes was also observed in MTC. The most prominent group of genes that are overexpressed in sporadic MTC are genes coding for RTKs. As a consequence, the epidermal growth factor receptor (EGFR), an RTK very similar to RET, is frequently overexpressed and is associated with the regulation of cell growth, proliferation and apoptosis. EGFR is frequently upregulated in various types of thyroid carcinomas and plays a vital role in cancer development and progression (Mitsiades *et al.* 2006, Croyle *et al.* 2008, Rodriguez-Antona *et al.* 2010). The degree of overexpression of EGFR varies among MTCs and in some cases only a very focal expression was observed (Erovic *et al.* 2012).

Another overexpressed protein observed during the pathogenesis of MTC is the vascular endothelial growth factor (VEGF) receptor (VEGFR). Three variants exist and mediate angiogenetic and lymphogenic effects. Overexpression of VEGF proteins and VEGFR-2 was identified in MTC, when compared to normal thyroid tissues (Capp *et al.* 2010). The VEGF proteins are secreted by tumours and act as ligands, which bind to VEGFR-2 on endothelial cells to promote a signalling cascade through different pathways. Among the downstream

signalling cascades are MAPK and PI3K/Akt pathways that stimulate proliferation, migration and survival, as well as neoangiogenesis in cancer cells (Kerbel 2008). Similar to the overexpression of EGFR, MTCs showing an overexpression of VEGFR-2 have an increased tendency to metastasise (Rodriguez-Antona *et al.* 2010).

1.5 Recent advances in treating MTC

The general first line treatment of clinically apparent MTC lacking distant metastasis is total thyroidectomy and subsequent hormone supplement. C-cells do not concentrate radioactive iodine nor are sensitive to chemotherapy (Machens *et al.* 2009, Moley 2010). For patients with metastasis the surgical extirpation of the primary tumour and the involved lymph nodes is the only chance for a cure (Milan *et al.* 2010). Detectable calcitonin levels in the blood of patients after surgery indicate disease progression and the levels of this tumour marker relates to tumour mass (Barbet *et al.* 2005, Machens *et al.* 2009). Patients with persistently elevated calcitonin levels after surgery experience clinical recurrence at different time intervals, depending on the progression rate. In 60–90% of patients without lymph node involvement undetectable basal calcitonin levels between 2–3 months after surgery indicates no tumour growth. In contrast, less than 20% of patients with lymph node metastases show low calcitonin levels (Ball 2007, Schlumberger *et al.* 2008).

Genetic alterations have been described in most primary thyroid cancers, but their role in MTC tumourigenesis is still under investigation. Increasing our understanding of the molecular pathogenesis of MTC may help to identify new treatment options for individual patients in the future (Cheng, S. Y. *et al.* 2009).

The recent advances in the understanding of thyroid tumourigenesis and the associated genetic changes, allowed the development of specific inhibitors against targets commonly altered in thyroid cancers. Multikinase inhibitors like Vandetanib, Cabozantinib and Sorafenib were developed. These are small molecule tyrosine kinase inhibitors (TKI) that bind to the adenosine triphosphate (ATP) binding pocket of receptors and thereby block any interaction between receptor and its downstream interaction partners by preventing transphosphorylation of the receptor's tyrosine residues (Lackey *et al.* 2000, Lyons *et al.* 2001, Hennequin *et al.* 2002, Yakes *et al.* 2011). Interestingly, the TKIs currently employed to treat MTC were typically developed to combat other malignancies (Giunti *et al.* 2013).

The multikinase inhibitor Vandetanib is an orally available TKI of RET, VEGFR-2, VEGFR-3 and EGFR, which inhibits downstream pathways critical for tumour growth and angiogenesis. Of note, Vandetanib shows sensitivity against most of the RET oncoproteins, with the exception of the RET^{V804G} oncoprotein, due to steric hindrance (Carlomagno *et al.* 2004). In

clinical trials it was demonstrated that Vandetanib shows minimal toxicity and specific activity in patients with locally advanced or metastatic MTC (Wells *et al.* 2009). The most common treatment-related adverse events were diarrhoea and skin rashes, as well as hypertension and irregular heartbeat (Morabito *et al.* 2009). In approximately 20% of patients a partial remission was observed, while 60% experienced a stable disease (Wells *et al.* 2009). Vandetanib and structurally/chemically similar inhibitors, share the ability of neutralising the effect of *RET* mutations and additionally inhibit signalling propagated by VEGFRs. The suppression of growth of new blood vessels via angiogenesis as shown in Figure 8 is thereby an addition beneficial effect (Schlumberger *et al.* 2008).

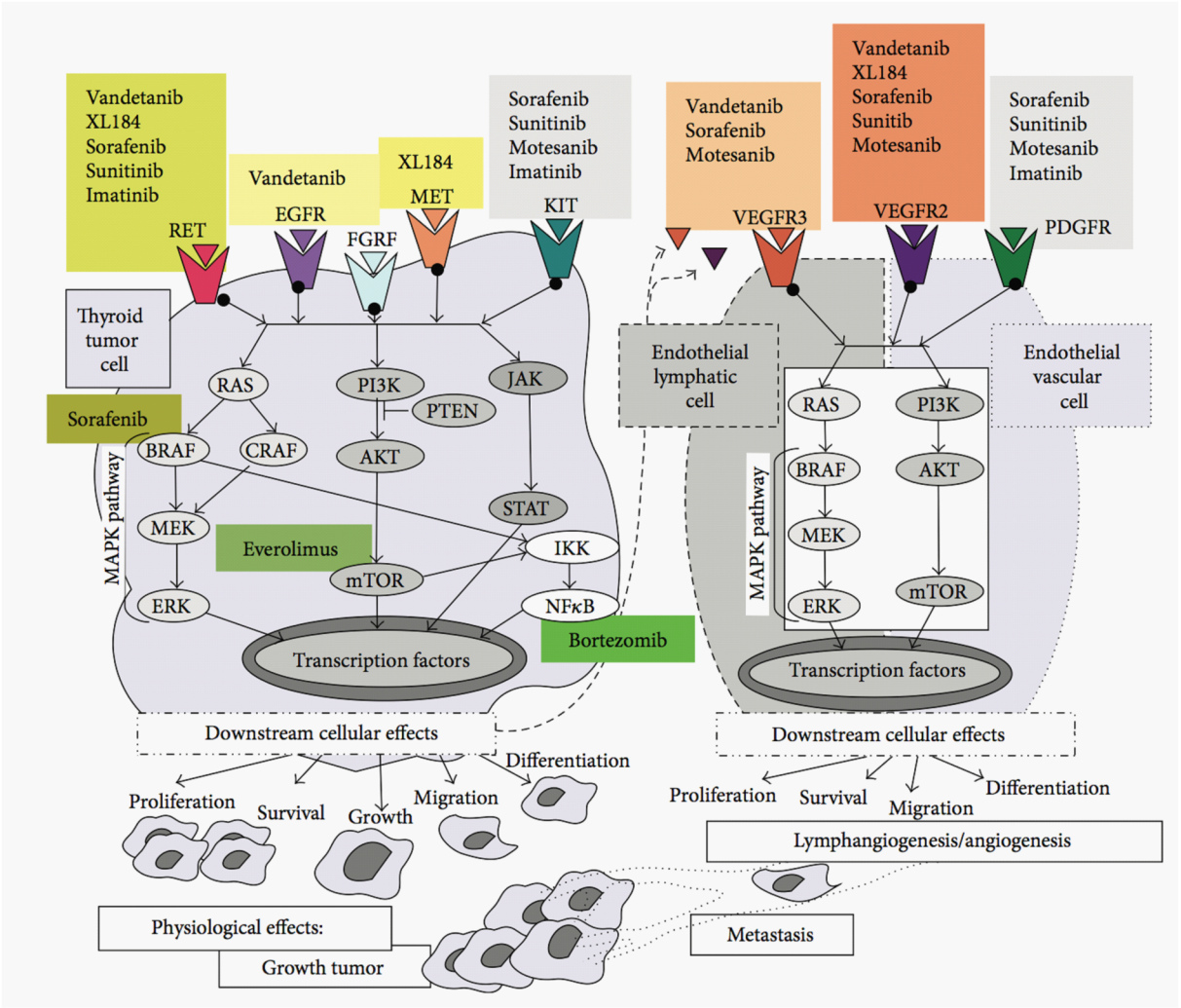

Figure 8: TKIs and their targets. The main TKIs and their targets are shown, such as RET, EGFR and VEGFR, as well as some of their downstream effectors. The two most important oncogenic signalling pathways are PI3K/AKT and RAS-MAPK. The activation of the pathways may transduce different transcription factors and induce tumour cell proliferation, survival and migration, with subsequent tumour growth, angiogenesis and metastasis (with permission from Giunti *et al.* 2013).

The response of patients to TKIs similar to Vandetanib showed variable efficacy. For example, Cabozantinib (denoted XL184 in Figure 8) is a selective inhibitor of RET, MET and VEGFR-2, which showed clinical benefits for MTC patients in phase I trials and prolongation of progression-free survival in phase III trials (Figure 8) (Kurzrock *et al.* 2011). Common cabozantinib-associated adverse events included diarrhea, decreased weight and appetite, as well as nausea and fatigue (Elisei *et al.* 2013). Cabozantinib has been approved by the US Food and Drugs administration for the treatment of MTC patients in November 2012 (Elisei *et al.* 2013). Sorafenib is a multikinase inhibitor similar to Cabozantinib and targets BRAF, VEGFR-2 and VEGFR-3, which is being tested in phase II clinical trials as depicted in Figure 8 (Carlomagno *et al.* 2006, Ahmed *et al.* 2011). Patients displaying adverse reactions to Sorafenib suffered from hand-foot syndrome, diarrhea, skin rashes, fatigue and weight loss. Since Sorafenib is a VEGF inhibitor, cardiovascular adverse effects were present, especially hypertension, acute myocardial infarctions and congestive heart disease (Thomas *et al.* 2014). Further inhibitors are currently being developed and tested.

1.6 Animal models of MTC

In order to test the efficacy of novel MTC therapies xenografts have been created, where human cells from MTC cell lines or primary cells were subcutaneously injected into nude mice and these cells were allowed to grow into a tumour. This has been performed using MTC cells of sporadic origin as well as tumour cells from MTC patients affected by MEN2 (Johanson *et al.* 2007).

Over the past years the focus has shifted away from attempting to develop *in vivo* mouse models to study the multistep tumourigenesis of MTC. Nonetheless, the developed mice strains, were grouped into two major categories. The first group consists of transgenic mouse models expressing human RET oncoproteins with MEN2A- and MEN2B-associated *RET* mutations. For example, among the first transgenic mouse model developed contained a human *RET* gene with a C634R mutation in thyroid's C-cells. The generated lines developed multifocal and bilateral MTC with complete penetrance by the age of 14 months (Michiels *et al.* 1997). The second major category of MTC mouse models introduced mutant murine Ret proteins into mice, which developed MTC along with carcinomas in other organs (Sweetser *et al.* 1999, Acton *et al.* 2000, Kawai *et al.* 2000). Transgenic mouse models by introducing the *Ret* M919T mutation (equivalent to human *RET* M918T) into mice resulted only in the development of C-cell hyperplasias (Smith-Hicks *et al.* 2000).

Other transgenic mouse models were developed containing non-*Ret* mutations. These transgenic mice carry mutations in oncogenes and tumour suppressors previously associated with the predisposition of MTC. One attempt to create a transgenic mouse model

was achieved by generating *Cdkn2c* and *Cdkn1b* knockouts, encoding p18 and p27, repectively (Franklin *et al.* 1998). In addition, the generation of the *Cdkn1b*;*Men1* double knockout showed a high incidence of MTC (Bai *et al.* 2007).

Transgenic mice were also created by overexpressing oncogenes, playing different roles in the pathogenesis of MTC. The E2F-family of transcription factors is involved in the progression of the cell cycle. Mice double knockouts for *Rb1*;*E2f3* showed strong MTC development (Ziebold *et al.* 2003).

One of the downstream effectors of RET is RAS, whose role in MTC was studied by generating *HRAS* transgenic mice. MTC was generated in the majority of animals after one year (Johnston *et al.* 1998, Kostoglou-Athanassiou *et al.* 2004).

Some mouse models did not target cell cycle regulatory genes or components of the RET signalling pathway. The generation of prolactin receptor knockout mice lead to a high incidence of MTC in both genders. Unfortunately, this strain is the only MTC mouse model currently listed in the Mouse Genome Informatics database. In addition, there are no MTC related rat strains listed in the Rat Genome Database (Kedzia *et al.* 2005, Begley *et al.* 2012, Laulederkind *et al.* 2013, Blake *et al.* 2014, Smith *et al.* 2014). Despite previous efforts, the lack of MTC animal models listed in the databases underlines the need for a suitable animal in order to study the pathogenesis of MTC.

1.7 MEN-like syndrome in rats

We discovered a novel hereditary cancer syndrome in a Sprague-Dawley rat colony that is transmitted as a recessive gene mutation. Animals homozygous for this mutation develop multiple neuroendocrine malignancies within the first year of life, showing a phenotypic overlap between human MEN1 and MEN2 syndromes. Among the affected rats the appearance of bilateral adrenal pheochromocytomas (incidence 100%), anterior pituitary adenomas (incidence 100%), bilateral C-cell neoplasias (incidence 78%), bilateral parathyroid hyperplasias (incidence 65%) and multiple extra-adrenal pheochromocytomas (incidence 10%) was identified. The onset of neuroendocrine tumours is preceded by the development of bilateral juvenile cataracts. Cataracts were not identified in MEN4 patients, which is the human equivalent. Interestingly, the spectrum of affected tissues is reminiscent of the human forms of MEN, but germ-line mutations in the *RET* or *MEN1* genes were never detected (Fritz *et al.* 2002, Pellegata 2012).

Due to the overlap with MEN1 and MEN2 syndromes and to the unique combination of phenotypic organs, this multi tumour syndrome was termed MEN-like syndrome (MENX).

One of the most distinctive features is the reduced life span of affected homozygous mutant rats animals averaging only 10 months. In contrast, the life span of wild-type animals is between 24-30 months of age (Fritz *et al.* 2002).

This reduced life span of homozygous mutant rats is due to the early onset of tumour development, which is already evident in the thyroid glands of 2 month old homozygous mutant animals, by an increase in the number of C-cells as depicted in Figure 9. In addition, lesions occur in the adrenal glands, where hyperplastic areas are visible in affected rats at 2 months of age. At the age of 4 months homozygous mutant rats also show multifocal pituitary hyperplasias. At 6 months of age and older, affected animals develop infiltrating pheochromocytomas, multifocal pituitary adenomas and C-cell adenomas. By the age of 8 months animals develop C-cell tumours in the thyroid, which are histologically similar to human MTC (Pellegata *et al.* 2006).

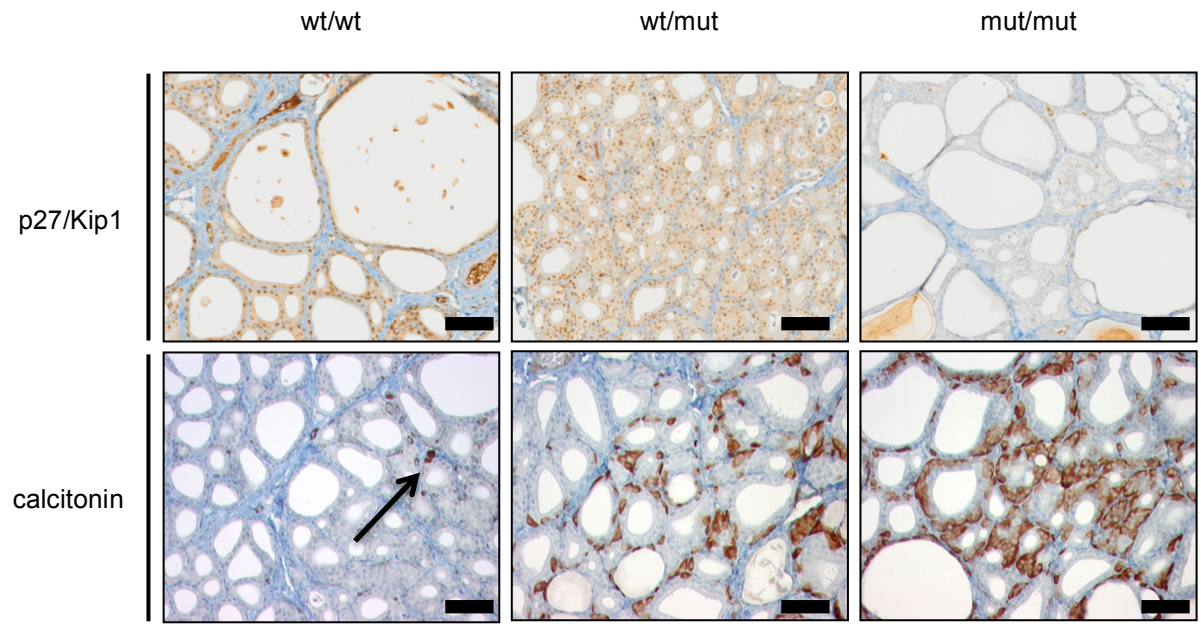

Figure 9: Inverse expression pattern of p27 and calcitonin in MENX rat thyroid glands. The loss of p27 leads to an increased number of C-cells. This can be seen most clearly in thyroid glands of homozygous mutant animals, where the lack of p27 expression leads to the highest number of C-cells detected. The expression of p27 in heterozygous animals is not reduced, yet an increase in the number of C-cells can be detected, when compared to the glands of wild-type animals. Affected animals develop thyroid tumours with a clear progression from hyperplasia to tumours with time. The arrow indicates an individually stained C-cell in thyroid gland of wild-type animals. The scale bar indicates a length of 50 microns (Magnification: 200x).

Examination of MENX-affected rats by linkage studies revealed the *Cdkn1b* gene, encoding the CKI p27, as the cause for the MENX syndrome. The subsequent sequencing of the *Cdkn1b* gene revealed a tandem duplication of eight base pairs in exon 2 of the affected rats. This mutation leads to a frame-shift after codon 176 resulting in the addition of 42 p27-

unrelated amino acids to the c-terminus (p27fs177 protein) of the protein (Pellegata *et al.* 2006). In contrast to wtp27, p27fs177 is highly unstable and rapidly degraded in every phase of the cell cycle. Consequently, the levels of p27 in the tissues of affected rats is absent. The degree of degradation is organ-dependent as p27 is much lower than the corresponding wild-type tissues and cannot be detected in the thyroid, adrenal and pituitary glands, as well as in the lungs, kidneys, liver and testis of affected animals. In contrast, slight reduction in p27 levels when compared to wild-type animals were detected in the thymus, the parathyroid and the brain (Pellegata *et al.* 2006).

Animals heterozygous for the p27 mutation live longer than homozygous MENX rats, but significantly shorter than wild-type littermates. At necropsy, male and female heterozygous mutant rats were found to develop multiple neuroendocrine tumours with time, including pheochromocytomas, pituitary adenomas, thyroid C-cell hyperplasias as well as tumours and parathyroid hyperplasias. Heterozygous mutant rats were significantly more susceptible to tumourigenesis than wild-type rats, but oncogenesis occurs at later ages than homozygous animals. The tumour spectrum is similar in both heterozygous and homozygous mutant rats. Heterozygous mutant rats develop bilateral calcitonin-positive and thyroglobulin-negative C-cell lesions. The first detectable pathological changes occur in the thyroid at the age of 2 months, while tumours of the adrenal medulla and adenohypophysis appear late in life, at an age of 6 months. In contrast to homozygous mutant animals, cataracts were not identified in heterozygous littermates. The C-cell hyperplasias, detected at 2 months of age, progresses to MTC in all heterozygous mutant animals after 9 months of age. The thyroid tumours grow in size up to 4,5 mm in diameter and expand to almost entirely efface the gland, with only a few residual normal follicles displaced at the periphery of the tumour mass. Vascular, muscular as well as perineural invasion was a common feature in the large tumours. Interestingly, a liver metastasis was found in a 20 month-old heterozygous mutant rat indicating that thyroid tumours in MENX rats have metastatic potential (Molatore *et al.* 2011).

Similar to the thyroid gland in humans, C-cells only make up a small percentage of the cell population in healthy thyroid glands of wild-type animals and do not form a coherent tissue within the organ. In contrast to the calcitonin-staining to wild-type littermates, homozygous and heterozygous rats show an increased number of C-cells but still do not form coherent tissues at an age of 2 months. Figure 9 shows the calcitonin staining of thyroid glands in wild-type, heterozygous and homozygous mutant rats. C-cells hyperplasias consist of only small C-cell populations, while benign tumours are not developed. For this reason normal thyroid tissues from wild-type rats cannot be used as representative controls for C-cells.

1.8 MicroRNAs

MicroRNAs (miRNAs) comprise a large family of non-coding RNAs that have been discovered in *Caenorhabditis elegans* (*C. elegans*) in 1993 as additional post-transcriptional regulators of gene expression. Since then, miRNAs have been identified in many plant and animal species (Lee *et al.* 1993, Chen *et al.* 2008, Fabian *et al.* 2010). MiRNAs account for approximately 1% of the human genome. They are usually located in the intergenic regions, in non-coding transcriptional units or within introns of protein coding transcriptional units. In addition, a sizeable percentage of miRNAs are clustered together as polycistronic transcription units, while some miRNAs are regulated by individual promoters (Rodriguez *et al.* 2004, Baskerville *et al.* 2005, Menon *et al.* 2009). Specific subsets of overexpressed or downregulated miRNAs have been identified in various cancer types, suggesting that aberrations in miRNA expression may be important in tumour development and progression (Nikiforova *et al.* 2008, Croce 2009, Menon *et al.* 2009, Nikiforova *et al.* 2009).

1.8.1 MiRNA biogenesis

MiRNAs are typically transcribed by RNA polymerase II as primary miRNAs (pri-miRNAs), which range from hundreds to thousands of nucleotides in length (Du *et al.* 2005, Ha *et al.* 2014). Folding into double stranded RNA-like hairpins, the maturation of pri-miRNAs occurs in two steps, both catalysed by enzymes belonging to the ribonuclease (Rnase) type III family, along with proteins containing double-strand RNA-binding domains as seen in Figure 10 (Filipowicz *et al.* 2005, Ha *et al.* 2014). The first processing is conducted by the microprocessor composed of Drosha and its partner DiGeorge syndrome critical region gene 8 (DGCR8) that excise a 70-nucleotide stem loop known as a precursor miRNA (pre-miRNA) (Inui *et al.* 2010). For this processing a large terminal loop in the hairpin is required. The pre-miRNA is then exported from the nucleus to the cytoplasm by Exportin 5, which specifically recognises the characteristic end structure of the pre-miRNA (Yi *et al.* 2003, Lund *et al.* 2004, Du *et al.* 2005, Ha *et al.* 2014). Double-stranded RNA-specific endorinuclease (Dicer), another RNase type III endonuclease and the transactivation response RNA-binding protein (TRBP) cleave the precursor and generate an approximately 20 nucleotide long mature miRNA duplex (Filipowicz *et al.* 2008, Koscianska *et al.* 2011).

MiRNA biogenesis is stringently controlled and is often subjected to feedback regulation. Multiple steps of miRNA biogenesis are specifically regulated during processes like differentiation and tumour progression (Thomson *et al.* 2006, Choudhry *et al.* 2011). For example in cancer, many pri-miRNAs are expressed but are not efficiently converted into

mature miRNAs, leading to a widespread downregulation of miRNAs in cancers (Thomson *et al.* 2006, Garzon *et al.* 2009, Siomi *et al.* 2010).

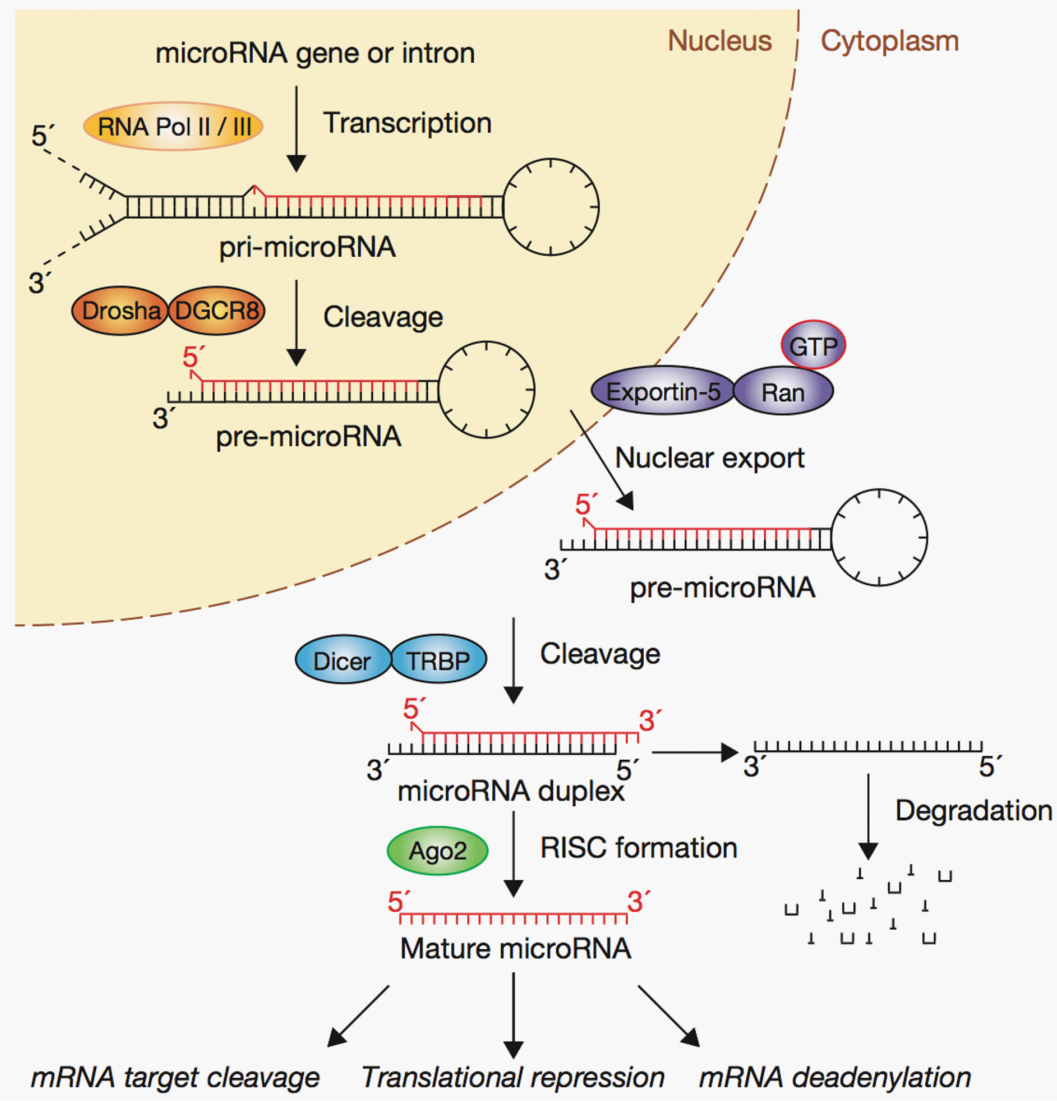

Figure 10: Biogenesis of miRNAs. The canonical miRNA processing pathway includes the production of the pri-miRNA by RNA polymerase II or III and cleavage of the pri-miRNA by the microprocessor complex Drosha/DGCR8 in the nucleus. The resulting pre-miRNA is exported from the nucleus by Exportin-5/Ran-GTP. In the cytoplasm, the RNase Dicer in complex with the double-stranded RNA-binding protein TRBP cleaves the pre-miRNA hairpin to its mature length. The functional strand of the mature miRNA is loaded together with Argonaut (Ago) proteins into the RNA induced silencing complex (RISC), where it guides RISC to silence target mRNAs through mRNA cleavage, translational repression or deadenylation. The passenger strand is degraded (with permission from Winter *et al.* 2009).

Regulation of individual miRNAs can be achieved independently, but miRNAs are frequently encoded in the genome as clusters and are transcribed as long polycistronic primary transcripts (Kim *et al.* 2009, Winter *et al.* 2009). However, in most incidences only one miRNA is expressed from the primary transcript as the miRNA transcript is post-transcriptionally regulated (Guil *et al.* 2007, Siomi *et al.* 2010).

The first mechanism regulating miRNAs occurs at the stage of transcription of the pri-miRNA. Most pri-miRNAs are transcribed by RNA polymerase II and therefore bear a 7-methyl-guanosine cap and are poly-adenylated at the 3'-end. The promoters of pri-miRNAs contain CpG islands, TATA box sequences, initiation elements and histone modifications, subjecting miRNAs to regulation by enhancers, silencing elements and chromatin modifications (Lee *et al.* 2004, Lee *et al.* 2009, Libri *et al.* 2013).

Processing of the pri-miRNA into the pre-miRNA is the first step of post-transcriptional modifications and may be regulated by a variety of protein cofactors that are recruited to the microprocessor, composed of Drosha and DGCR8 (Gregory *et al.* 2004, Fukuda *et al.* 2007, Libri *et al.* 2013). The recruitment of the helicases $p68^{DDX5}$ (p68) and $p72^{DDX17}$ (p72) to the microprocessor facilitates processing of pri-miRNAs. Many proteins such as SMADs, p53 and BRCA1 are able to stabilise the interaction of p68/p72 with the microprocessor (Suzuki *et al.* 2009, Blahna *et al.* 2012, Kawai *et al.* 2012). Inhibitory effects of proteins like the oestrogen receptors was also observed, where signalling is preventing the processing of specific pri-miRNAs by intercepting p68 (Yamagata *et al.* 2009).

Pre-miRNA processing by Dicer is very efficient, since relative low levels of pre-miRNAs are present, when compared to pri-miRNAs and mature miRNAs. Dicer is typically regulated by the retention of pre-miRNAs in the nucleus, where they are not exposed to Dicer (Lee *et al.* 2008). The levels of Dicer can also be regulated by its products, which in some cases bind to Dicer mRNA directly, therefore regulating its expression and thus creating a negative feedback loop (Forman *et al.* 2008). Furthermore, Dicer protein levels are regulated by TRBP through direct interaction. Signalling cascades like the RAS-MAPK pathways are able to stabilise the Dicer-TRBP complex and enhance miRNA production (Melo *et al.* 2009, Paroo *et al.* 2009).

1.8.2 MiRNA targeting mechanism and mRNA degradation

Two different miRNAs can be generated from the miRNA duplex. However, usually only one miRNA strand gets incorporated into the RISC and guides the complex to the target mRNAs (Schwarz *et al.* 2003). A selection between the two strands is based on thermodynamic stability of base pairs, where the miRNA strand with a less stable base pair at its 5' end in the duplex is loaded onto RISC (Khvorova *et al.* 2003, Winter *et al.* 2009).

It is believed that miRNAs regulate approximately one third of all human genes, where each miRNA have numerous putative targets with distinct functions (Menon *et al.* 2009). Through mutual base pairing to mRNAs with nearly perfect complementary the miRNA binds to its target mRNA (Filipowicz *et al.* 2008).

The most stringent requirement for miRNAs to bind the target mRNA is a continuous and perfect base pairing of the miRNA nucleotides 2-8, representing the seed region, which recognises the target mRNA and nucleates the pairing between the miRNA and the mRNA (Filipowicz *et al.* 2008, Hibio *et al.* 2012). Binding of the miRNA‘s 3’-half with the complementary mRNA region is quite relaxed. It generally stabilises the interaction, particularly when the seed matching is suboptimal (see Figure 11). Typically, miRNA-mRNA duplexes contain mismatches and bulges in the central region that prevent premature endonucleolytic cleavage of the mRNA by an RNA interference (RNAi)-like mechanism (Fabian *et al.* 2010). Interestingly, an mRNA tends to contain several binding sites for either the same or different miRNAs. This suggests a potential importance of synergetic binding of the miRNA to the target and a possible regulation of an mRNA by multiple miRNAs (Doench *et al.* 2004, Fabian *et al.* 2010).

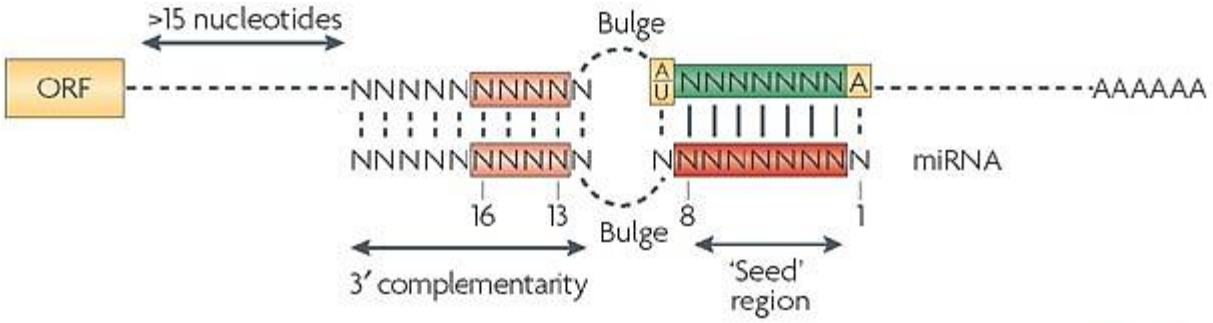

Figure 11: The interaction between miRNAs and target mRNAs. MiRNAs interacting with their mRNA targets by base pairing follow a set of rules. One rule for miRNA–target base paring is perfect and continuous base pairing of miRNA nucleotides 2 to 8, representing the 'seed' region which nucleates the miRNA–mRNA association. GU pairs or mismatches and bulges in the seed region greatly affect repression. However, an A residue across position 1 of the miRNA, and an A or U across position 9 improve the site efficiency. Another rule is that bulges or mismatches must be present in the central region of the miRNA–mRNA duplex, precluding the Ago-mediated endonucleolytic cleavage of mRNA. The third rule is that there must be reasonable complementarity to the miRNA 3'-half to stabilise the interaction. Mismatches and bulges are generally tolerated in this region, although good base pairing becomes important when matching in the seed region is suboptimal (with permission from Filipowicz *et al.* 2008).

Following the binding of the miRNA to its mRNA target, the miRNA can regulate gene expression through multiple mechanisms. These include the inhibition of translation of the mRNA, as well as subsequent storage or degradation (Fabian *et al.* 2010).

Typically, the binding of miRNAs to their targets triggers the endonucleolytic mRNA degradation by an RNAi-like mechanism, a biological process in which RNA molecules inhibit gene expression, typically by causing the destruction of a specific mRNA molecule (Fire *et al.* 1998, Filipowicz *et al.* 2008). Essential for the mRNA repression is the formation of RISC-like miRNA ribonucleoprotein particles (miRNP) composed of proteins of the Ago family, giving

miRNAs the ability to achieve an RNAi-like downregulation (Filipowicz *et al.* 2005, Fabian *et al.* 2012).

MiRNAs function in cooperation with Ago proteins, forming catalytic components of the miRNP. Ago proteins bind different classes of non-coding RNAs and in cooperation identify specific targets through sequence complementarity (Ghildiyal *et al.* 2009, Cenik *et al.* 2011). Some Ago proteins have endonuclease activity directed against the target mRNA, which is known as slicer activity (Tolia *et al.* 2007). Previous studies demonstrated that miRNA expression levels are tied to Ago protein levels (Diederichs *et al.* 2007). Ago proteins are also subjected to various levels of transcriptional and post-transcriptional regulation, which consequently influence the expression of miRNAs. This occurs especially in cancer, where signalling pathways such as EGFR-MAPK pathways upregulate the expression of Ago proteins leading to an enhanced expression of miRNAs (Adams *et al.* 2009).

Translational repression induced by miRNA was initially observed during the development of *C. elegans*, where the translating polysomes remain bound to the targeted mRNA yielding a reduction in protein levels (Fabian *et al.* 2010). Three main mechanisms have been described where by interfering with translation miRNAs achieve a downregulation of protein expression (Figure 12) (Wilczynska *et al.* 2015). Eukaryotic translation of mRNAs is divided into the initiation, elongation and termination processes, where the initiation represents the rate-limiting step and requires the participation of at least 10 initiation factors. Initiation of translation of most cellular mRNAs starts with the recognition of the mRNA 5'-terminal 7-methylguanosine cap by the eukaryotic translational initiation factor (eIF) 4E and the poly(A) tail is recognised by the poly(A) binding protein (Filipowicz *et al.* 2008). Additional important initiation factors are eIF4A, eIF4F and eIF4G participating in the circulation of the mRNA (Fabian *et al.* 2010).

The first mechanism, by which miRNAs accomplish translational repression is the inhibition of the cap-dependent translation. An interaction between the miRNP and the cap binding complex was observed in various experiments with reporter miRNAs and cell extracts (Pillai *et al.* 2005, Mathonnet *et al.* 2007, Zdanowicz *et al.* 2009).

A second mode of miRNA-mediated translational repression was shown to be the inhibition of the 60S ribosomal subunit joining with the 40S subunit of the ribosome as seen in Figure 12 (Wang *et al.* 2008). A proposed mechanism involves an interaction between the miRNP and eIF6, which prevents joining of the 60S and 40S subunits and the generation of the 80S ribosome (Filipowicz *et al.* 2008).

A third type of repression mechanism involves numerous post-initiation interferences (Figure 12), where an inhibition through interfering with peptide elongation or promoting premature ribosome dissociation has been described (Lytle *et al.* 2007, Filipowicz *et al.* 2008).

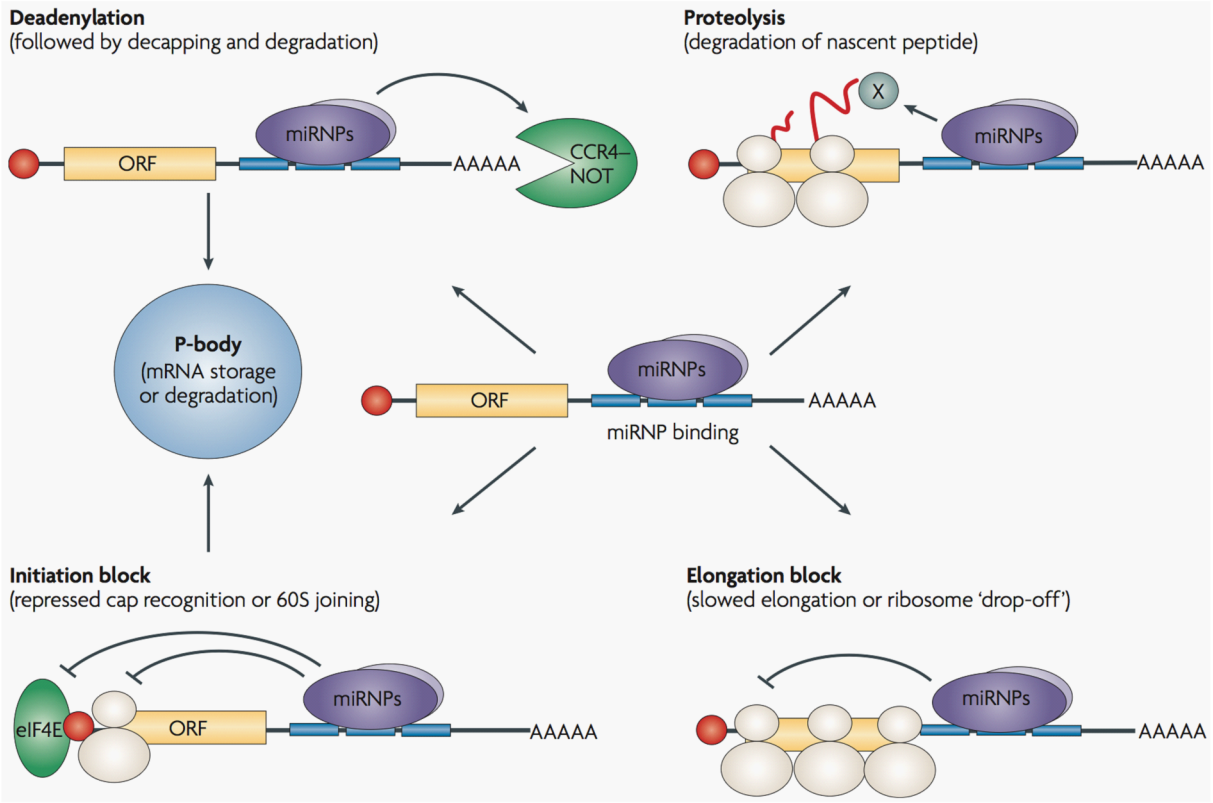

Figure 12: MiRNA mediated regulation of protein translation. Binding of miRNPs, possibly complexed with accessory factors, to mRNA 3'-UTR can induce deadenylation and decay of target mRNAs. Alternatively, miRNPs can repress translation initiation at either the cap-recognition stage or the 60S subunit joining stage. The mRNAs repressed by deadenylation or at the translation-initiation stage are moved to processing bodies (P-bodies) for either degradation or storage. The repression can also occur at post-initiation phases of translation, owing to either slowed elongation or ribosome 'drop-off' (with permission from Filipowicz *et al.* 2008).

Following the inhibition of translation, the repressed mRNAs may be degraded via several proposed mechanisms (Figure 12). In most cases mRNA decay by animal miRNAs does not occur through endonucleolytic activity of Ago proteins, but instead by mRNA-degradation machinery, consisting of GW182 proteins in P-bodies (Eulalio *et al.* 2007). P-bodies are discrete cytoplasmic domains where functions in translational repression, mRNA silencing or quality control of mRNA transcripts are observed (Eulalio *et al.* 2007). The translationally repressed mRNAs can accumulate in P-bodies, in response to the action of miRNA or physiological conditions such as stress. Frequently, the translational repressed miRNAs are degraded. P-bodies may also store repressed mRNAs, allowing for a delayed release of the mRNA and a postponed gene expression (Fabian *et al.* 2010).

The mRNA quality control mechanisms have evolved to ensure that only fully processed and error-free mRNAs are translated. Nonsense-mediated mRNA decay pathways recognise and degrade mRNAs that contain premature translation termination codons and thereby limiting the translation of faulty proteins. The nonsense-mediated mRNA decay pathways are triggered by the premature termination of translation and escorted to P-bodies, where the mRNAs are degraded (Eulalio *et al.* 2007).

As a common initialising step in all mechanisms, the poly(A) tail of the mRNA is removed, through members of the exonuclease III family of nucleases, which undergoes nucleophilic attacks on phosphodiester bonds (Parker *et al.* 2004). Following this initial shortening of the mRNA's poly(A) tail, the mRNA body can then be degraded by progressive 3'-5' decay, which is catalysed by the exosome, or by the removal of the cap followed by 5'-3' degradation which is catalysed by the XRN1 exonuclease. The miRNP allows the controlled degradation as it recruits specific components of the degradation machinery (Filipowicz *et al.* 2008).

.

2 Aim of the project

With the discovery of miRNAs a new level of gene expression regulation has been identified, thereby increasing our understanding of gene deregulation such as that witnessed in cancer cells. The overexpression or downregulation of cancer-specific miRNAs have a profound impact on thyroid tumour development and progression (Nikiforova *et al.* 2008, Nikiforova *et al.* 2009).

The differential expression of specific mRNAs and miRNAs has been used to classify thyroid tumours. The analysis of gene mutations commonly associated with thyroid cancer and expression profiles of miRNAs improve the characterisation of the tumours. A higher understanding of the molecular pathomechanisms of cancer may ultimately lead to targeted therapeutic approaches (Cheng, S. Y. *et al.* 2009). For instance, tumours in which miRNAs are lost or overexpressed could then be treated with miRNAs or specific miRNA inhibitors, respectively (Croce 2009, Berindan-Neagoe *et al.* 2014).

Compared with other thyroid malignancies, MTC shows a higher tendency to metastasise and is often associated with a poor prognosis (David *et al.* 2010, Kaatsch *et al.* 2013, Santarpia *et al.* 2013). The molecular mechanisms leading to aggressive MTC phenotypes are still elusive. A molecular characterisation of MTC tumours during different stages of tumour progression would shed light into the mechanisms of MTC development. Several independent studies have characterised miRNA deregulation on snap-frozen PTC and FTC tissues, revealing several specific miRNAs associated with progression of tumours (Nikiforova *et al.* 2009).

In contrast to studying thyroid tumours arising from follicular cells, only few investigations have focussed on the miRNA expression in MTC. This is primarily due to the difficulty in obtaining a representative normal tissue of C-cells that can be used as a reference and in part caused by the low incidence of MTC itself (Maliszewska *et al.* 2013).

Animal models resembling MTC have been generated by introducing human as well as mouse *RET* mutations associated with MEN2A and MEN2B into mice with varying success (Michiels *et al.* 1997, Sweetser *et al.* 1999). The introduction of mutant murine Ret proteins into mice was partially successful (Sweetser *et al.* 1999, Smith-Hicks *et al.* 2000). Transgenic mice created by overexpressing oncogenes and knocking-out tumour suppressor genes, ocassionally developed MTC. Interestingly, to date few animal models have been generated that closely resemble the human disease (Begley *et al.* 2012, Laulederkind *et al.* 2013, Blake *et al.* 2014, Smith *et al.* 2014).

The aim of this study was to determine the miRNA expression signatures of MTC in MENX rats. The development of histologically similar MTC in homozygous and heterozygous mutant rats allows the investigation of the influence of p27 levels on MTC pathogenesis. The prolonged life span of heterozygous mutant rats allows the investigation of effects of tumour progression on miRNA expression. In order to reach these aims, RNA was isolated from MENX rat thyroid tumours and miRNA profiles were generated.

A further aim of our investigation was to determine the suitability of MENX rats as a model of human MTC. We addressed this issue by collecting patient tumour samples and generating miRNA profiles. The patients were grouped according to their genetic background and separated into patients with MEN2A-associated *RET* mutations and sporadic patients. The obtained miRNA expression data sets were compared with those obtained using rat tumours in order to identify any significant overlap.

3 Materials and methods

3.1 Materials

Table 1: Equipment.

Product	Company
Adhesive seal applicator	3M Deutschland, Neuss (Germany)
Centrifuge Biofuge fresco	Heraeus Instruments, Osterode (Germany)
Rotor: 3325B 1.5 ml	Thermo Fisher Sci., Waltham (MA, USA)
Centrifuge Biofuge pico	Heraeus Instruments, Osterode (Germany)
Rotor: 3325B 1.5 ml	Thermo Fisher Sci., Waltham (MA, USA)
Centrifuge Eppendorf 5415D	Eppendorf, Hamburg (Germany)
Rotor: F45-24-11 1.5 ml	Eppendorf, Hamburg (Germany)
Centrifuge Fisherbrand Mini	Fisher Scientific, Schwerte (Germany)
Rotors 0.2 ml, 1.5 ml	Fisher Scientific, Schwerte (Germany)
Centrifuge Rotanta 460R	Andreas Hettich, Tuttlingen (Germany)
Rotor: 5624 15 /50 ml	Andreas Hettich, Tuttlingen (Germany)
Centrifuge Rotina 420R	Andreas Hettich, Tuttlingen (Germany)
Rotor: 4790 1.5 ml	Andreas Hettich, Tuttlingen (Germany)
Centrifuge PerfectSpin P	PeqLab Biotechnologie, Erlangen (Germany)
Centrifuge Variofuge 3.0R	Heraeus Sepatech, Osterode (Germany)
Rotor: #8074, inserts #8078 15/50 ml	Heraeus Sepatech, Osterode (Germany)
Centrifude MIKRO 200 R Centrifuge	Andreas Hettich, Tuttlingen (Germany)
Angle rotor for 24 x 1.5/2 ml, max.	Andreas Hettich, Tuttlingen (Germany)
RCF 21,382 – Cat. No. 2424-B	
Counting chamber Improved Double Neubauer Ruling	Brand, Wertheim (Germany)
Cryostat CM1950 OUVVM	Leica, Wetzlar (Germany)
Electrophoresis Cell GT MINI-SUB®	Bio-Rad Laboratories, Munich (Germany)
Freezer -20 °C Liebherr Comfort	Liebherr, Biberach an der Riss (Germany)
Freezer -80 °C HFC86-360	Heraeus Instruments, Osterode (Germany)
Freezing container NALGENE™ Cryo 1 °C	Thermo Fisher Sci., Roskilde (Denmark)
Fridge +4 °C Liebherr Premium	Liebherr, Biberach an der Riss (Germany)
Gas burner Fuego SCS basic	WLD-TEC, Goettingen (Germany)
Gel documentation system	Vilber Lourmat, Eberhardzell (Germany)

Table 1 continued: Equipment.

Product	Company
Heating block Thermomixer® comfort 1.5 ml	Eppendorf, Hamburg (Germany)
Hood Uniflow UVUB 1800	UniEquip, Planegg (Germany)
Hotplate stirrer IKAMAG® RCT	IKA®-Werke, Staufen (Germany)
Ice machine	Ziegra, Isernhagen (Germany)
Incubator innova CO-170	New Brunswick Sci., Edison (NJ, USA)
Incubator shaker Model G25	New Brunswick Sci., Edison (NJ, USA)
Infinite200 NanoQuant	TECAN, Männedorf (Switzerland)
Luna automated cell counter	Biozym, Hessisch Oldendorf (Germany)
Magnetic stir bars, various sizes	NeoLab, Heidelberg (Germany)
Magnetic stirrer MR2000	Heidolph Instr., Schwabach (Germany)
Microplate Reader Model 680	Bio-Rad Laboratories, Munich (Germany)
Microscope EVOS xl	AMG, Bothell (WA, USA)
Microtome MH 335	Carl Zeiss, Jena (Germany)
Microwave Whirlpool ProMicro 825	Bauknecht Hausg., Stuttgart (Germany)
MSC-Advantage™ Class II Biological Safety Cabinets	Thermo Fisher Sci., Waltham (MA, USA)
PCR cycler GeneAmp® PCR system 9700	Applied Biosystems Darmstadt (Germany)
PCR cycler Real-Time 7900HT	Applied Biosystems Darmstadt (Germany)
PCR cycler SensoQuest labcycler	SensoQuest, Goettingen (Germany)
pH meter inoLab® Level 1	WTW, Weilheim (Germany)
Pipette Discovery 0.5-10 µl	Abimed, Langenfeld (Germany)
Pipette Discovery 10-100 µl	Abimed, Langenfeld (Germany)
Pipette Discovery 100-1000 µl	Abimed, Langenfeld (Germany)
Pipette Discovery 2-20 µl	Abimed, Langenfeld (Germany)
Pipette Discovery 20-200 µl	Abimed, Langenfeld (Germany)
Pipette P10	Gilson, Middleton (WI, USA)
Pipette P100	Gilson, Middleton (WI, USA)
Pipette P1000	Gilson, Middleton (WI, USA)
Pipette P20	Gilson, Middleton (WI, USA)
Pipette P200	Gilson, Middleton (WI, USA)
Pipettor accu-jet®	Brand, Wertheim (Germany)
Pipettor pipetus®-akku	Hirschmann Laborg., Eberstadt (Germany)
Power supply PowerPac 300	Bio-Rad Laboratories, Munich (Germany)
Pressure cooking pot Tender Cooker	Nordic Ware, Minneapolis (MN, USA)

Table 1 continued: Equipment.

Product	Company
Rainin Pipet-Lite XLS+ Multichanel pipette	Mettler Toledo, Gießen (Germany)
Reaction tube rotator L29	A. Hartenstein, Würzburg (Germany)
Scales Sartorius basic	Sartorius, Göttingen (Germany)
Scales Sartorius universal	Sartorius, Göttingen (Germany)
Spectrophotometer NanoDrop® ND-1000	Thermo Fisher Sci., Waltham (MA, USA)
Spectrophotometer UV/VIS Novaspec II	Pharmacia LKB, Uppsala (Sweden)
System Microscope BX43	Olympus GmbH, Hamburg (Germany)
Tweezers	A.Dumont&Fils, Montignez (Switzerland)
Vortexer Vortex-Genie 2	Scientific Industries, Bohemia (NY, USA)
Water bath shaker #1083	G. f. Labortechnik, Burgwedel (Germany)
Water bath shaker SW21	Julabo Labortechnik, Seelbach (Germany)

Table 2: Consumable Products.

Product	Company
Adhesive seal films MicroAMP™	Applied Biosystems, Darmstadt (Germany)
Cryo-Gel™ High Viscosity Water Soluble Media For Frozen Sections	Leica, Wetzlar (Germany)
Glass slides SuperFrost® 76 x 26 mm	Carl Roth, Karlsruhe (Germany)
GeneChip miRNA 1.0 Arrays	Affymetrix, High Wycombe (UK)
Matrigel® invasion chambers (8 µm pore size) cell culture inserts	BD Falcon, Heidelberg (Germany)
microRNA Ready-to-use microRNA PCR Rat Panel I	Exiqon, Vedbaek (Denmark)
Microplates, TC 96 well, clear bottomed, white walled	Lonza, Basel (Switzerland)
Needles Sterican® Ø 0.80 x 50 mm 21G x 2”	B. Braun, Melsungen (Germany)
Parafilm®	Carl Roth, Karlsruhe (Germany)
PCR plate (0.2 ml) Thermo-Fast® 96-well, non-skirted	Thermo Fisher Sci., Waltham (MA, USA)
PCR plate (0.2 ml) Thermo-Fast® 96-well, semi-skirted	Thermo Fisher Sci., Waltham (MA, USA)
PET track-etched membrane (8 µm pore size) cell culture inserts	BD Falcon, Heidelberg (Germany)

Table 2 continued: Consumable Products.

Product	Company
Pipette tips Graduated Filter Tips TipOne® 0.1-10 µl	Starlab, Ahrensburg (Germany)
Pipette tips Graduated Filter Tips TipOne® 1-20 µl	Starlab, Ahrensburg (Germany)
Pipette tips Graduated Filter Tips TipOne® 1-100 µl	Starlab, Ahrensburg (Germany)
Pipette tips Graduated Filter Tips TipOne® 1-200 µl	Starlab, Ahrensburg (Germany)
Pipette tips Graduated Filter Tips TipOne® 101-1000 µl	Starlab, Ahrensburg (Germany)
Pipette tips, DIAMOND® Standard Tips D1000	Gilson S.A.S, Villiers le Bel (France)
Pipette tips, DIAMOND® Standard Tips D200	Gilson S.A.S, Villiers le Bel (France)
Pipette tips, DIAMOND® Standard Tips DL10	Gilson S.A.S, Villiers le Bel (France)
Pipettes, Pasteur glass 3.2 ml	Carl Roth, Karlsruhe (Germany)
Pipette tips Rainin Bioclean-Tips 1-20 µl	Mettler Toledo, Gießen (Germany)
Pipettes, serological CELLSTAR® 10 ml	Greiner BioOne, Frickenhausen (Germany)
Pipettes, serological CELLSTAR® 25 ml	Greiner BioOne, Frickenhausen (Germany)
Pipettes, serological CELLSTAR® 5 ml	Greiner BioOne, Frickenhausen (Germany)
Reaction tubes 1.5 ml	Eppendorf, Hamburg (Germany)
Reaction tubes 2 ml	Eppendorf, Hamburg (Germany)
Reaction tubes Falcon™ Blue Max 15 ml	BD Falcon, Heidelberg (Germany)
Reaction tubes Falcon™ Blue Max 50 ml	BD Falcon, Heidelberg (Germany)
Reaction tubes, RNase-free 1.5 ml	Zymo Research, Orange (CA, USA)
RNaseZAP®	Sigma-Aldrich, St. Louis (MO, USA)
Scalpel, sterile, disposable	Aesculap, Tuttlingen (Germany)
Syringe, single-use 50 ml (60 ml)	Henke-Sass-Wolf, Tuttlingen (Germany)
Tissue culture flasks 25 cm^2, filter cap Nunclon™	Nunc, Roskilde (Denmark)
Tissue culture flasks 75 cm^2, filter cap	Greiner BioOne, Frickenhausen (Germany)
Tissue culture plates 24 well MULTIWELL™	BD, Franklin Lakes (NJ, USA)
Tissue culture plates 6 well Nunclon™	Nunc, Roskilde (Denmark)
TissueTec OCT compound for Cryostat Sectioning	Sakura Finetec, Staufen (Germany)

Table 3: Reagents.

Product	Company
3-(4,5-dimethylthiazol-2-yl)-2,5-diphenyltetrazoliumbromide (*pur*.)	Sigma, Munich (Germany)
Agarose LE for gel electrophoresis	Biozym, Hessisch Oldendorf (Germany)
Albumin from bovine serum (*pur*.)	Sigma-Aldrich, Steinheim (Germany)
Ampicillin sodium salt	Sigma-Aldrich, Steinheim (Germany)
Ampuwa® water	Fresenius KABI, Bad Homburg (Germany)
β-mercaptoethanol (*puriss*.)	Sigma-Aldrich, Steinheim (Germany)
Chloroform (*puriss*.)	Merck, Darmstadt (Germany)
Calf Intestinal Alkaline Phosphotase (CIP)	New England Biolabs, Ipswich (MA, USA)
Dako Real Antibody Diluent	Dako, Hamburg (Germany)
Dimethyl sulfoxide (DMSO; *puriss*.)	Sigma-Aldrich, Steinheim (Germany)
Dulbecco's modified Eagle's serum (DMEM) + GlutaMAX™-I, 4.5 g/l D-glucose, pyruvate	Gibco, Darmstadt (Germany)
DMEM modified to 1500 mg/L sodium bicarbonate.	LGC Standards GmbH, Wesel (Germany)
dNTP Mix 10 mM	Fermentas, St. Leon-Rot (Germany)
dATP	Fermentas, St. Leon-Rot (Germany)
dCTP	Fermentas, St. Leon-Rot (Germany)
dTTP	Fermentas, St. Leon-Rot (Germany)
dGTP	Fermentas, St. Leon-Rot (Germany)
Dithiothreitol (DTT) 0.1 M (*p. A*.)	Invitrogen, Grand Island (NY, USA)
Eosin	Bio-Optica, Milano (Italy)
Ethanol (*p. A*.)	Merck, Darmstadt (Germany)
Ethidium bromide (*p. S*.)	Sigma-Aldrich, Steinheim (Germany)
F12 Kaighn's Modification	Gibco, Darmstadt (Germany)
Fetal bovine serum	Gibco, Darmstadt (Germany)
First strand buffer 5x	Invitrogen, Grand Island (NY, USA)
Flat Bottom Immobiliser	Genisphere Hatfield (PA, USA)
Gel loading dye, blue 6x	New England Biolabs, Ipswich (MA, USA)
Glycerol (*puriss*.)	Sigma-Aldrich, Steinheim (Germany)
Glycogen (*puriss*.)	Roche Diagnostics, Mannheim (Germany)
Haematoxilin	Bio-Optica, Milano (Italy)
HCl 5 M (*puriss*.)	NeoLab, Heidelberg (Germany)
Horse Serum	Gibco, Darmstadt (Germany)

Table 3 continued: Reagents.

Product	Company
Instant haematoxylin	Standon, Pittsbrug (PA, USA)
Isopropanol (*puriss*.)	Merck, Darmstadt (Germany)
Lysogeny Broth (LB) broth base	Invitrogen, Grand Island (NY, USA)
Lipofectamine 2000	Invitrogen, Grand Island (NY, USA)
Methanol (*p. A.*)	Merck, Darmstadt (Germany)
Magnesium Chloride (50 mM)	Invitrogen, Grand Island (NY, USA)
*mir*Vana™ miRNA-124-3p Inhibitor	Life Technologies, Carlsbad (CA, USA)
*mir*Vana™ miRNA-29a-3p Inhibitor	Life Technologies, Carlsbad (CA, USA)
*mir*Vana™ miRNA-29b-3p Inhibitor	Life Technologies, Carlsbad (CA, USA)
*mir*Vana™ miRNA-29c-3p Inhibitor	Life Technologies, Carlsbad (CA, USA)
*mir*Vana™ miRNA Inhibitor Negative Control #1	Life Technologies, Carlsbad (CA, USA)
NEBuffer	New England Biolabs, Ipswich (MA, USA)
Opti-MEM® Reduced Serum Medium	Invitrogen, Grand Island (NY, USA)
Paraformaldehyde (PFA; *puriss.*)	Merck, Darmstadt (Germany)
Phosphate buffered saline (PBS) powder	Sigma-Aldrich, St. Louis (MO, USA)
Penicillin-Streptomycin, liquid	Invitrogen, Grand Island (NY, USA)
Phenol Red	Sigma-Aldrich, Steinheim (Germany)
*Pme*I Restriction Enzyme	New England Biolabs, Ipswich (MA, USA)
Reverse transcriptase SuperScript® II	Invitrogen, Grand Island (NY, USA)
RNAlater RNA Stabilization Agent	Qiagen, Hilden (Germany)
RNase inhibitor RNaseOUT™	Invitrogen, Grand Island (NY, USA)
SOC Medium	Invitrogen, Grand Island (NY, USA)
Sodium acetate (*p. A.*)	Merck, Darmstadt (Germany)
Sodium citrate (*p. A.*)	Merck, Darmstadt (Germany)
Streptavidin-horseradish peroxidase (HRP)	Thermo Fisher Sci., Waltham (MA, USA)
2x SYBR Green PCR master mix	Exiqon, Vedbaek (Denmark)
T4 Ligase	New England Biolabs, Ipswich (MA, USA)
T4 Ligase Buffer	New England Biolabs, Ipswich (MA, USA)
TaqMan® miRNA Assays	Applied Biosystems, Darmstadt (Germany)
TaqMan® mRNA assays	Applied Biosystems, Darmstadt (Germany)
TaqMan® universal PCR master mix 2x	Applied Biosystems, Darmstadt (Germany)

Table 3 continued: Reagents.

Product	Company
Taq Polymerase	Fermentas, St. Leon-Rot (Germany)
Tris/Borate/EDTA (TBE) 10x	Bio-Rad Lab., Hercules (CA, USA)
Tetramethylethylenediamine (TEMED)	Amresco, Solon (OH, USA)
3,3',5,5'-Tetramethylbenzidine (TMB) stop solution	Thermo Fisher Sci., Waltham (MA, USA)
TMB substrate solution	Thermo Fisher Sci., Waltham (MA, USA)
Toluodine Blue	Merck, Darmstadt (Germany)
Tris/HCl	Carl Roth, Karlsruhe (Germany)
Triton X-100	Sigma-Aldrich, Steinheim (Germany)
Trizma® base (puriss.)	Sigma-Aldrich, Steinheim (Germany)
TRIzol® reagent	Invitrogen, Grand Island (NY, USA)
Trypan blue solution 0.4 %	Sigma-Aldrich, St. Luis (MO, USA)
Trypsin, 0.05% with EDTA	Gibco, Darmstadt (Germany)
Tween 20	Carl Roth, Karlsruhe (Germany)
*Xho*I Restriction Enzyme	New England Biolabs, Ipswich (MA, USA)
Yeast extract	Carl Roth, Karlsruhe (Germany)

Table 4: Antibodies.

Product	Dilution	Weight	Host	Company	Catalog number (Lot)
anti-Calcitonin	1:200	3kDa	rabbit	DCS, Hamburg (Germany)	CI670R06 (Lot B397)
anti-p27	1:300	27 kDa	rabbit	BD Bioscience, Heidelberg (Germany)	610241 (Lot 35156)

Table 5: Buffers and Solutions.

Agarose	1 % (w/v) agarose in 1x TBE boil until dissolved, cool to approximately 60 °C add 0.005 % ethidium bromide
Citrate buffer pH 6.0	1.8 mM citric acid 8.2 mM Na citrate $2H_2O$ adjusted to pH 6.0 with HCl

Table 5 continued: Buffers and Solutions.

Hydrogen Peroxide	3% (v/v) in H_2O
LB Medium (for 1 l)	10 g tryptone 5 g yeast extract 10 g NaCl
PFA pH 7.4	2 % (w/v) in PBS 15 µl phenol red adjust pH to 7.4 with HCl
PBS pH 7.4	137 mM NaCl 2.7 mM KCl 10 mM Na_2HPO_4 2 mM KH_2PO_4 adjusted to pH 7.4 with HCl
Polymerase chain reaction (PCR) buffer 10x (50 ml)	3 g sucrose 100 µl dATP (100 mM) 100 µl dCTP (100 mM) 100 µl dTTP (100 mM) 100 µl dGTP (100 mM) 5 ml 10x buffer 1.5 ml $MgCl_2$ 20 µl Cresol red (100 µg/ml) add water to 50 ml
TBE pH 8.6	89 mM Tris/HCl 89 mM Boric Acid 2 mM EDTA adjusted to pH 8.6 with HCl
Tris buffered saline (TBS) pH 7.4	50 mM Tris/HCl 150 mM NaCl adjusted to pH 7.4 with HCl

Table 5 continued: Buffers and Solutions.

	0.5 M Tris/HCl
TBS-T pH 7.6	1.5 M NaCl
	0.05% (v/v) Tween 20
	adjust to pH 7.6 with HCL
Toluidine blue 2%	2% (w/v) in 50 ml Methanol

Table 6: Bacteria.

Product	Company
One Shot® TOP10 *E. coli* competent cells	Invitrogen, Grand Island (NY, USA)

Table 7: Vector

Product	Company
pmirGLO Dual-Luciferase miRNA Target Expression Vector	Promega, Mannheim (Germany)

Table 8: Cell lines.

Cell Line	Company	Description
TT cell line	Banca Biologica e Cell Factory, Genoa (Italy)	Human cell lines isolated from a hereditary MTC patient with mutant RET^{C634R}
6-23 MTC cell line	ATCC LGC Standards GmbH, Wesel (Germany)	Rat cell lines isolated from a rat thyroid tumour with wtRET

Table 9: Commercially Available Kits.

Product	Company
Dual Luciferase reporter assay system	Promega, Mannheim (Germany)
flashtag Biotin HSR RNA labelling Kit	Genisphere, Hatfield (PA, USA)
High-Capacity cDNA Archive Kit	Applied Biosystems, Darmstadt (Germany)
HistoMark Biotin Streptavidin–HRP System	KPL, Wedel (Germany)
KPL HistoMark DAB substrate Kit	KPL, Wedel (Germany)
Miniprep Kit QIAprep® Spin (50)	Qiagen, Hilden (Germany)

Table 9 continued: Commercially Available Kits.

Product	Company
miRCURY LNA Universal RT microRNA PCR System	Exiqon, Vedbaek (Denmark)
miRNeasy Micro Kit	Qiagen, Hilden (Germany)
QIAquick Gel Extraction Kit	Qiagen, Hilden (Germany)
QIAprep Spin Miniprep Kit	Qiagen, Hilden (Germany
MycoAlert™ Plus Mycoplasma Detection Kit	Lonza, Basel (Switzerland)
Viromer Blue transfection system	Lipocalyx, Halle (Germany)

Table 10: Standards.

Product	Company
DNA Molecular Weight Marker VIII (19-1114 bp)	Roche Diagnostics, Mannheim (Germany)

Table 11: Primer Sequences. Restriction sites for *Pme*I (red) and *Xho*I (blue) are indicated.

Designation	Sequence	Melting Temperature
MAPK14-fw	5´ATGGTTTAAACAAGGCCTTTTCACGGGAACT-3´	51.8 °C
MAPK14-rev	5´ATGCTCGAGGTCTTCACTGGCAAACCTGC-3´	53.8 °C
RAB27A-fw-1	5´ATGGTTTAAACGCCATAGCACTCGCAGAGAA-3´	53.8 °C
RAB27A-rev-1	5´ATGCTCGAGCTCGGCATAAGCACCAGCTA-3´	53.8 °C
RAB27A-fw-2	5´ATGGTTTAAACTTGTGGTGGCAAATGTTTGGT-3´	50.5 °C
RAB27A-rev-2	5´ATGCTCGAGTGGCACATGGTTCACTGAAGA-3	52.4 °C
SPHK1-fw	5´ATGGTTTAAACGAGAAGTATCGGCGTCTGGG-3´	55.9 °C
SPHK1-rev	5´ATGCTCGAGTTGGATTTGGTTCGTGGGGT-3´	51.8 °C

Table 12: Taqman® microRNA assays for quantitative miRNA RT-PCR. Taqman® microRNA assays consisting of a primer specific for a specific miRNA and corresponding quantitative RT-PCR probe.

Assay Name	miRNA	Species	Reporter	Assay ID
hsa-miR-10a	hsa-miR-10a-3p	human	FAM	000387
hsa-miR-26b	hsa-miR-26b-5p	human	FAM	000407
hsa-miR-29a	hsa-miR-29a-3p	human	FAM	002112
hsa-miR-29b	hsa-miR-29b-3p	human	FAM	000413
hsa-miR-29c	hsa-miR-29c-3p	human	FAM	000587
hsa-miR-124	hsa-miR-124-3p	human	FAM	001182
hsa-miR-148b	hsa-miR-148b-3p	human	FAM	000470
hsa-miR-183	hsa-miR-183-5p	human	FAM	002269
hsa-miR-192	hsa-miR-192-5p	human	FAM	000491
hsa-miR-335	hsa-miR-335-5p	human	FAM	000546
hsa-miR-584a	hsa-miR-584a-3p	human	FAM	001538
hsa-miR-1281	hsa-miR-1281	human	FAM	241042_mat
U6	U6 snRNA	human	FAM	001973

Table 13: Quantitative RT-PCR probes.

Assay Name	Species	Reporter	Assay ID
RAB27A	human	FAM	Hs00608302_m1
SPHK1	human	FAM	Hs01116530_g1
TATA box binding protein (TBP)	human	FAM	Hs99999910_m1

Table 14: Software.

Product	Company
Carmaweb	Institute for Genomics and Bioinformatics, Graz University of Technology, Graz (Austria)
Ingenuity Pathway Analysis	IPA®,QIAGEN, Redwood City (CA,USA)
Microsoft Excel	Microsoft Deutschland, Unterschleißheim (Germany)
Microsoft PowerPoint	Microsoft Deutschland, Unterschleißheim (Germany)

Table 14 continued: Software.

Product	Company
Microsoft Word	Microsoft Deutschland, Unterschleißheim (Germany)
miRanda	Memorial Sloan-Kettering Cancer Centre, New York (NY, USA)
miRNA QC tool (version 1.0.33.0)	Affymetrix, High Wycombe (UK)
PicTar	Max Delbruck Centrum, Berlin (Germany)
RQ manager software (version 1.2.1)	Applied Biosystems, Darmstadt (Germany)
SDS Software (version 2.4.2)	Applied Biosystems, Darmstadt (Germany)
SigmaPlot	Systat Software Inc., San Jose (CA, USA)
Statistical Programming Environment R	R Foundation for Statistical Computing, Vienna (Austria)
TargetScan	Whitehead Institute of Biomedical Research, Cambridge (MA, USA)
Venny	BioinfoGP, Madrid (Spain)

3.2 Methods

3.2.1 Animal maintenance and tissue collection

Animals were maintained according to animal husbandry regulations of Helmholtz Zentrum München, Munich, Germany. Animals were subjected to complete necropsy either at the first indication of morbidity or at defined ages to analyse age-related tumour progression.

Thyroid tissues from 9 month-old homozygous, 9 month-old heterozygous and 18 month-old heterozygous mutant rats were collected, snap-frozen in liquid nitrogen and stored at -80 °C until used.

3.2.2 Histopathological evaluation of thyroid tumours

Cryosections of rat thyroid tissues were histologically evaluated before a macrodissection was conducted in order to isolate tissue only from the tumour area. For this purpose rat thyroid tissues were cut using a cryotomes into sections and a H&E staining was conducted. For this purpose, the cyrosections were air dried for 5 min at room temperature followed by the fixation of the tissues with acetone for 5 min at room temperature. The staining of the nuclei was achieved by immersing the tissue slides into haematoxylin for 4 min at room temperature and any excess haematoxylin was removed by washing the slides in running water for 5 min. The staining of the nuclei should fade from violet to blue. The tissue slides were counterstained using eosin for 20 sec and subsequently washed with running water for an additional 5 min. Finally, the stained tissue slides were dehydrated using an ascending alcohol series (50%, 70%, 96% and 100% for 5 min each) and treated with xylol for 2x 10 min. The slides were sealed with cover slips and microscopically evaluated using the System Microscope BX43.

3.2.3 Immunohistochemistry of thyroid tumours

In order to investigate protein expression of MTC tumours *in situ*, an immunohistochemistry analysis was performed. For this purpose, formalin-fixed and paraffin embedded (FFPE) tissues were dewaxed using xylol and rehydrated via a descending alcohol series (100%, 96%, 70%, 50% and distilled water). In addition, fresh frozen section were air dried and fixed as described in section 3.2.2. Epitope retrieval was conducted using microwave cooking in 0.01 M citrate buffer (pH 6) at 1.000 W for 30 min. Non-specific epitopes were blocked using 5% normal goat serum for 30 min at room temperature. The primary antibody was applied to the tissue sections according to the conditions listed in Table 4. The tissue sections were thoroughly washed in TBS buffer and specific antibody binding was made visible with the

HistoMark Biotin Streptavidin–HRP System. For this purpose, the biotinylated secondary antibody was applied for 45 min at room temperature. After repeated thorough washing in TBS, streptavidin-horseradish peroxidase was added for 30 min at room temperature. Following a final washing step, Diaminobenzidine (DAB) was added, making the antibody specific binding visible. The colour reaction was quenched with tap water. A haematoxylin counterstain was applied, as described previously in section 3.2.2.

3.2.4 Collection of human MTC tumours

Our cooperation partner Prof Dr Sergio Pereira De Almeida Toledo of the Hospital das Clínicas da Faculdade de Medicina da Universidade de São Paulo, Endocrine Genetics Unit, Sao Paulo, Brazil, has the largest cohort of snap frozen MEN2 related MTC tumours in Brazil. Fresh frozen tissues from MTC patients were also provided by Prof Dr Christine Spitzweg, Department of Internal Medicine II of the Ludwigs-Maximillians Universität, Munich, Germany, and Dr Thomas Negele of the Klinikum Martha Maria, Munich, Germany. We have obtained a total of 34 primary MTC tumours of which 15 were identified as hereditary of and 19 of sporadic origin. 6 of the hereditary cases were male, while 9 were female and 9 of the sporadic MTC patients were male and 10 female.

3.2.5 RNA isolation

Thyroid tumours from both rats and humanswere pathologically confirmed by Dr Frauke Neff of the Institute of Pathology at the Helmholtz Zentrum München, Munich, Germany. Following the histologically evaluation and examination by immunostaining the areas of comprising the tumour were then isolated by macrodissection. RNA was extracted using the miRNeasy micro Kit according to the manufacturer's protocol.

3.2.6 Establishing miRNA profiles of rat thyroid tumours

A high-throughput PCR analysis was performed using the mirCURY LNA universal RT miRNA Ready-to-Use PCR Mouse and Rat 1, V2.R plates. Of the 384 well in the PCR plate, 373 wells contain different primer sets for 373 miRNAs of known sequence present in miR-Base version 16. In addition, 11 wells were used for the following controls: an empty well, three inter-plate calibrators, a primer pair specific to synthetic oligo-RNA template in the complementary DNA (cDNA) synthesis master mix and wells for the reference genes miR-423-3p, miR-103-3p and miR-191a-5p, as well as the small nucleolar RNAs U6, RNU5G and RNU1A1 (Pai *et al.* 2014).

The cDNA synthesis of extracted rat RNA was performed using the miRCURY LNA Universal RT microRNA PCR system according to the manufacturer's instructions. In brief, the RNA was tailed with a poly(A) sequence at their 3'-end and then reverse transcribed into cDNA using a universal poly(T) primer with a 3'-end degenerate anchor and a 5' end universal tag.

Table 15: Reaction setup for miRCURY LNA Universal RT microRNA PCR.

Reagent	Volume
5x Reaction buffer	4 µl
Nuclease-free water	9 µl
Enzyme Mix	2 µl
Synthetic RNA spike ins	1 µl
Template total RNA (5 ng/µl)	4 µl
Total Volume	20 µl

The reaction was set up according to Table 15, mixed very gently by pipetting up and down and spun down gently using a microfuge (microcentri, ficher scientific). The reaction mixture was incubated at 42 °C for 1 h. The reverse transcriptase was heat-inactivated by incubating the reaction mixture at 95 °C for 5 min.

The cDNA products of the MENX rat RNA was subsequently diluted 125 fold and transferred to the Ready-to-use microRNA PCR Rat Panel I containing 200 lyophilised rat specific LNA enhanced miRNA primers. Quantification was achieved with SYBR green based quantitative real time polymerase chain reaction (RT-PCR). The reagents to set up the amplification of the miRNAs RT-PCR product are shown in Table 16.

Table 16: Reagents for the Ready-to-use microRNA PCR Rat Panel I.

Reagent	Volume
2x SYBR Green PCR master mix	2000 µl
cDNA	20 µl
H_2O	1980 µl
Total Volume	4000 µl

The cDNA mix was gently mixed and briefly spun down. 10 µl of the reaction mix was aliquoted into each well of the Ready-to-use microRNA PCR Rat Panel. This corresponds to 0.05 ng of total RNA starting material per PCR reaction. The plates were sealed with optical sealing and the plate was briefly spun down for 1 min (Centrifuge PerfectSpin P).

Table 17: Quantitative RT-PCR cycle conditions for Ready-to-use microRNA PCR Rat Panel I.

Process Step	Temperature	Time
Polymerase activation	95 °C	10 min
Denaturation	95 °C	10 sec
Amplification	60 °C	1 min

The quantitative RT-PCRs were run on a 7900HT thermocycler using the thermal-cycling parameters recommended by Exiqon as shown in Table 17 followed by a melting curve analysis. A total of 40 cycles between steps 2 and 3 were conducted. Raw Ct values were calculated as recommended by Exiqon using the software SDS (version 2.4.2) with manual settings for threshold and baseline subtraction using cycles 1-14. All data was normalised with the corresponding RNU1A1 non-coding RNA transcription level using a comparative delta Ct method (Livak *et al.* 2001, Pfaffl 2001).

3.2.7 Establishing miRNA profiles of human MTC

The extracted total RNA from human MTC samples requires to be labelled, in order to allow detection after hybridisation to the miRNA array. RNAs isolated from tissue sections were labelled with the *FlashTag* Biotin HSR RNA labelling kit according to the manufacturer's protocol. The labelling reaction requires a minimum of 250 ng of total RNA isolated from tissue sections.

Initially the RNA is elongated with a poly(A) tail using a poly(A) polymerase, which acts as a spacer for ligating the biotinylated signal molecule. The signal molecule is composed of single and doubled stranded DNAs arranged to a branched structure. Conjugated to the signalling molecules are biotin labels. Detection is achieved via streptavidin tagged luminescent dyes that bind to the biotin conjugated signal molecules (Nilsen *et al.* 1997, Stears *et al.* 2000).

A total of 250 ng sample RNA was used and volumes were adjusted to 8 µl with nuclease-free water. 2 µl of the RNA spike control oligos were added to the input RNA. For the addition of the poly(A) tail, the reagents were set up as shown in Table 18. The reactions mix was incubated for 15 min at 37 °C.

Table 18: Polyadenylation Reaction setup.

Reagent	Volume
10x Reaction buffer	1.5 µl
25 mM $MnCl_2$	1.5 µl
ATP Mix	1 µl
Poly(A) Polymerase	1 µl
RNA (250 ng)	8 µl
RNA Spike Control Oligos	2 µl
Total Volume	15 µl

After the addition of the poly(A) tail, the signal molecules were ligated to the RNAs. For this purpose, the *FlashTag* Biotin HSR ligation reaction was set up as shown in Table 19. Reactants were gently mixed, microfuged (microcentri, ficher scientific) and incubated at room temperature for 25 min. The reaction was stopped by the addition of 2.5 µl of HSR stop solution. 21.5 µl of the reaction mixture was used for hybridisation with GeneChip miRNA 1.0 arrays from Affymetrix.

Table 19: Reaction setup for *FlashTag* Biotin HSR Ligation.

Reagent	Volume
Poly (A) tailed RNA	15 µl
5x *FlashTag* Biotin HSR Ligation mix	4 µl
T4 DNA Ligase	2 µl
Total Volume	21 µl

The RNA microarray study was conducted using the GeneChip miRNA 1.0 array from Affymetrix. The hybridisation and the scanning of the microarrays were conducted in cooperation with Dr Martin Irmler at the Institute of Experimental Genetics, Helmholtz Zentrum München, Munich, Germany. The experimental procedure was carried out according to the Affymetrix GeneChip miRNA 1.0 array manual.

3.2.8 Validation of miRNA profiles with quantitative RT-PCR

Validation of mature miRNA expression levels in thyroid tumours was performed by quantitative RT-PCR using TaqMan® microRNA Assays. Briefly, 10 ng total RNA was reverse transcribed with specific miRNA primers (Table 12) using the High-Capacity cDNA Archive kit.

Table 20: Reverse Transcription reaction setup for quantitative miRNA RT-PCR.

Reagent	Volume
dNTPs	0.15 µl
10x Buffer	1.5 µl
Enzyme	1 µl
RNasin	0.19 µl
Sample RNA (5 ng/µl)	2 µl
Specific miRNA Primer (Table 12)	3 µl
H_2O	7.16 µl
Total Volume	15 µl

The reagents for the reverse transcription of RNA to conduct a quantitative miRNA RT-PCR using specific miRNA Taqman® primers was set up according to Table 20. The miRNA quantitative RT-PCR mix was reverse transcribed using the program shown in Table 21 on a thermal cycler.

Table 21: Thermal cycler program for quantitative miRNA RT-PCR.

Time	Temperature
30 min	16 °C
30 min	42 °C
5 min	85 °C
∞	4 °C

For the quantification, the reaction mix was set up as shown in Table 22 and aliquoted into 96 well plates and 2 µl of the miRNA RT-PCR product was added to each well. All quantitative RT-PCRs were performed in triplicates.

Table 22: Reagents for the quantitative miRNA RT-PCR amplification.

Reagent	Volume
2x Taqman® master mix	5 µl
H_2O	2.5 µl
miRNA specific Assay	0.5 µl
Total Volume	8 µl

The plates were sealed with optical sealing and the plate was briefly spun down for 1 min (Centrifuge PerfectSpin P).The quantitative RT-PCRs were run on a 7300HT thermocycler using the thermal-cycling parameters shown in Table 23.

Table 23: Quantitative RT-PCR cycle conditions for miRNA and mRNA amplification.

Process Step	Temperature	Time
Initiation	50 °C	2 min
Polymerase activation	95 °C	10 min
Denaturation	95 °C	15 sec
Amplification	60 °C	1 min

A total of 40 cycles between steps 2 and 3 were conducted. Raw Ct values were calculated using the software SDS (version 2.4.2) with manual settings for threshold and baseline substraction using cycles 1-14. All data was normalised with the corresponding U6 snRNA non-coding RNA transcription level using a comparative delta Ct method (Livak *et al.* 2001, Pfaffl 2001).

3.2.9 Cell culture

The human MTC cell line TT was maintained in F12 Kaighn's Modification containing 15% fetal bovine serum and 1% penicillin/streptomycin at 37 °C in a humidified atmosphere of 5% CO_2 (Spitzweg *et al.* 2007).

The 6-23 cells were cultured in DMEM, 4 mm l-glutamine, and 2.1 g/l sodium bicarbonate supplemented with 15% horse serum in a humidified atmosphere containing at 37 °C and 5% CO_2 (Zeytinoglu *et al.* 1980, Zeytinoglu *et al.* 1980).

Cells were cultured in 75 cm^2 flasks and were split after 7 days to the required concentrations. For this purpose, the cell medium was removed and the cells were washed with 6 ml 1x PBS. Subsequently, 2 ml Trypsin was added and incubated at 37 °C for 5 min. The detached cells were resuspended in 9 ml complete medium and transferred to new flasks at the appropriate concentration.

In order to freeze cells for conservation, cells with high confluence were trypsinised, suspended in complete medium and centrifuged at 1,000 RPM (Centrifuge Rotanta460 R, Rotor: 5623 15 ml, 50 ml) for 5 min at 5 °C. The medium was aspirated and discarded. The cell pellet was re-suspended in 90% serum and 10% DMSO and 1 ml aliquots were transferred to cryovials for final long-term storage in liquid nitrogen.

To thaw cells, cells were retrieved from liquid nitrogen and thawed in a water bath at 37 °C. The thawed cells were transferred to a 15 ml conical tube and 10 ml of pre-warmed medium was added. The cells were spun down at 1,000 RPM (Centrifuge Rotanta460 R, Rotor: 5623 15 ml, 50 ml) for 5 min at 5 °C. The supernatant was aspirated and discarded to ensure the

removal of DMSO. The cells were resuspended in full medium and transferred to a culture flask.

In order to determine any contaminations in the cell lines, cells were tested for mycoplasma using the MycoAlert™ Plus Mycoplasma Detection Kit according to the manufacturer's protocol. Detection occurs through measuring ATP levels generated by mycoplasmal enzymes in a sample both before and after the addition of the MycoAlert™ PLUS Substrate, thereby establishing mycoplasma contamination.

3.2.10 Transfection of MTC cell lines with specific inhibitors of miRNA expression

According to the manufacturer, the *mir*Vana™ miRNA inhibitors are small chemically modified single-stranded RNA molecules designed to specifically bind and inhibit endogenous miRNA molecules. This enables miRNA functional analysis by downregulation of miRNA activity. The *mir*Vana™ miRNA Inhibitor Negative Control #1 is intended for use as a negative control for experiments using *mir*Vana™ miRNA Inhibitors.

Cells were seeded at the appropriate concentrations and incubated overnight at 37 °C and 5% CO_2. TT and 6-23 MTC cell lines were transfected with the Viromer Blue transfection system according to the manufacturer's protocol. For this purpose, specific miRNA expression inhibitors or unspecific control miRNA inhibitor were diluted to 11 µM using Buffer F (pH 7.2). 11 µl of the Viromer Blue transfection agent was diluted with 989 µl of Buffer F. For complexation, 11 µl of the diluted miRNA expression inhibitor was combined with 99 µl of diluted Viromer Blue in Buffer F. The mixture was carefully pipetted up and down and incubated for 20 min to allow complexation, giving a final concentration of 1.1 µM. Different transfer volumes for cell culture plate formats were added to the seeded cells, resulting in a final miRNA concentration of 100 nM per experiment. The inhibition of miRNA expression was validated 48 h post-transfection with quantitative RT-PCR as described in section 3.2.8.

3.2.11 Cell viability assay

The MTT assay measures cell viability, where the tetrazolium dye MTT is converted by NADH-dependent oxidoreductase enzymes to its formazan salt. The MTT assay is therefore dependent on cellular metabolic activity. In cells with low metabolic activity, a decreased reduction of MTT is observed, whereas cells with high metabolic activity, an elevated reduction of MTT is observed (Mosmann 1983, Berridge *et al.* 1993, Berridge *et al.* 2005).

MTT was dissolved in PBS at 5 mg/ml and filtered to sterilise and remove insoluble any residue (Mosmann 1983). Cells were plated onto 96 well plates at a concentration of 15,000

cells per well in full medium in replicates of five. The cells were grown overnight in a humidified atmosphere at 37 °C and 5% CO_2. Cells were then transfected with either the unspecific control miRNA inhibitor or specific miRNA expression inhibitors as described in section 3.2.10. Cells were incubated for a further 48 h in a humidified atmosphere at 37 °C and 5% CO_2. MTT stock solution (10 µl per 100 µl medium) was added to all wells and plates were incubated at 37 °C and 5% CO_2 for 4 h. After the removal of the medium, cells were lysed through the addition of 150 µl of 0.04 M HCl in isopropanol per well. The lysates were mixed for 15 min and any undissolved crystals were dissolved by pipetting up and down. The plates were read on an ELISA microplate reader model 680 using a detection wavelength of 560 nm, detecting the formazan salt and a reference wavelength of 655 nm, set to detect the background. The cell viability was assessed by subtracting the reference from detection values. Any change in cell viability was determined as the fold change between cells transfected with miRNA specific inhibitors and cells transfected with the unspecific control miRNA inhibitor. A total of three independent experiments were performed.

3.2.12 Migration assay

The migration assay employing the boyden chamber quantifies migrating cells exposed to different nutritional concentrations. The chamber contains two compartments separated by a porous filter through which the cells migrate towards higher nutritional concentrations (Toetsch *et al.* 2009). Our experimental setup employs serum to create a chemotactic gradient, where serum was placed in the lower compartment.

Cells were plated on 6 well plates at a concentration of 300,000 cells per well and incubated overnight at 37 °C and 5% CO_2. Cells were then transfected with either an unspecific control miRNAs inhibitor or miRNA inhibitors blocking the endogenous expression of specific miRNAs as described in section 3.2.10. The transfected cells were further incubated at 37 °C and 5% CO_2 for 48 h.

Cells were harvested with 300 µl Trypsin, incubated at 37 °C for 5 min and neutralised with medium containing 1% serum. Cells were centrifuged at 1,000 RPM (Centrifuge Rotanta460 R, Rotor: 5623 15 ml, 50 ml) for 5 min and the supernatant was aspirated. The resulting cell pellet was resuspended with 3 ml serum free medium. Cells were counted and suspensions in 750 µl serum-free medium containing 60,000 cells were prepared and transferred to PET track-etched membrane (8 µm pore size) cell culture inserts. Meanwhile, 750 µl of full medium was added to the bottom of 24 well culture plates. The cell culture inserts containing the cell suspensions were then transferred to the 24 well culture plates containing the full medium and incubated for 48 h at 37 °C and 5% CO_2. After incubation, cells on the lower

surface of the membrane were fixed with 2% PFA for 2 min at room temperature and stained with 2% toluidine blue for 10 min. Cells that did not migrate through the pores were mechanically removed by a cotton swab. The membranes were dried at 37 °C and mounted onto slides with mounting medium. The images of migrated cells were acquired by microscopy (System Microscope BX43) with a magnification of 200x. The number of migrated cells was counted from five randomly selected fields in a blind way (Qin *et al.* 2010). Any change in migration was determined as the fold change between cells transfected with specific miRNA inhibitor and cells transfected with the unspecific control miRNA inhibitor. A total of three independent experiments were performed.

3.2.13 Invasion assay

Native tissues are surrounded by the extracellular matrix (ECM), rich in fibrous materials such as collagen, laminin, and fibronectin and therefore presenting heterogeneous properties. Synthetic matrices are widely employed in studying the interaction between cells and the ECM. The invasion assay's experimental setup is similar to the migration assay with the addition of a synthesised matrix occluding the porous membranes. For cells to migrate along the nutritional gradient, the simulated ECM has to be degraded, thereby simulating the process of local invasion in cancer (Toetsch *et al.* 2009).

The invasion assay was conducted in the same manner as the migration assay described in section 3.2.12, with the exception of the substitution of Matrigel® invasion chambers (8 µm pore size) cell culture inserts with the PET track-etched membrane inserts. Before conducting the experiments, 500 µl of serum free medium was added to the thawed Matrigel® invasion chambers and incubated at 37 °C and 5% CO_2 for 2 h. The invasion assay was evaluated in the same manner as the migration assay, as described in section 3.2.12. A total of three independent experiments were performed.

3.2.14 Reverse transcription

In order to gain cDNA, a reverse transcription of template RNA was conducted. For this purpose, 0.25-1 mg of sample RNA was isolated from the sample tissues and volumes were adjusted to 10 µl with nuclease-free water. The template RNA was preincubated with 1 µl of random primers at room temperature for 10 min.

Table 24: Reverse transcription reaction setup.

Reagents	Volume
5x First strand buffer	4 µl
0.1 M DTT	2 µl
RNaseOUT	1 µl
SuperScript II reverse transcriptase	1 µl
10 mM dNTP mix	1 µl
Sample RNA pre-incubated with random primers	11 µl
Total Volume	20 µl

The reagents were set up according to Table 24, mixed gently, microfuged (microcentri, fischer scientific) and incubated at 42 °C for 1 h. The reaction was stopped by denaturing the reverse transcriptase at 95 °C for 5 min. The cDNA can be stored at -20 °C until further use.

3.2.15 PCR of target gene sequences

The target genes of miRNAs determined *in silico* require to be validated experimentally. The 3'-untranlated region (UTR) of selected target genes were cloned into the pmiRGLO vector containing dual luciferase reporter gene activity. Section 3.2.15-3.2.19 were conducted in cooperation with Simone Mörtl of the Institute of Radiation Biology, Helmholtz Zentrum München, Munich, Germany. Candidate gene cDNA sequences were obtained by PCR amplification of reverse transcribed TT cell mRNA using the protocol described in section 3.2.14. Primer sets indicated in Table 11 were designed to amplify the miR-124-3p binding site of the target gene, with flanking regions of 1,000 bp. *Pme*I and *Xho*I restriction enzyme sites were included to the 5' ends of the forward and reverse primers, respectively, in order to ligate the amplified DNA into the pmiRGLO vector.

Table 25: PCR reagents for cloning 3'-UTR Sequences.

Reagent	Volume
10x PCR buffer	20 µl
dNTPs (10 mM)	4 µl
Forward Primer (10 µM)	4 µl
Reverse Primer (10 µM)	4 µl
Taq Polymerase (5 units/µl)	1.6 µl
cDNA	8 µl
H_2O	158.4 µl
Total Volume	200 µl

The reagents for the PCR were set up according to Table 25, mixed and briefly microfuged (microcentri, ficher scientific). The PCR was conducted under the conditions listed in Table 26 with steps 2 and 4 cycled 40 times.

Table 26: PCR cycle conditions.

Process Step	Temperature	Time
Polymerase activation	95 °C	3 min
Denaturation	95 °C	45 sec
Annealing	see Table 11	45 sec
Elongation	72 °C	1:30 min
Final Elongation	72 °C	10 min

The PCR products were separated by gel electrophorese using a 2% agarose gel. The separated PCR products were then purified using the QIAquick Gel Extraction Kit according to the manufacturer's instructions.

3.2.16 Digestion with restriction enzymes

In order to insert cDNA sequences obtained by PCR amplification into the pmiRGLO Dual-Luciferase miRNA Target Expression Vector, the plasmid has to be linearised by restriction enzyme digestion with *Pme*I and *Xho*I.

Table 27: Reagents for the restriction enzyme of the plasmid.

Reagent	Volume
*Pme*I	5 µl
*Xho*I	5 µl
NEBuffer	10 µl
Plasmid DNA	1 µl
H_2O	79 µl
Total Volume	100 µl

In addition, the cDNA fragments containing the 3'-UTR sequences obtained by PCR were also digested with *Pme*I and *Xho*I restriction enzymes in order to ligate them into the fragments into the vector.

Table 28: Reagents for the restriction enzyme of the cDNA fragments

Reagent	Volume
*Pme*I	5 µl
*Xho*I	5 µl
NEBuffer	10 µl
cDNA Fragments	1 µl
H_2O	79 µl
Total Volume	100 µl

For digestion of the pmiRGLO vector and the cDNA fragments, reagents were set up according to Table 27 and Table 28, respectively, and incubated at 37 °C overnight.

The linearised pmiRGLO Vector and the DNA fragments containing the miRNA target sites were separated with 2% agarose gel electrophoresis followed by the purification using the QIAquick Gel Extraction Kit according to the manufacturer's instruction.

3.2.17 Desphosphorylation of digested pmiRGLO vector

In order to prevent self-ligation of the linearised pmiRGLO vector, the 5' ends of the cut vector were dephosphorylated using a CIP.

Table 29: Vector desphosphorylation reaction setup.

Reagent	Volume
Linearised pmiRGLO Vector (500 ng)	1 µl
CIP	0.2 µl
1x NEBuffer	80 µl
Total Volume	81.2 µl

Reagents were set up according to Table 29, mixed and briefly microfuged (microcentri, ficher scientific) and incubated at 37 °C for 1 h.

3.2.18 Ligation of target gene sequences with the pmiRGLO vector

The linearised CIP treated vector and the double stranded 3'-UTR fragments were covalently linked using the T4 DNA ligase. For this purpose, a 2:1 ratio between insert and vector was used.

Table 30: DNA ligation reaction setup.

Reagent	Volume
CIP treated Vector	1 µl
Insert	4 µl
T4 DNA Ligase	0.5 µl
T4 Ligation buffer	4 µl
H_2O	10.5 µl
Total Volume	20 µl

The reagents were set up according to Table 30 and incubated at 4 °C overnight. As control for the ligation, the ligation reaction was carried out without the insert. In addition, the ligation reaction was carried out with the plasmids not dephosphorylated as a control of the alkaline phosphatase reaction.

3.2.19 Transformation of competent bacterial cells with pmiRGLO constructs

10 µl of the products from the ligation reaction were used to transform 50 µl of chemical competent *Escherichia coli* (*E. coli*) cells, followed by an incubation on ice for 30 min. The bacteria were heat shocked at 42 °C for 1 min and immediately put back on ice for 2 min. The cells were incubated with 400 µl SOC-medium for 1.5 h at 37 °C. The cells were harvested by centrifugation at 4,000 RPM (Centrifuge Variofuge 3.0R, Rotor: #8074, inserts #8078 15 ml, 50 ml) for 5 min at room temperature. The supernatant was discarded. The cell pellet was re-suspended with 150 µl LB-medium and platted onto LB_{amp} agarose plates and cultivated overnight at 37 °C. Colonies were selected and used to inoculate LB_{amp} medium. The inoculated culture was incubated overnight at 37 °C and 150 RPM. Plasmid DNA was isolated through the QIAprep Spin Miniprep kit according to the manufacturer's instructions. The identity and integrity of all constructs was confirmed by DNA sequencing.

3.2.20 Luciferase reporter assay to identify miRNA targets

The pmiRGLO vector uses dual-luciferase technology, with *Firefly* luciferase (luc2) being the reporter used to quantify miRNA regulation of translation and *Renilla* luciferase (hRluc-neo) being the non-regulated internal control (Kraemer *et al.* 2013).

For the co-transfection of the reporter constructs and the miRNA inhibitors, cells were seeded into clear bottomed, white walled 96 well plates at a concentration of 5,000 cells per well in replicates of five. Cells were incubated overnight in a humidified atmosphere at 37 °C and 5% CO_2. Transfection of reporter constructs into TT cells was performed using

Lipofectamine 2000 according to the manufacturer's instructions. The miRNA inhibitor blocking the endogenous expression of miR-124-3p or the unspecific control miRNA inhibitor were transfected into TT cells as described in section 3.2.10. The specific miRNA inhibitor/ unspecific control miRNA inhibitor was transfected along with 0.2 µg of the pmirGLO Dual-Luciferase construct harbouring cDNA of putative miR-124-3p regulated targets. 48 h post transfection, cells were lysed with passive lysis buffer and the activities of *Firefly* luciferase and *Renilla* luciferase were measured using the Dual Luciferase Reporter Assay System. The ratio of *Firefly* luciferase and *Renilla* luciferase was expressed as normalised luciferase activity to compensate differences in transfection efficiencies. The relative luciferase activity was determined as the ratio between normalised luciferase activities of cells transfected with the specific miR-124-3p inhibitor and the unspecific control miRNA inhibitor (Kraemer *et al.* 2013). A total of three independent experiments were conducted.

3.2.21 Quantitative RT-PCR to determine mRNA expression levels

The expression of differentially expressed genes in MTC were analysed using quantitative RT-PCR. The cDNA was obtained by reverse transcription as described in section 3.2.14. The reagents for the quantitative RT-PCR were set up as follows using specific Taqman® probes listed in Table 13.

Table 31: Reagents for quantitative RT-PCR.

Reagent	Volume
2x Taqman® master mix	10 µl
H2O	5 µl
Taqman® Probe	1 µl
cDNA	4 µl
Total Volume	20 µl

The 20 µl reaction mix as shown in Table 31 was aliquoted into 96 well plates with samples being analysed as doublets. The quantitative RT-PCRs were run on a 7300HT thermocycler using the thermal-cycling parameters as shown in Table 23. A total of 40 cycles between steps 2 and 3 were conducted. All data was normalised with the corresponding TBP RNA transcription level using a comparative delta Ct method (Livak *et al.* 2001, Pfaffl 2001).

3.2.22 Statistical and bioinformatics analysis

High-throughput PCR analysis of rat thyroid tumours were normalised using the inter-plate-calibrator spike-in controls UniSP3. For this purpose the calibration factor was calculated as

the difference between the plate average and overall average for each plate. Each plate is subsequently calibrated by subtracting the calibration factor from all Ct values in the plate.

The normalised PCR plates as well as quantitative RT-PCR experiments for mRNA and miRNA were analysed using a comparative Ct method. The Ct value is defined as the as the cycle, where amplification of the cDNA is exponential. The first delta Ct (ΔCt) is the difference between the target miRNA of interest and the reference miRNA: $\Delta Ct = Ct_{\text{miRNA of interest}} - Ct_{\text{reference miRNA}}$. Delta delta Ct (ΔΔCt) is calculated by employing the equation: $\Delta Ct_{\text{sample population A}} - \Delta Ct_{\text{sample population B}}$. The normalised target miRNA expression level is then stated as $2^{-\Delta\Delta Ct}$ (Livak *et al.* 2001, Pfaffl 2001).

The resulting data set of the high-throughput PCR analysis was statistically evaluated through the use of the statistical environment R implemented in CARMAweb (https://carmaweb.genome.tugraz.at/carma/) (Rainer *et al.* 2006, R Development Core Team 2008). Similar to the statistical analysis of the miRNA arrays, Genewise testing for differential expression was done by employing the limma t-test and the Benjamini-Hochberg (BH) multiple testing correction. False discovery rate (FDR) multiple testing correction of p-values was applied (Benjamini *et al.* 1995). Heatmaps and cluster dendograms were generated with CARMAweb. All miRNAs were updated to the current designations as listed in miRBase 21.

Array data was processed with the miRNA QC tool (Version 1.0.33.0) using settings recommended by Affymetrix. Briefly, background was detected and removed by RMA global background correction, followed by quantile normalisation and summarisation using median polishing. Statistical analysis of the resulting data set was performed by utilising the statistical programming environment R implemented in CARMAweb as described above. Genewise testing for differential expression was done employing the limma t-test and the BH multiple testing correction. False discovery rate (FDR) multiple testing correction of p-values was applied (Benjamini *et al.* 1995). Heatmaps and cluster dendrograms were generated with CARMAweb. Array data was submitted to GEO and a link for referees was created. All miRNAs were updated to the current designations as listed in miRBase 21.

To obtain information about biological mechanisms, pathways and network relationships of the differentially expressed miRNAs the Ingenuity Pathway Analysis (IPA) was used (IPA®, Ingenuity Systems, http://www.Ingenuity.com). For this purpose, all the differentially expressed miRNAs and fold changes were imported into IPA. The IPA software is based on computational algorithms that analyse the functional connectivity of the miRNA target genes from information obtained within the IPA database (Mayburd *et al.* 2006, Kramer *et al.* 2014).

To determine the top biological functions associated with the observed miRNA expression profiles, an IPA Downstream Effects Analysis was performed, extracting the most drastic affected functions (BH-p-value 0.05). The right tailed exact test was used to determine the probability that association between a set of molecules and a function or pathway might be due to random chance (Kramer *et al.* 2014).

Putative miRNA targets were identified using PicTar (www.pictar.mbc-berlin.de), TargetScans (www.targetscan.org), miRanda (www.microRNA.org) and Ingenuity miRNA target filter (www.ingenuity.com). Putative target gene were analysed using IPA Downstream Effects Analysis as described above.

Data are presented as mean ±S.E.M unless stated otherwise and graphically interpreted with the SigmaPlot statistical software. Venn Diagrams were produced using VENNY (http://bioinfogp.cnb.csic.es/tools/venny/index.html) (Oliveros 2007). The results (raw data) were statistically analysed using the Student t test with SigmaPlot statistical software (***p≤0.001; **p≤0.01; *p≤0.05 were considered significant; # p>0.05 was considered not significant).

3.2.23 Ethic vote

The local ethic committees of the Ludwig Maximilian Universität München, Munich, Germany, and the Technische Universität München, Munich, Germany, approved the use of human material for analysis.

4 Results

4.1 Thyroid tumours of MENX rats

The deregulation of miRNAs is a frequent event observed in human cancers and therefore many investigations focussed on the suitability of miRNAs as markers for cancer diagnosis and prognosis (Croce 2009, Berindan-Neagoe *et al.* 2014). The miRNA profiling of MENX rat thyroid tumours will aid in assessing the potential role of miRNAs in MTC tumour generation and will give a better understanding of MTC tumourigenesis in MENX rats.

As described in section 1.7, MENX rats develop a phenotype overlapping human MEN1 and MEN2 tumour spectra and have a lifespan of approximately 9 months. The onset of MTC in homozygous mutant rats is noticeable at an age of 2 months, but fully progressed thyroid tumours develop towards the end of their life span. The prolonged life span of heterozygous mutant rats of over 18 months of age allows the investigation of thyroid tumour progression.

The major limitation in investigating the miRNA expression of MTCs in rats is the low number of C-cells within the normal thyroid gland, as described in section 1.7. Unfortunately, C-cells comprise only 1% of the thyroid's cell population and do not form a coherent tissue. Therefore, RNA isolation from individual C-cells of the thyroid glands of wild-type rats was not performed. As a consequence a comparison between C-cells of wild-type animals and tumours of mutant animals is not possible. The distribution of C-cells in healthy thyroid glands represents the main limitation in investigating MTC, as the tumour initiation and progression from healthy to transformed cells is not possible. Since only tumour tissues may be compared, we compared the miRNA expression of MTCs between age-matched homozygous and heterozygous mutant rats as well as the miRNA expression between tumours of a late stage of older heterozygous mutant animals with less progressed early stage MTC tumours of younger heterozygous mutant animals.

4.1.1 Profiling miRNA expression in MTC of homozygous MENX rats

The miRNA profiling of rat thyroid tumours was conducted using a quantitative RT-PCR approach in a 384 well plate format. The plates contain specific quantitative RT-PCR primers for more than 200 rat miRNAs, allowing the study of well characterised miRNAs.

Thyroid tissues were isolated and a comparison of the miRNA expression of thyroid tumours between 9 month-old homozygous and age-matched heterozygous mutant rats was conducted. Thyroid tumours of both genotypes were classified as carcinomas, with signs of local invasion. Thyroid tumours at similar histological classifications were thus collected from

homozygous and heterozygous mutant rats in order to determine the influence of the p27 levels on the miRNA expression signatures of MTC.

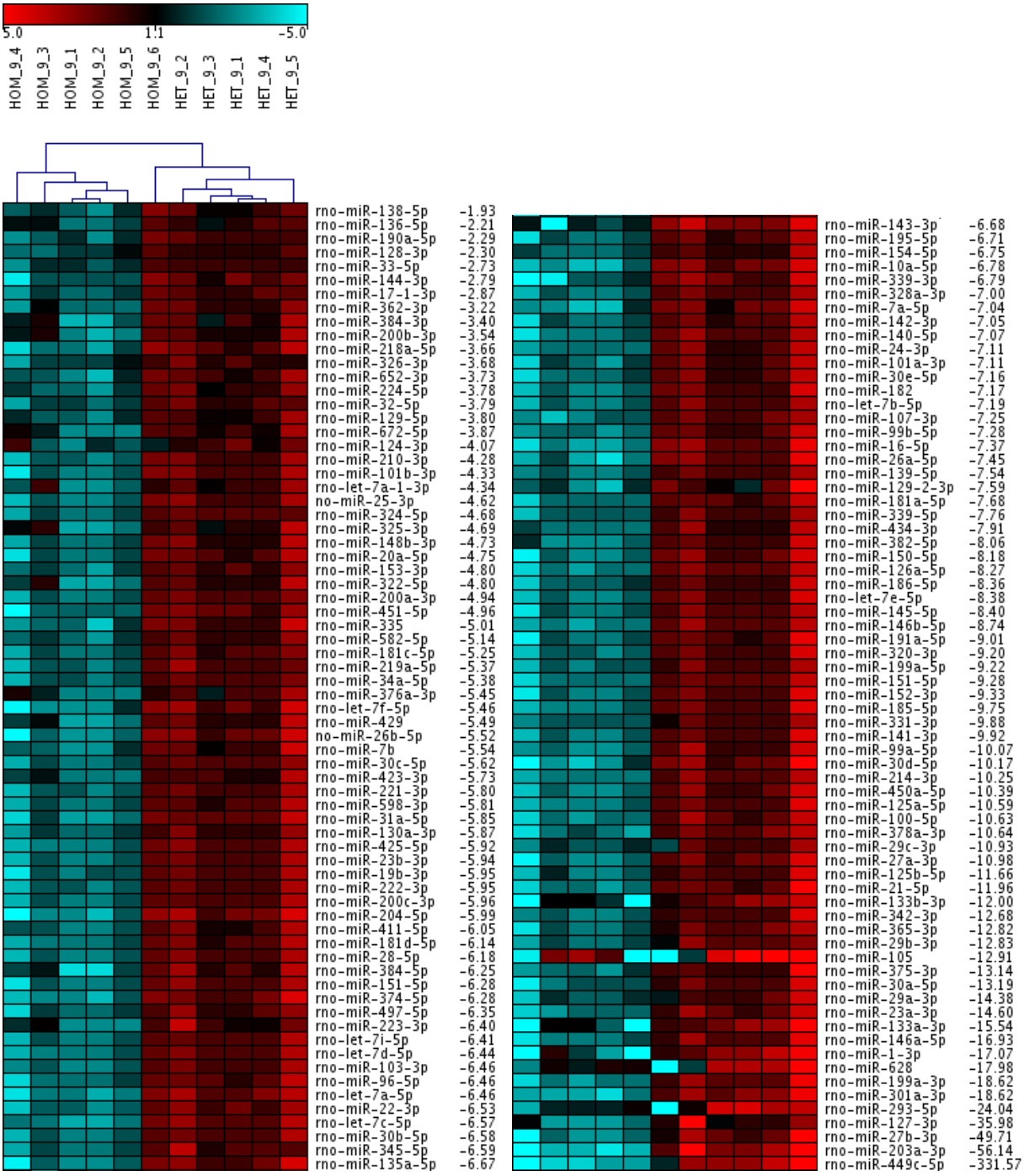

Figure 13: Unsupervised hierarchical clustering with the corresponding heat map of miRNA expression profile of 9 month-old homozygous and age-matched heterozygous mutant rats. The heat map was split to simplify legibility. The clustering at the top represents the similarity between miRNA expression profiles of rat samples. The corresponding heat map shows high expressed miRNAs in red and low expressed miRNAs in green. Undetected miRNAs were labelled in dark grey. All data was normalised to corresponding RNU1A1 transcription levels using a comparative delta CT method (Livak *et at*. 2001, Pfaffl 2001).

Table 32: Differentially expressed miRNAs in tumour of homozygous *versus* heterozygous mutant MENX rats. Differentially expressed miRNAs are shown with the corresponding fold changes.

miRNA	Fold Change	miRNA	Fold Change	miRNA	Fold Change	miRNA	Fold Change	miRNA	Fold Change
rno-miR-138-5p	-1,93	rno-miR-335	-5,01	rno-let-7i-5p	-6,41	rno-miR-181a-5p	-7,68	rno-miR-342-3p	-12,68
rno-miR-136-5p	-2,21	rno-miR-582-5p	-5,14	rno-let-7d-5p	-6,44	rno-miR-339-5p	-7,76	rno-miR-365-3p	-12,82
rno-miR-190a-5p	-2,29	rno-miR-181c-5p	-5,25	rno-miR-103-3p	-6,46	rno-miR-434-3p	-7,91	rno-miR-29b-3p	-12,83
rno-miR-128-3p	-2,30	rno-miR-219a-5p	-5,37	rno-miR-96-5p	-6,46	rno-miR-382-5p	-8,06	rno-miR-105	-12,91
rno-miR-33-5p	-2,73	rno-miR-34a-5p	-5,38	rno-let-7a-5p	-6,46	rno-miR-150-5p	-8,18	rno-miR-375-3p	-13,14
rno-miR-144-3p	-2,79	rno-miR-376a-3p	-5,45	rno-miR-22-3p	-6,53	rno-miR-126a-5p	-8,27	rno-miR-30a-5p	-13,19
rno-miR-17-1-3p	-2,87	rno-let-7f-5p	-5,46	rno-let-7c-5p	-6,57	rno-miR-186-5p	-8,36	rno-miR-29a-3p	-14,38
rno-miR-362-3p	-3,22	rno-miR-429	-5,49	rno-miR-30b-5p	-6,58	rno-let-7e-5p	-8,38	rno-miR-23a-3p	-14,60
rno-miR-384-3p	-3,40	no-miR-26b-5p	-5,52	rno-miR-345-5p	-6,59	rno-miR-145-5p	-8,40	rno-miR-133a-3p	-15,54
rno-miR-200b-3p	-3,54	rno-miR-7b	-5,54	rno-miR-135a-5p	-6,67	rno-miR-146b-5p	-8,74	rno-miR-146a-5p	-16,93
rno-miR-218a-5p	-3,66	rno-miR-30c-5p	-5,62	rno-miR-143-3p	-6,68	rno-miR-191a-5p	-9,01	rno-miR-1-3p	-17,07
rno-miR-326-3p	-3,68	rno-miR-423-3p	-5,73	rno-miR-195-5p	-6,71	rno-miR-320-3p	-9,20	rno-miR-628	-17,98
rno-miR-652-3p	-3,73	rno-miR-221-3p	-5,80	rno-miR-154-5p	-6,75	rno-miR-199a-5p	-9,22	rno-miR-199a-3p	-18,62
rno-miR-224-5p	-3,78	rno-miR-598-3p	-5,81	rno-miR-10a-5p	-6,78	rno-miR-151-5p	-9,28	rno-miR-301a-3p	-18,62
rno-miR-32-5p	-3,79	rno-miR-31a-5p	-5,85	rno-miR-339-3p	-6,79	rno-miR-152-3p	-9,33	rno-miR-293-5p	-24,04
rno-miR-129-5p	-3,80	rno-miR-130a-3p	-5,87	rno-miR-328a-3p	-7,00	rno-miR-185-5p	-9,75	rno-miR-127-3p	-35,98
rno-miR-672-5p	-3,87	rno-miR-425-5p	-5,92	rno-miR-7a-5p	-7,04	rno-miR-331-3p	-9,88	rno-miR-27b-3p	-49,71
rno-miR-124-3p	-4,07	rno-miR-23b-3p	-5,94	rno-miR-142-3p	-7,05	rno-miR-141-3p	-9,92	rno-miR-203a-3p	-56,14
rno-miR-210-3p	-4,28	rno-miR-19b-3p	-5,95	rno-miR-140-5p	-7,07	rno-miR-99a-5p	-10,07	rno-miR-449c-5p	-331,57
rno-miR-101b-3p	-4,33	rno-miR-222-3p	-5,95	rno-miR-24-3p	-7,11	rno-miR-30d-5p	-10,17		
rno-let-7a-1-3p	-4,34	rno-miR-200c-3p	-5,96	rno-miR-101a-3p	-7,11	rno-miR-214-3p	-10,25		
no-miR-25-3p	-4,62	rno-miR-204-5p	-5,99	rno-miR-30e-5p	-7,16	rno-miR-450a-5p	-10,39		
rno-miR-324-5p	-4,68	rno-miR-411-5p	-6,05	rno-miR-182	-7,17	rno-miR-125a-5p	-10,59		
rno-miR-325-3p	-4,69	rno-miR-181d-5p	-6,14	rno-let-7b-5p	-7,19	rno-miR-100-5p	-10,63		
rno-miR-148b-3p	-4,73	rno-miR-28-5p	-6,18	rno-miR-107-3p	-7,25	rno-miR-378a-3p	-10,64		
rno-miR-20a-5p	-4,75	rno-miR-384-5p	-6,25	rno-miR-99b-5p	-7,28	rno-miR-29c-3p	-10,93		
rno-miR-153-3p	-4,80	rno-miR-151-5p	-6,28	rno-miR-16-5p	-7,37	rno-miR-27a-3p	-10,98		
rno-miR-322-5p	-4,80	rno-miR-374-5p	-6,28	rno-miR-26a-5p	-7,45	rno-miR-125b-5p	-11,66		
rno-miR-200a-3p	-4,94	rno-miR-497-5p	-6,35	rno-miR-139-5p	-7,54	rno-miR-21-5p	-11,96		
rno-miR-451-5p	-4,96	rno-miR-223-3p	-6,40	rno-miR-129-2-3p	-7,59	rno-miR-133b-3p	-12,00		

For the detailed comparison, a total of 360 miRNAs and non-coding RNAs were quantified in all specimens. Of these, 189 miRNAs and non-coding RNAs were filtered for detection. In order to be included for further analysis, detection of a miRNA had to be positive in all specimens of a group. In addition, only rat miRNAs and non-coding RNAs were considered for analysis. After BH-correction (FDR < 10%) of the data, a cut-off BH-p-value of <0.05 was chosen, resulting in a total of 139 differentially expressed miRNAs, listed in Table 32.

The analysis of the unsupervised hierarchical clustering between homozygous and age-matched heterozygous mutant rats showed that the samples cluster according to their genotype, with the exception of the sample Hom_9_6, which clusters with MTC samples from heterozygous instead of homozygous mutant rats (Figure 13). This indicates that the process of tumourigenesis is different in the respective genotypes and suggests the miRNA expression is dependent on the p27 levels. Heterogeneity within each respective group is minimal suggesting high identity among rat MTC specimens with their genotypes.

Analysis of the differentially expressed miRNAs between thyroid tumours of homozygous and age-matched heterozygous mutant rats revealed that miRNAs are globally downregulated in tumours of the homozygous mutant animals. Table 32 shows that rno-miR-449c-5p (-331.57 fold), rno-miR-203a-3p (-56.14 fold), rno-miR-27b-3p (-49.71 fold), rno-miR-127-3p (-35.98 fold) and rno-miR-293-5p (-24.04 fold) were the most significantly downregulated miRNAs in homozygous mutant rat tumours. MiRNAs are categorised into different groups named miRNA families based on the mature miRNA sequence and/or the structure of pre-miRNAs (Ding *et al.* 2011, Kozomara *et al.* 2011). Among the 20 most differentially expressed miRNAs between age-matched homozygous and heterozygous mutant rats, we found rno-miR-29a-3p (-14.38 fold) and rno-miR-29b-3p (-12.83 fold); when considering the 25 most significantly downregulated miRNAs, rno-miR-29c-3p (-10.93 fold) was also detected. The analysis revealed that the members of the miR-29 family showed the strongest downregulation in thyroid tumours from homozygous, when compared to tumours of age-matched heterozygous mutant rats. The only miRNA family showing a similar trend in expression to that of miR-29 members was the miR-27 family with rno-miR-27b-3p (-49.71 fold) and rno-miR-27a-3p (-10.98 fold), which are also significantly downregulated in thyroid tumours of homozygous MENX rats. These miRNA families seem to be highly affected by the p27 levels.

4.1.2 Investigating MTC tumour progression in MENX rats

To complete the miRNA expression analysis of MENX-associated thyroid tumours, we investigated the changes in miRNA levels that accompany tumour progression in heterozygous mutant rats. Specifically, the miRNA expression profiles of progressed late

stage MTC in 18 month-old heterozygous mutant animals were compared with the signatures of less progressed early stage MTC in 9 month-old heterozygous mutant animals. Late stage MTC, in contrast to early stage tumours, showed an advanced invasive phenotype and occasional distant metastases. Profiling the miRNA expression of these advanced tumours may help in determining factors leading to invasive/metastatic MTC phenotypes.

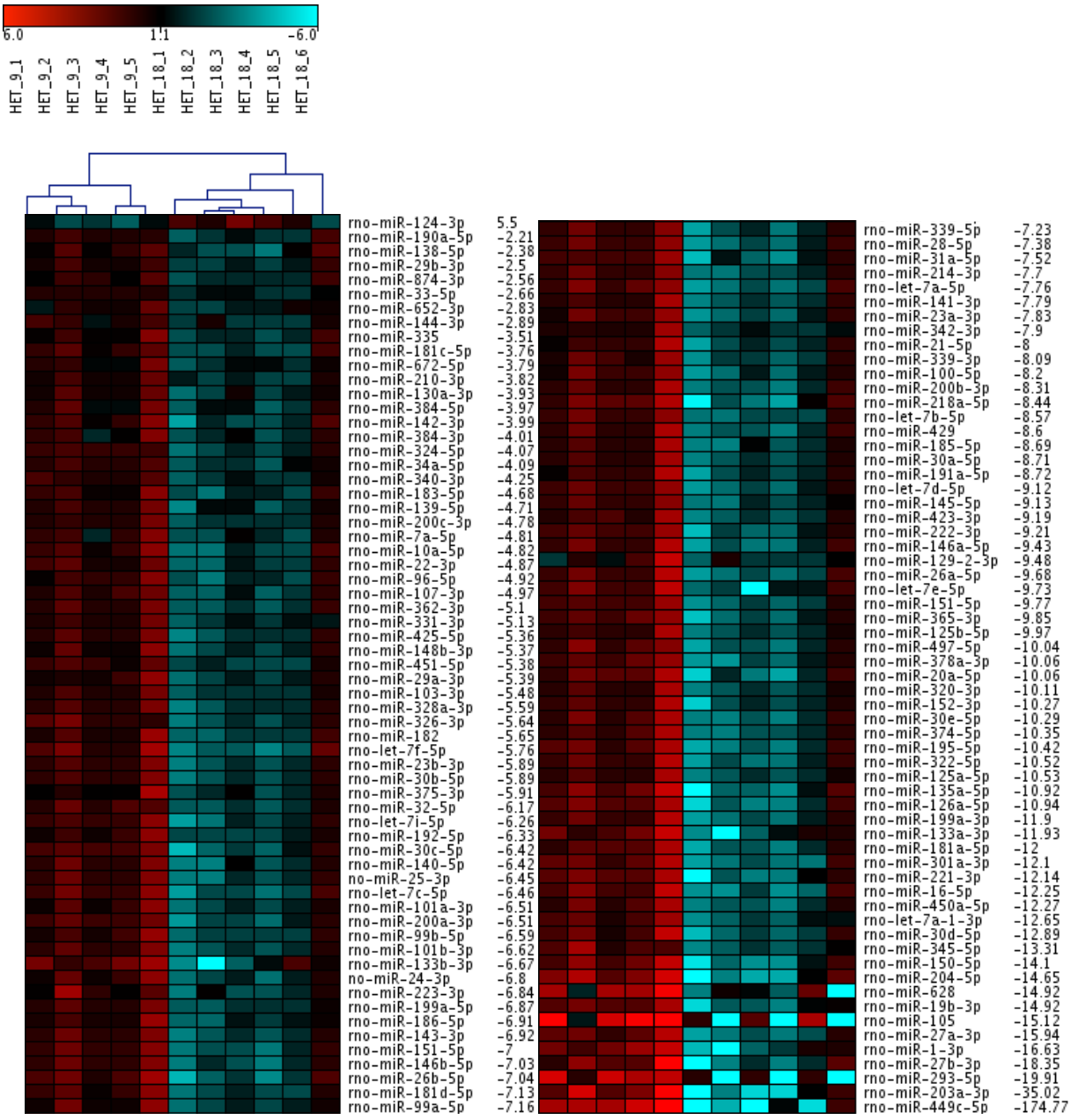

Figure 14: Unsupervised hierarchical clustering with the corresponding heat map of miRNA expression profiles of 18 month-old v*ersus* 9 month-old heterozygous mutant rats. The heat map was split to simplify legibility. The clustering at the top represents the similarity between miRNA expression profiles of rat samples. The corresponding heat map shows high expressed miRNAs in red and low expressed miRNAs in green. Undetected miRNAs were labelled in dark grey. All data was normalised to corresponding RNU1A1 transcription levels using a comparative delta CT method (Livak *et at*. 2001, Pfaffl 2001).

Table 33: Differentially expressed miRNAs in late stage MTC *versus* early stage MTC in heterozygous mutant rats. Differentially expressed miRNAs are shown with corresponding fold changes.

miRNA	Fold Change	miRNA	Fold Change	miRNA	Fold Change	miRNA	Fold Change	miRNA	Fold Change
rno-miR-124-3p	5,5	rno-miR-96-5p	-4,92	rno-miR-99b-5p	-6,59	rno-miR-218a-5p	-8,44	rno-miR-322-5p	-10,52
rno-miR-190a-5p	-2,21	rno-miR-107-3p	-4,97	rno-miR-101b-3p	-6,62	rno-let-7b-5p	-8,57	rno-miR-125a-5p	-10,53
rno-miR-138-5p	-2,38	rno-miR-362-3p	-5,1	rno-miR-133b-3p	-6,67	rno-miR-429	-8,6	rno-miR-135a-5p	-10,92
rno-miR-29b-3p	-2,5	rno-miR-331-3p	-5,13	no-miR-24-3p	-6,8	rno-miR-185-5p	-8,69	rno-miR-126a-5p	-10,94
rno-miR-874-3p	-2,56	rno-miR-425-5p	-5,36	rno-miR-223-3p	-6,84	rno-miR-30a-5p	-8,71	rno-miR-199a-3p	-11,9
rno-miR-33-5p	-2,66	rno-miR-148b-3p	-5,37	rno-miR-199a-5p	-6,87	rno-miR-191a-5p	-8,72	rno-miR-133a-3p	-11,93
rno-miR-652-3p	-2,83	rno-miR-451-5p	-5,38	rno-miR-186-5p	-6,91	rno-let-7d-5p	-9,12	rno-miR-181a-5p	-12
rno-miR-144-3p	-2,89	rno-miR-29a-3p	-5,39	rno-miR-143-3p	-6,92	rno-miR-145-5p	-9,13	rno-miR-301a-3p	-12,1
rno-miR-335	-3,51	rno-miR-103-3p	-5,48	rno-miR-151-5p	-7	rno-miR-423-3p	-9,19	rno-miR-221-3p	-12,14
rno-miR-181c-5p	-3,76	rno-miR-328a-3p	-5,59	rno-miR-146b-5p	-7,03	rno-miR-222-3p	-9,21	rno-miR-16-5p	-12,25
rno-miR-672-5p	-3,79	rno-miR-326-3p	-5,64	rno-miR-26b-5p	-7,04	rno-miR-146a-5p	-9,43	rno-miR-450a-5p	-12,27
rno-miR-210-3p	-3,82	rno-miR-182	-5,65	rno-miR-181d-5p	-7,13	rno-miR-129-2-3p	-9,48	rno-let-7a-1-3p	-12,65
rno-miR-130a-3p	-3,93	rno-let-7f-5p	-5,76	rno-miR-99a-5p	-7,16	rno-miR-26a-5p	-9,68	rno-miR-30d-5p	-12,89
rno-miR-384-5p	-3,97	rno-miR-30b-5p	-5,89	rno-miR-339-5p	-7,23	rno-let-7e-5p	-9,73	rno-miR-345-5p	-13,31
rno-miR-142-3p	-3,99	rno-miR-23b-3p	-5,89	rno-miR-28-5p	-7,38	rno-miR-151-5p	-9,77	rno-miR-150-5p	-14,1
rno-miR-384-3p	-4,01	rno-miR-375-3p	-5,91	rno-miR-31a-5p	-7,52	rno-miR-365-3p	-9,85	rno-miR-204-5p	-14,65
rno-miR-324-5p	-4,07	rno-miR-32-5p	-6,17	rno-miR-214-3p	-7,7	rno-miR-125b-5p	-9,97	rno-miR-628	-14,92
rno-miR-34a-5p	-4,09	rno-let-7i-5p	-6,26	rno-let-7a-5p	-7,76	rno-miR-497-5p	-10,04	rno-miR-19b-3p	-14,92
rno-miR-340-3p	-4,25	rno-miR-192-5p	-6,33	rno-miR-141-3p	-7,79	rno-miR-378a-3p	-10,06	rno-miR-105	-15,12
rno-miR-183-5p	-4,68	rno-miR-30c-5p	-6,42	rno-miR-23a-3p	-7,83	rno-miR-20a-5p	-10,06	rno-miR-27a-3p	-15,94
rno-miR-139-5p	-4,71	rno-miR-140-5p	-6,42	rno-miR-342-3p	-7,9	rno-miR-320-3p	-10,11	rno-miR-1-3p	-16,63
rno-miR-200c-3p	-4,78	no-miR-25-3p	-6,45	rno-miR-21-5p	-8	rno-miR-152-3p	-10,27	rno-miR-27b-3p	-18,35
rno-miR-7a-5p	-4,81	rno-let-7c-5p	-6,46	rno-miR-339-3p	-8,09	rno-miR-30e-5p	-10,29	rno-miR-293-5p	-19,91
rno-miR-10a-5p	-4,82	rno-miR-200a-3p	-6,51	rno-miR-100-5p	-8,2	rno-miR-374-5p	-10,35	rno-miR-203a-3p	-35,02
rno-miR-22-3p	-4,87	rno-miR-101a-3p	-6,51	rno-miR-200b-3p	-8,31	rno-miR-195-5p	-10,42	rno-miR-449c-5p	-174,77

A total of 274 miRNAs and non-coding RNAs were quantified across all MTC specimens. The miRNAs were filtered for detection and in order to be considered, detection had to be positive in all samples of the group. Furthermore, only rat miRNAs were included for analysis. After BH-correction (FDR < 10%) of the data, a cut-off BH-p-value of <0.05 was chosen resulting in a total of 125 significantly differentially expressed miRNAs, which are listed in Table 33.

Unsupervised hierarchical cluster analysis between late and early stage MTC of heterozygous mutant rats show that specimens separate according to tumour progression with the exception of the late stage sample Her_18_6, which cluster together with less progressed early stage MTC specimens (Figure 14). Heterogeneity of specimens within each particular group is minimal, suggesting high identity among samples.

Analysis of the differentially expressed miRNAs in heterozygous mutant rats showed a global downregulation of miRNAs in tumours of late stage MTCs, indicating a downregulation of miRNAs accompanying tumour progression. The analysis of the individual miRNAs revealed the downregulation of rno-miR-449c-5p (-174.77 fold), rno-miR-203a-3p (-35.02 fold), rno-miR-293-3p (-19.91 fold), rno-miR-27b-3p (-18.35 fold) and rno-miR-1-3p (-16.63 fold) as the most significant differentially expressed miRNAs in late stage *versus* early stage MTC tissues of heterozygous mutant rats. Among the 25 most significantly differentially expressed miRNAs belonging to the same family, rno-miR-27a-3p (-15.94 fold) and rno-miR-27b-3p (-18.35 fold) were identified as downregulated.

The miRNA signature of late stage MTC revealed the upregulation of rno-miR-124-3p (5.50 fold). This result suggests that rno-miR-124-3p increases with tumour progression and therefore shows an opposite trend in expression, with respect to the majority of the differentially expressed miRNAs. Furthermore, the expression trend of rno-miR-124-3p with tumour progression suggests oncogenic properties.

4.1.3 MiRNA expression in MENX rats

Comparative analysis of the miRNA signatures of MENX rat thyroid tumours identified miRNAs dependent on the p27 levels, as well as miRNAs associated with tumour progression. The comparison in miRNA expression between homozygous and age-matched heterozygous mutant rats shows a p27-dependent downregulation of rno-miR-449c-5p, rno-miR-203a-3p and rno-miR-27b-3p. A similar expression trend was observed by comparing their expression levels between late and early stage MTC of heterozygous mutant rats.

The expression of members of the miR-29 family is p27-dependent: lower in the tumours of homozygous mutant rats. The expression analysis of these miRNAs detected a

downregulation of rno-miR-29a-3p (-5.39 fold) and rno-miR-29b-3p (-2.50 fold) in the miRNA signatures of late stage *versus* early stage MTCs in heterozygous mutant rats. Aberrant expression of this miRNA family suggests an important role in MTC tumourigenesis. Furthermore, the expression of the miR-29 family is not only dependent on tumour progression, but also on the p27 levels. The expression of differentially expressed miRNAs suggests that loss of p27 is an initiating event in MTC and deregulation of many miRNAs is dependent on tumour progression.

Tumour progression correlates with the increased expression of rno-miR-124-3p (5,50 fold) in heterozygous MENX rats. Interestingly, a differentially expressed of rno-miR-124-3p (-4.07 fold) was also observed in thyroid tumours of homozygous mutant rats. The analysis shows that downregulation of rno-miR-124-3p correlates with depletion of p27, suggesting that rno-miR-124-3p is regulated by p27. Unfortunately, investigating the tumour progression including thyroid tissues from wild-type rats was not possible due to the low C-cell population in the gland. As a consequence, a definite influence of p27 on the expression of rno-miR-124-3p cannot be determined.

4.1.4 Causal analysis of MENX-associated MTC miRNA expression

The differentially expressed miRNAs identified by profiling thyroid tumours of homozygous rats *versus* age-matched heterozygous mutant rats were subjected to causal analysis using the IPA Downstream Effects Analysis. For the comparison between tumours of age-matched homozygous and heterozygous mutant rats, 139 miRNAs were considered eligible for analysis. For the comparison of differentially expressed miRNAs identified between late stage and early stage MTC in heterozygous mutant rats, 125 were considered eligible for analysis by employing the IPA Downstream Effects Analysis (QIAGEN Redwood City, www.qiagen.com/ingenuity).

The IPA Downstream Effects Analysis predicts any enrichment in downstream biological activities occurring in the tissues studied. There are a total of 85 high level functional categories, divided into the three categories “Diseases and Disorders”, “Physiological System Development” and “Molecular and Cellular Functions”. Using the directional change of miRNAs in the data sets, IPA computes the likely effect on diseases and cell biological functions such as cancer, apoptosis and cell migration and therefore biological information is organised for a high level overview (IPA®, QIAGEN Redwood City, www.qiagen.com/ingenuity).

High level functional categories contain high quality Gene Ontology information that can be further broken down into specific biological processes caused by the directional change of

the miRNAs that were measured in both data sets (IPA®, QIAGEN Redwood City, www.qiagen.com/ingenuity).

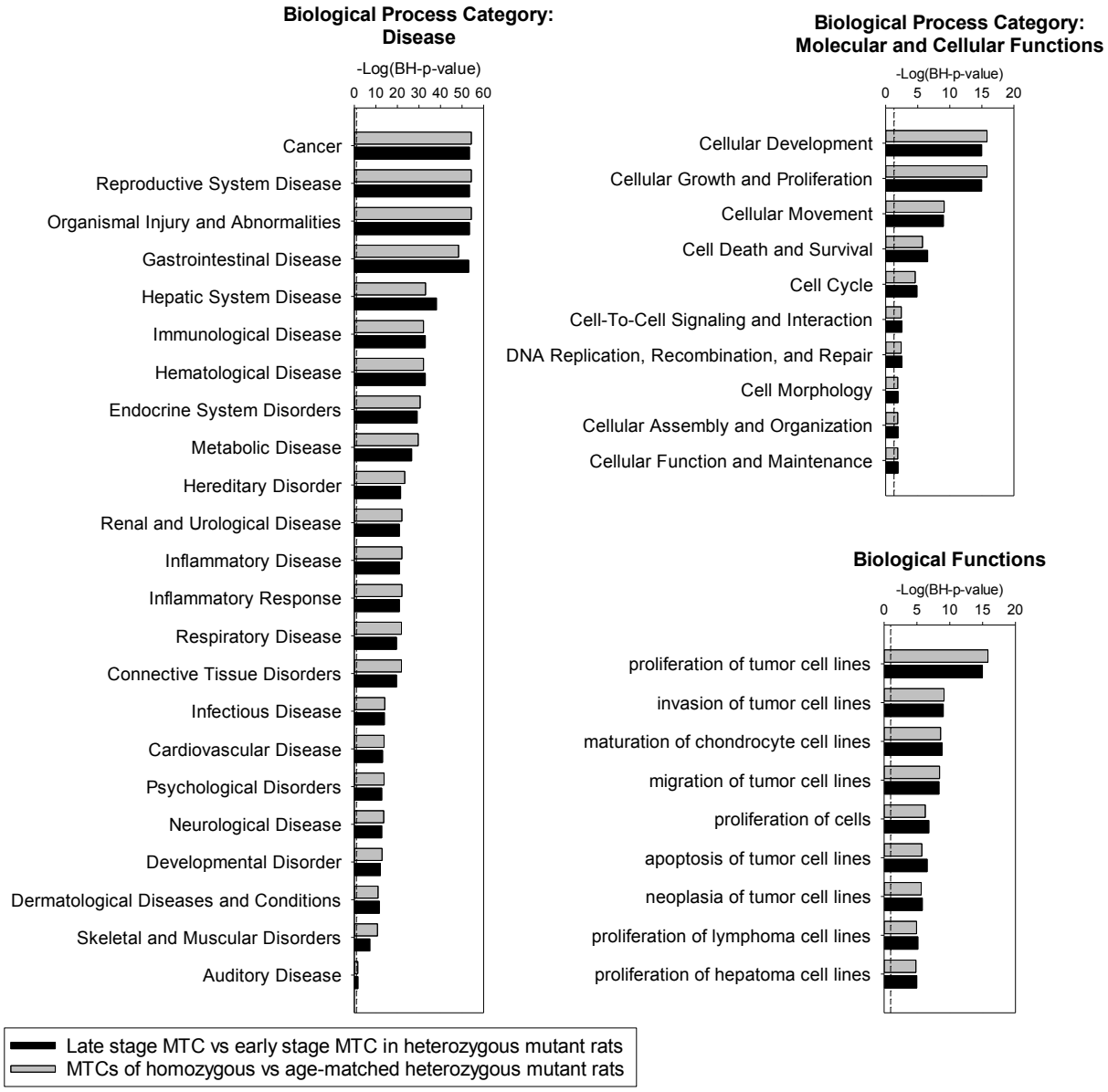

Figure 15: IPA high level functional categories and biological functions specifically enriched among miRNAs differentially expressed in rat MTC profiles. The histogram displays perturbed IPA categories. The y-axis reports the significance of the perturbation and is plotted as log of the BH multiple testing corrected p-value calculated by IPA based on the specific data sets. The dotted line is the threshold BH-p-value of <0.05.

The differentially expressed miRNAs identified in our profiling were subjected to IPA in the areas of “Diseases and Disorders” as well as “Molecular and Cellular Functions” as these contained cancer relevant high level functional categories. Figure 15 shows the enriched high level functional categories above the threshold of BH-p-value of <0.05 for both miRNA expression comparisons of MENX rats. The causal analysis showed a similar enrichment of categories for both miRNA expression comparisons, and the most significantly enriched

category in the area “Disease and Disorders” in both comparisons was “Cancer”. This suggests that a large proportion of the miRNAs we found differentially expressed in MTC of MENX rats had been previously associated to oncogenic functions, implying important roles in tumour formation.

In the area “Molecular and Cellular Functions” the most significantly enriched categories in both miRNA expression comparisons was “Cellular Development”, “Cellular Growth and Proliferation”, “Cellular Movement”, “Cell Death and Survival” as well as “Cell Cycle” (Figure 15). This implies that differentially expressed miRNAs of MENX rats are involved in the regulation of processes that fall into the significantly enriched functional categories.

The high level functional categories in the area “Molecular and Cellular Functions” were further broken down into biological functions using the IPA Downstream Effect Analysis. Figure 15 shows that the most significantly perturbed functions for both data sets was “proliferation of tumour cell lines”, “invasion of tumour cell lines” as well as “migration of tumour cell lines”. These results indicate that differentially expressed miRNA signatures of MENX rat thyroid tumours lead to an aggressive phenotype by increasing cell proliferation, cell migration and invasion.

4.2 MiRNA expression in human MTC

4.2.1 Patients and tumour characteristics

Thyroid tissues from human MTC patients were collected over a time period of three years in order to conduct a miRNA profiling study. Through our collaboration partner Prof Dr Sergio Pereira De Almeida Toledo of the University Hospital, Sao Paulo, Brazil, we were able to obtain fresh frozen hereditary MTC tumours. In addition, we were able to obtain fresh frozen and FFPE MTC tissues through collaboration with Prof Dr Christine Spitzweg of the Ludwigs-Maximillians-Universität München, Munich, Germany and Dr Thomas Negele of the Klinikum Martha Maria, Munich, Germany. Detailed information of patients is listed in Table 34.

In contrast to sporadic MTC, hereditary MTC is historically and clinically defined through the presence of germinal mutations in the *RET* proto-oncogene as part of the MEN2 syndrome or if patients have a family history of MTC. Sporadic MTC can arise clinically at any age but its incidence peaks beginning with the fourth decade of life (Leboulleux *et al.* 2004, Lodish *et al.* 2008). Studies estimate the prevalence of *RET* mutation carriers are 1:80,000 in Germany, with approximately 300 RET families. According to these data, the majority of patients carry a mutation in codon 634 (222-296 out of 1,000 *RET* mutation carriers), while mutations in codons 620 (36-48 out of 1,000 RET mutation carriers), 791 (24-32 out of 1,000

RET mutation carriers) and 918 (28-56 out of 1,000 RET mutation carriers) are more rare (Machens *et al.* 2013).

Table 34: Patient List.

No	Age at diagnosis (years)	Sex	Tumour size (cm)	Clinical Diagnosis	RET Mutation	Follow up (months)	Residual Disease	Lateral Metastasis	Distant Metastasis	Clinical Outcome
Her_M_1	12	M	0.5 x 0.3	MEN2A	C620R	36	no	yes	no	cured
Her_M_2	9	M	0.8 x 0.6	MEN2A	C620R	36	no	no	no	cured
Her_M_3	20	M	1.1 x 0.9	MEN2A	C620R	36	no	yes	no	cured
Her_M_4	5	M	0.5 x0.3	MEN2A	C620R	42	no	no	no	cured
Her_M_5	29	M	1.4 x 1.2	MEN2A	C620R	24	yes	yes	no	not cured
Her_M_6	37	M	2,4	MEN2A	n.a.	27	yes	yes	yes	not cured
Her_F_1	9	F	0.5 X 0.4	MEN2A	C634R	300	no	no	no	cured
Her_F_2	41	F	2.1 x 1.3	MEN2A	C634Y/791Y	72	yes	yes	no	not cured
Her_F_3	19	F	1.3 x 1.1	MEN2A	C634R	36	yes	yes	no	not cured
Her_F_4	86	F	9.1 x 4.3	MEN2A	C634R	2	yes	yes	yes	not cured
Her_F_5	9	F	0.6 x 0.5	MEN2A	C634R	24	no	no	no	cured
Her_F_6	25	F	n.a.	MEN2A	n.a.	n.a.	yes	yes	yes	not cured
Her_F_7	58	F	0.7 x 1.7	MEN2A	n.a.	65	no	yes	no	cured
Her_F_8	32	F	0.2x0.2	MEN2A	n.a.	53	no	yes	yes	stable disease
Her_F_9	21	F	n.a.	MEN2A	n.a.	154	no	no	no	stable disease
Spor_M_1	42	M	3	sporadic	negative	23	no	no	no	cured
Spor_M_2	64	M	1,1	sporadic	n.a.	1	no	yes	no	cured
Spor_M_3	42	M	6,2	sporadic	negative	11	no	yes	no	stable disease
Spor_M_4	43	M	6,3	sporadic	negative	13	no	yes	yes	stable disease
Spor_M_5				sporadic						
Spor_M_6	50	M	1,9	sporadic	negative	92	yes	yes	yes	not cured
Spor_M_7	40	M	1,7	sporadic	negative	106	no	no	no	n.a.
Spor_M_8	37	M	n.a.	sporadic	n.a.	n.a.	no	yes	no	stable disease
Spor_M_9	48	M	3	sporadic	negative	70	no	yes	no	cured
Spor_F_1	78	F	1.3 x 0.3	sporadic	n.a.	13	no	yes	no	stable disease
Spor_F_2	48	F		sporadic	negative	122	no	yes	no	stable disease
Spor_F_3	63	F		sporadic	negative	56	no	no	no	cured

Table 34 continued: Patient list.

No	Age at diagnosis (years)	Sex	Tumour size (cm)	Clinical Diagnosis	RET Mutation	Follow up (months)	Residual Disease	Lateral Metastasis	Distant Metastasis	Clinical Outcome
Spor_F_4	70	F	2,5	sporadic	negative	5	yes	yes	no	stable disease
Spor_F_5	42	F	2,2	sporadic	n.a.	5	yes	yes	yes	n.a.
Spor_F_6	42	F	n.a.	sporadic	n.a.	338	yes	yes	yes	not cured
Spor_F_7	53	F	n.a.	sporadic	n.a.	155	no	yes	no	cured
Spor_F_8		F	n.a.	sporadic						
Spor_F_9		F	3,7	sporadic						
Spor_F_10	49	F	1.8 x 1.3	sporadic	negative	319	no	yes	no	stable disease

In most European countries, the distribution of *RET* missense mutations is similar to Germany. Outside of Europe, national health care systems differ regarding the availability and comprehension of *RET* gene sequencing and therefore is usually used for molecular confirmation of clinically manifested MEN2A and MEN2B (Machens *et al.* 2013).

This study was conducted on 34 patients with detailed patient histories and long follow-up periods. 15 patients with identified germline *RET* mutations were diagnosed as MEN2A. After surgery, 10 hereditary patients suffered from lateral metastasis. In four hereditary patients, the presence of distant metastasis was discovered. A total of 19 sporadic MTC patients were collected. In a total of 13 out of 19 sporadic MTC specimens lateral metastasis, while in three specimens distant metastasis were detected after surgery. Residual disease was observed in six hereditary MTC patients and four sporadic MTC patients. Hereditary MTC patients were followed up for a mean of 64 months and patients with sporadic MTC were followed for a mean of 92 months.

The *RET* gene contains 21 exons and therefore sequencing the gene presents a huge undertaking (Ceccherini *et al.* 1993). When screening for germline *RET* mutations, exons10, 11 and 13-16 are usually sequenced as these contain mutation hotspots (Margraf *et al.* 2009). In consideration of the size of the *RET* gene, sequencing is only conducted if patients have family histories or are suspected as MEN2. Nonetheless, *RET* sequencing was conducted for 10 out of 19 sporadic MTC specimens, identifying no *RET* mutations. Unfortunately, for nine sporadic MTC specimens used in this study the *RET* mutation status is unknown, as these specimens were not sequenced.

Interestingly, patients suffering from MEN2A related hereditary MTC, nine patients carried the *RET* mutation C620R with one patient carrying the *RET* mutation C634R and one patient carrying the C634Y/791Y double mutation. The fact that most hereditary MTC patients carry the same *RET* mutations makes this data set unique, especially when considering the frequency of hereditary mutations in MTC and the incidence of MTC itself.

4.2.2 Histological evaluation of MTC tumours

Fresh frozen tissues were used to undertake a miRNA profiling of hereditary *versus* sporadic MTC. In addition, MTC patients with available FFPE tissues were selected to be utilised for histological investigations. All MTC specimens were histologically investigated in cooperation with Dr Frauke Neff. The thyroid specimens were diagnosed and pathologically confirmed as MTC by Dr Frauke Neff.

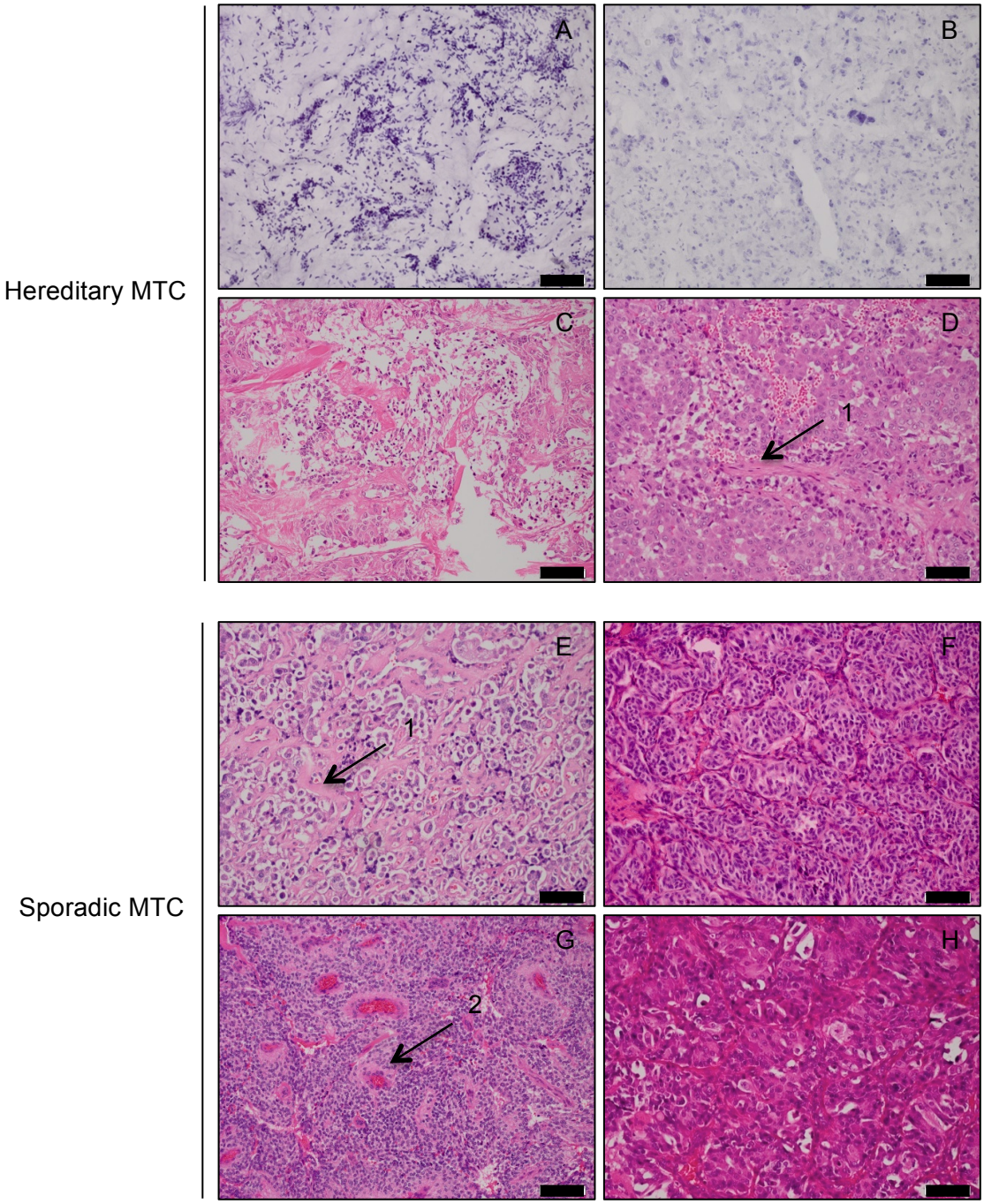

Figure 16: H&E staining of MTC Specimens. A-D: H&E staining of hereditary MTC from patients Her_F_1, Her_F_2, Her_F_6 and Her_M_6. **E-H:** H&E staining of sporadic MTC from patients Spor_F_6, Spor_F_7, Spor_F_8 and Spor_M_7. The distribution of plump stroma is marked with the arrows labelled 1, while psammon bodies are indicated by the arrow labelled 2. The scale bar indicates a length of 50 microns. (Magnification: 200x).

The histological evaluation of the specimens confirmed MTC in all patients. Tumour areas were identified in the examined specimens. Figure 16 shows representative H&E stainings of MTC specimens. Interestingly, hereditary and sporadic MTCs cannot be distinguished according to histological features. A similar distribution of delicate and plump stroma (indicated by the arrows labelled 1) was identified in tumourr areas of both hereditary and sporadic MTCs . A minor distinguishing feature between the two groups is an increase in cell

polymorphisms in hereditary MTC. MTC in both hereditary and sporadic patients frequently showed areas of necrosis, bleeding and local invasion into neighbouring tissues. In some MTC specimens, psammon bodies were identified (indicated by the arrow labelled 2). The MTC tumour specimens collected all show invasive phenotypes and seem to be at comparable stages of tumour progression.

4.2.3 MiRNA profiles of human MTC

MTC accounts for only 2-3% of all thyroid malignancies (Kaatsch *et al.* 2013). Despite this low frequency, there are a disproportionate number of deaths from MTC, when compared to other thyroid malignancies. Regrettably, 50% of MTC patients with metastatic or recurring disease have an average survival rate of 4 years (Santarpia *et al.* 2013). To assess the potential role of miRNAs in MTC tumour progression, a miRNA array expression analysis was conducted.

As described in section 1.2, a comparison of the miRNA expression between primary MTC tumours and normal C-cells is not possible because of the low numbers of C-cells present in the thyroid cell mass. As a consequence, only a comparison between C-cell tumours is possible and usually differences between hereditary and sporadic MTCs are investigated. Another approach is the comparison between primary and metastatic MTC tumours, but insufficient primary and corresponding metastatic tumours were collected in order to conduct this comparison.

For this investigation, the GeneChip miRNA 1.0 arrays from Affymetrix were used. The GeneChip miRNA 1.0 array contains 6,703 probe sets designed according to the Sanger miRBase database (Version 11) for miRNAs, with four identical probes per miRNA. The probes correspond to non-coding RNAs of different species, including human, mouse, rat, canine and rhesus monkey. Cancerous tissue was isolated from previously identified tumour areas of fresh frozen samples reported in Table 34 and hybridised onto the miRNA arrays. The normalisation and quality control analysis was conducted with the miRNA QC tool (Version 1. 0.33.0) according to the settings recommended by Affymetrix. Due to weak signal intensities, the samples Her_M_2 and Spor_F_2 were excluded from the analysis.

For the comparative analysis of miRNA expression between hereditary and sporadic MTC, a total of 311 miRNAs, small RNAs and non-coding RNAs were quantified across all specimens. Of these, 158 miRNAs, small RNAs and non-coding RNAs were filtered for detection. In order to be considered, detection needed to occur in at least five out nine hereditary and four out of seven sporadic MTC specimens. After BH correction of data, a cut-off p-value of <0.05 was chosen, resulting in a total of 48 significantly differentially expressed

non-coding RNAs. Of the 48 differentially expressed non-coding RNAs between hereditary and sporadic MTC, 30 were identified as miRNAs and which are listed in Table 35.

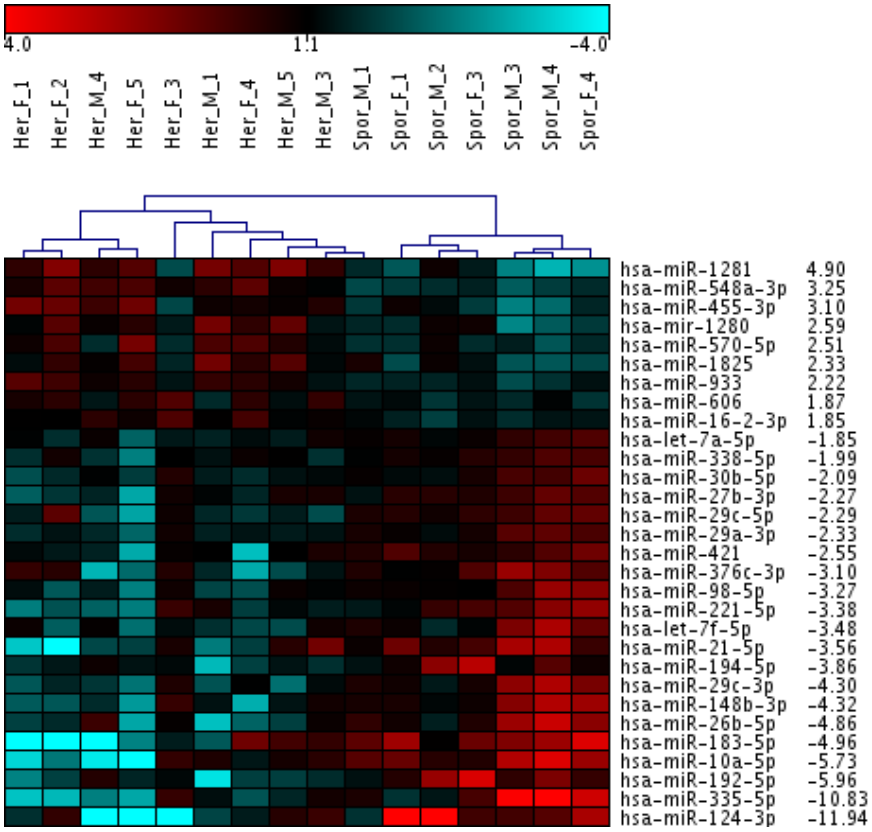

Figure 17: Unsupervised hierarchical clustering with the corresponding heat map of miRNA expression profiles of MTC patient samples. The clustering at the top represents the similarity between miRNA expression profiles of rat samples. Beneath the dendogram at the top, the corresponding heat map shows high expressed miRNAs in red and low expressed miRNAs in green. Undetected miRNAs were labelled in dark grey.

The miRNA expression profiles of MTC patient samples were subjected to unsupervised, hierarchical clustering and are shown together with the corresponding heat map in Figure 17. Interestingly, the miRNA expression patterns divide the samples into two major clusters, separating hereditary and sporadic MTC specimens, with the exception of the hereditary MTC specimen Her_F3, which clusters with the sporadic cases. This excludes major gender specific effects on miRNA expression and suggests that miRNA profiling is affected by the presence of germline *RET* mutations associated with MEN2A. The *RET* sequencing analysis of sporadic MTC patents identified no acquired mutations in five out of seven specimens, while the mutation status of two specimens remains unknown. As a consequence, miRNA expression profiles between *RET* mutation positive hereditary MTC specimens separated from *RET* mutation negative sporadic MTC specimens for the majority of cases, according to the hierarchical cluster analysis.

Within each group, differences among individual patient samples were observed, suggesting a heterogeneous population among MTC specimens. Nonetheless, MEN2A-associated MTC specimens have a specific pattern in miRNA deregulation, which indicates a common mechanism of pathogenesis within hereditary MTC specimens.

Table 35: Significantly differentially expressed miRNAs in hereditary *versus* sporadic MTC. Deregulated miRNAs with respective fold changes between hereditary and sporadic MTC.

miRNA	Fold Change	miRNA	Fold Change
hsa-miR-1281	4.90	hsa-miR-421	-2.55
hsa-miR-548a-3p	3.25	hsa-miR-376c-3p	-3.10
hsa-miR-455-3p	3.10	hsa-miR-98-5p	-3.27
hsa-mir-1280	2.59	hsa-miR-221-5p	-3.38
hsa-miR-570-5p	2.51	hsa-let-7f-5p	-3.48
hsa-miR-1825	2.33	hsa-miR-21-5p	-3.56
hsa-miR-933	2.22	hsa-miR-194-5p	-3.86
hsa-miR-606	1.87	hsa-miR-29c-3p	-4.30
hsa-miR-16-2-3p	1.85	hsa-miR-148b-3p	-4.32
hsa-let-7a-5p	-1.85	hsa-miR-26b-5p	-4.86
hsa-miR-338-5p	-1.99	hsa-miR-183-5p	-4.96
hsa-miR-30b-5p	-2.09	hsa-miR-10a-5p	-5.73
hsa-miR-27b-3p	-2.27	hsa-miR-192-5p	-5.96
hsa-miR-29c-5p	-2.29	hsa-miR-335-5p	-10.83
hsa-miR-29a-3p	-2.33	hsa-miR-124-3p	-11.94

Analysis of the miRNA signature of human MTC revealed that hsa-miR-124-3p (-11.94 fold) and hsa-miR-335-5p (-10.83 fold) show the highest degree of downregulation in hereditary *versus* sporadic MTC. The expression of hsa-miR-192-5p (-5.96 fold), hsa-miR-10a-5p (-5.73 fold), hsa-miR-183-5p (-4.96 fold) and hsa-miR-26b-5p (-4.86 fold) was reduced to a similar degree in hereditary MTC, when compared with sporadic MTC specimens. The only significant differential expression of miRNAs belonging to the same miRNA family, were hsa-miR-29c-3p (-4.30 fold) and hsa-miR-29a-3p (-2.33 fold), from the predominant transcript, as well as hsa-miR-29c-5p (-2.29 fold) from the opposite strand of the pre-miRNA (Ambros *et al.* 2003). A total of six miRNAs were overexpressed in hereditary MTC specimens, of which miR-1281 (4.90 fold) and miR-548a-3p (3.25 fold) showed the largest increase in expression.

4.2.4 Causal analysis of human MTC miRNA expression signatures

In order to analyse potential trends in miRNA expression in human MTCs, a causal analysis of the differentially expressed miRNAs between hereditary and sporadic MTC was performed using the IPA Downstream Effects Analysis, as previously described for the miRNA expression of MENX rats. The study of high level functional categories was chosen as it provides more robust results before studying individual miRNAs.

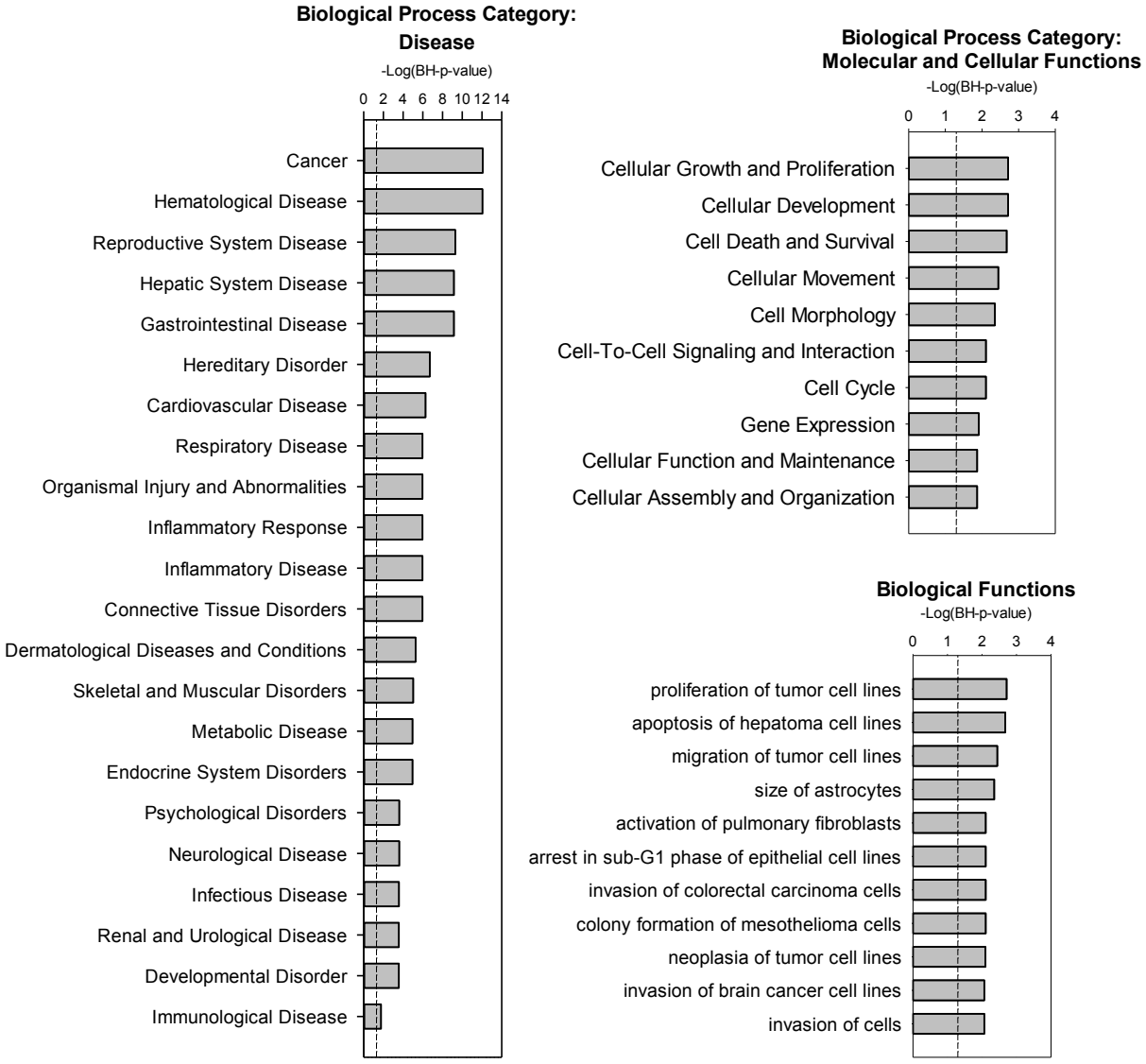

Figure 18: IPA high level functional categories and biological functions specifically enriched among miRNAs differentially expressed in hereditary *versus* sporadic MTC. The histogram displays perturbed IPA categories and functions. The y-axis reports the significance of the differential enrichment and is plotted as log of the BH multiple testing corrected p-value calculated by IPA based on the specific data set. The dotted line denotes the threshold BH-p-value of <0.05.

The quantified miRNAs found by the miRNA expression analysis between hereditary and sporadic MTC were subjected to IPA analysis. The IPA network included 30 differentially regulated miRNAs in hereditary *versus* sporadic MTC that were eligible for analysis.

The enriched high level functional categories based on the miRNA expression changes in the human MTC miRNA expression comparison were identified using IPA Downstream Effects Analysis. The analysis indicates the likelihood that the association between a set of miRNAs in our data set and a biological function is significant (IPA®, QIAGEN Redwood City, www.qiagen.com/ingenuity). The differentially regulated miRNAs in hereditary *versus* sporadic MTC were analysed by IPA in the areas of “Disease and Disorders” and “Molecular and Cellular Functions”. These areas were analysed as they contained cancer relevant high level functional categories. Figure 18 shows enriched IPA functional categories among the differentially expressed miRNAs above the threshold of a BH-p-value of <0.05. The most significantly affected functional category in area “Disease and Disorders” for the comparison between hereditary and sporadic MTC was “Cancer”, suggesting that detected miRNAs have been previously identified in cancer.

The area “Molecular and Cellular Functions” shows the perturbation of the high level functional categories “Cellular Growth and Proliferation”, “Cell Death and Survival” as well as “Cellular Movement”. IPA Downstream Effects Analysis suggests that the differential expression of the miRNAs correlate with a change in cell proliferation, migration and apoptosis.

Functional categories obtained by the IPA Downstream Effects Analysis can be broken down into specific biological processes caused by the directional change of the miRNAs that were measured (IPA®, QIAGEN Redwood City,www.qiagen.com/ingenuity). The area “Molecular and Cellular Functions” was further broken down and biological functions based on the differentially expressed miRNAs between hereditary and sporadic MTC. The most significantly enriched biological functions were “proliferation of tumour cell lines”, “apoptosis of tumour cell lines” as well as “migration of tumour cell lines”. These results further substantiate the implication that significantly differentially expressed miRNAs participate in the regulation of cell proliferation and cell migration in hereditary MTC. Furthermore, the miRNA signature of hereditary MTC implies that differentially expressed miRNAs regulate apoptosis in MTC cells.

4.2.5 Validation of miRNA expression in human MTC

Detection of miRNAs via miRNA arrays is based on hybridising labelled miRNAs onto the arrays and therefore this method has to be validated using a different method. Quantitative RT-PCR was used for validating the miRNA array results by selecting differentially expressed

miRNAs that can discriminate between hereditary and sporadic MTC. The expression of differentially expressed miRNAs between hereditary and sporadic MTC was conducted with MTC specimens used for the array analysis.

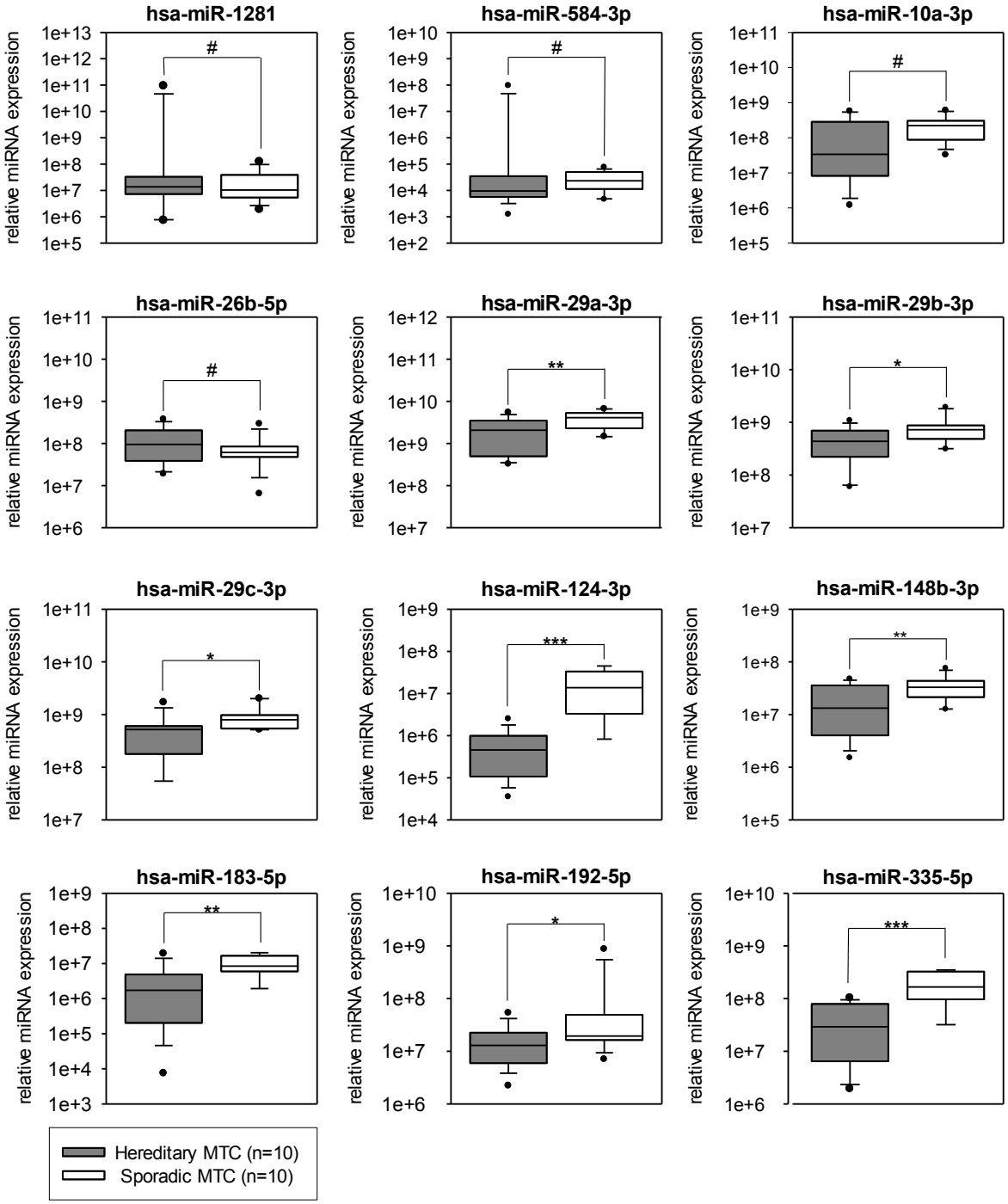

Figure 19: Validation of human MTC miRNA expression signatures. Validation of miRNA array results by quantitative RT-PCR. All data was normalised to U6 snRNA transcription levels using a comparative Ct method (Livak *et al.* 2001, Pfaffl 2001). All box plots show 25th to 75th percentiles (box) and 5th and 95th percentiles (whiskers). Solid dots are outliers below 5% and above 95%. The line in the box represents the median (#= not significant; *= p-value <0.05, **= p-value <0.01, ***= p-value <0.001).

The miRNAs hsa-miR-10a-3p, hsa-miR-26b-5p, hsa-miR-29a-3p, hsa-miR-29b-3p, hsa-miR-29c-3p, hsa-miR-124-3p, hsa-miR-148b-3p, hsa-miR-183-5p, hsa-miR-192-5p and hsa-miR-335-5p were selected for validation as they showed a significant downregulation between hereditary and sporadic MTC based on the miRNA array analysis. In addition, the significantly upregulated hsa-miR-584a-3p and hsa-miR-1281 were also chosen for validation. The miRNA array investigation had revealed that the expression of these miRNAs was up to two fold differentially expressed in hereditary, when compared to sporadic MTC specimens.

Validation with quantitative RT-PCR confirms a significant downregulation of hsa-miR-29a-3p, hsa-miR-29b-3p, hsa-miR-29c-3p, hsa-miR-124-3p, hsa-miR-148b-3p, hsa-miR-183-5p, hsa-miR-192-5p and hsa-miR-335-5p in hereditary *versus* sporadic MTCs (Figure 19). Differential expression of hsa-miR-10a-3p, hsa-miR-26b-5p, hsa-miR-548-3p and hsa-miR-1281 could not be validated with quantitative RT-PCR. Hence, eight out of twelve miRNAs identified as differentially expressed and most significantly discriminatory between hereditary and sporadic MTC by miRNA array and statistical testing, could be confirmed by quantitative RT-PCR, a method with higher sensitivity.

In summary, the expression of the significantly deregulated miRNAs, hsa-miR-124-3p, hsa-miR-183-5p, hsa-miR-192-5p and hsa-miR-335-5p, additionally to the expression of the miR-29 family, was validated in hereditary MTC indicating their significance in the pathogenesis of these tumours.

4.3 The MENX rats as an animal model of human MTC

4.3.1 Similarities in differentially expressed miRNAs

In this study, we determined the miRNA expression signature of MTC in both 9 month-old homozygous and heterozygous mutant rats, which allows to study the influence of p27 levels on miRNAs expression in tumours at the same stage of progression. Additionally, we determined the miRNA expression in heterozygous mutant rats at 18 and 9 months of age, where late and early stage tumours with similar p27 levels were investigated. We also investigated the miRNA expression in human hereditary *versus* sporadic MTCs. Due to the low numbers of C-cell within healthy thyroid glands of wild-type animals, the influence of the p27 levels on the miRNA expression of MTC cannot be fully comprehended. For the purpose of clarity, any further species designation of individual miRNAs will be omitted.

In order to determine whether the rat thyroid tumours are a suitable model of human MTC, a detailed comparison of miRNA signatures between rats and humans was conducted. Our

three comparisons of acquired data sets are composed of: 9 month-old homozygous *versus* age-matched heterozygous mutant rats; 18 month-old heterozygous and 9 month-old heterozygous mutant rats; human hereditary *versus* sporadic MTC. The miRNA miR-29b-3p was included in the comparison of miRNA signatures as its expression was validated in human MTCs by quantitative RT-PCR, whereas the expression of miR-10a-5p, miR-26-5p, miR-548-3p as well as miR-1281 was not validated and therefore not included in the comparison. Figure 20 shows the overlap of miRNA expression signatures of human and rat MTC.

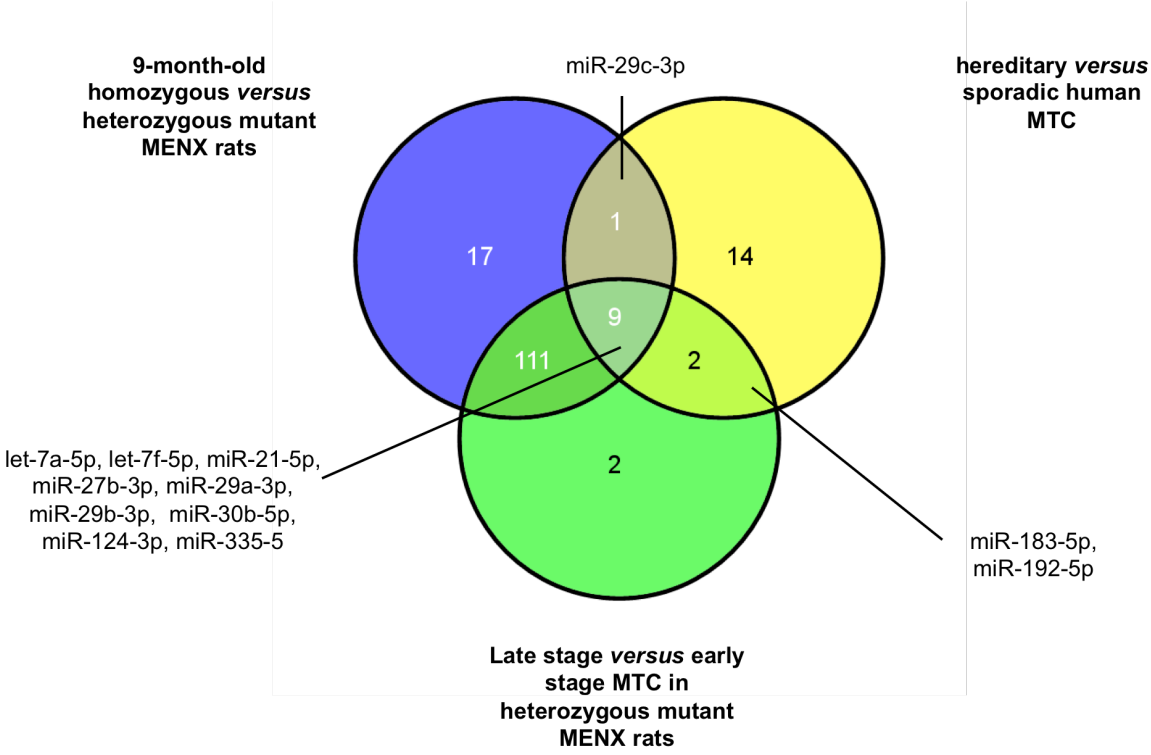

Figure 20: Venn diagram of investigated miRNA signatures. The diagram shows the overlap in miRNA expression between comparisons: 9 month-old homozygous *versus* age-matched heterozygous mutant rats (blue); 18 month-old heterozygous and 9 month-old heterozygous mutant rats (green); human hereditary *versus* sporadic MTC (yellow).

The early onset of MTC in homozygous mutant rats indicates that the loss of p27 expression is an initiating event. The loss of p27 expression leads to generation of MTC with an earlier onset, which is already evident in MENX rats at the age 2 months as indicated in Figure 9. Unfortunately, without the comparison to normal C-cells of wild-type littermates, the precise mechanisms of tumour initiation of MTC in MENX rats remain elusive.

The comparison between the miRNA signature of heterozygous rats (progression) and the human miRNA expression signature revealed a common differential expression of miR-183-5p and miR-192-5p. Interestingly, the only common differential expression found in the comparison of the miRNA expression signature of homozygous mutant MENX rats and the

miRNA expression signature of human MTCs revealed miR-29c-3p as a common deregulated miRNA.

A significant overlap was identified between all three miRNA signature comparisons, totalling to nine miRNAs. These include let-7a-5p, let-7f-5p, miR-21-5p, miR-27b-3p, miR-29a-3p, miR-29b-3p, miR-30b-5p, miR-124-3p as well as miR-335-3p. The degree of overlap observed includes 35% of the significantly differentially expressed miRNAs in human MTC. Interestingly, according to the Sanger miRBase database (version 21), the common differentially expressed miRNAs are conserved across both rats and humans, further implicating basic oncogenic mechanisms of MTC in both species.

Table 36: Common differentially expressed miRNAs in human and MENX rat MTC. Differentially expressed miRNAs are shown with respective fold changes in human and MENX rat MTC miRNA expression profiles.

miRNA	fold change hereditary *versus* sporadic MTC	fold change homozygous *versus* age-matched heterozygous mutant rats	fold change late stage *versus* early stage MTC in heterozygous mutant rats
let-7a-5p	-1.85	-6.46	-7.76
let-7f-5p	-3.48	-5.46	-5.76
miR-21-5p	-3.56	-11.96	-8.00
miR-26b-5p	-4.86	-5.52	-7.04
miR-29a-3p	-2.27	-49.71	-18.35
miR-29b-3p	-2.33	-14.38	-5.39
miR-30b-5p	-2.09	-6.58	-5.89
miR-124-3p	-11.94	-4.07	5.50
miR-335-5p	-10.83	-5.01	-3.51

Table 36 shows the fold changes of the deregulated miRNAs detected in all obtained comparisons. The most significantly differentially expressed miRNA in the hereditary human signature was miR-124-3p. Additionally, the differential expression of miR-124-3p was observed in rat miRNA expression comparisons, making it an interesting candidate for further analysis. Furthermore, members of the miR-29 family showed an extensive differential expression in rat and human miRNA expression comparisons making them also interesting candidates for further studies.

Expression of the miR-29 family was significantly downregulated in human hereditary MTC and represents the only globally deregulated miRNA family among common significantly differentially expressed miRNAs. A significantly differential expression of members of the

miR-29 family was noticed in the miRNA signatures of thyroid tumours of homozygous mutant rats and also in progressed tumours of heterozygous mutant rats. It is interesting to note that the expression of miR-124-3p in thyroid tumours of heterozygous mutant rats increases with progression in late stage MTC. In contrast, a decrease in expression in tumours of homozygous mutant rats and in the human miRNA signature was observed.

The established deregulation and validated expression of miR-29 and miR-124-3p in human and MENX rat MTC as well as the functional role suggested by IPA make these miRNAs ideal candidates for further study.

4.3.2 The expression of p27 in human MTC

Due to the high similarities in miRNA expression between rat and human MTCs, human specimens were further examined by immunohistochemistry for the expression of p27. Constitutively active RET correlates with reduced p27 expression and activity, indicating that p27 is a key regulator in the development of MTC (Joshi *et al.* 2007, Knight *et al.* 2011). Since the expression of miRNAs shows an expression dependent on the p27 levels in rats, human MTC tumour samples were stained for p27 in order to determine further similarities.

Investigating the p27 expression in human MTC revealed a differential expression of p27 in hereditary *versus* sporadic MTC. As seen in Figure 21, a reduced immunoreactivity was observed in the tumours areas of hereditary MTC, when compared to sporadic MTC specimens. The number of positively-stained nuclei and the intensity of the staining was lower in hereditary *versus* sporadic MTC.

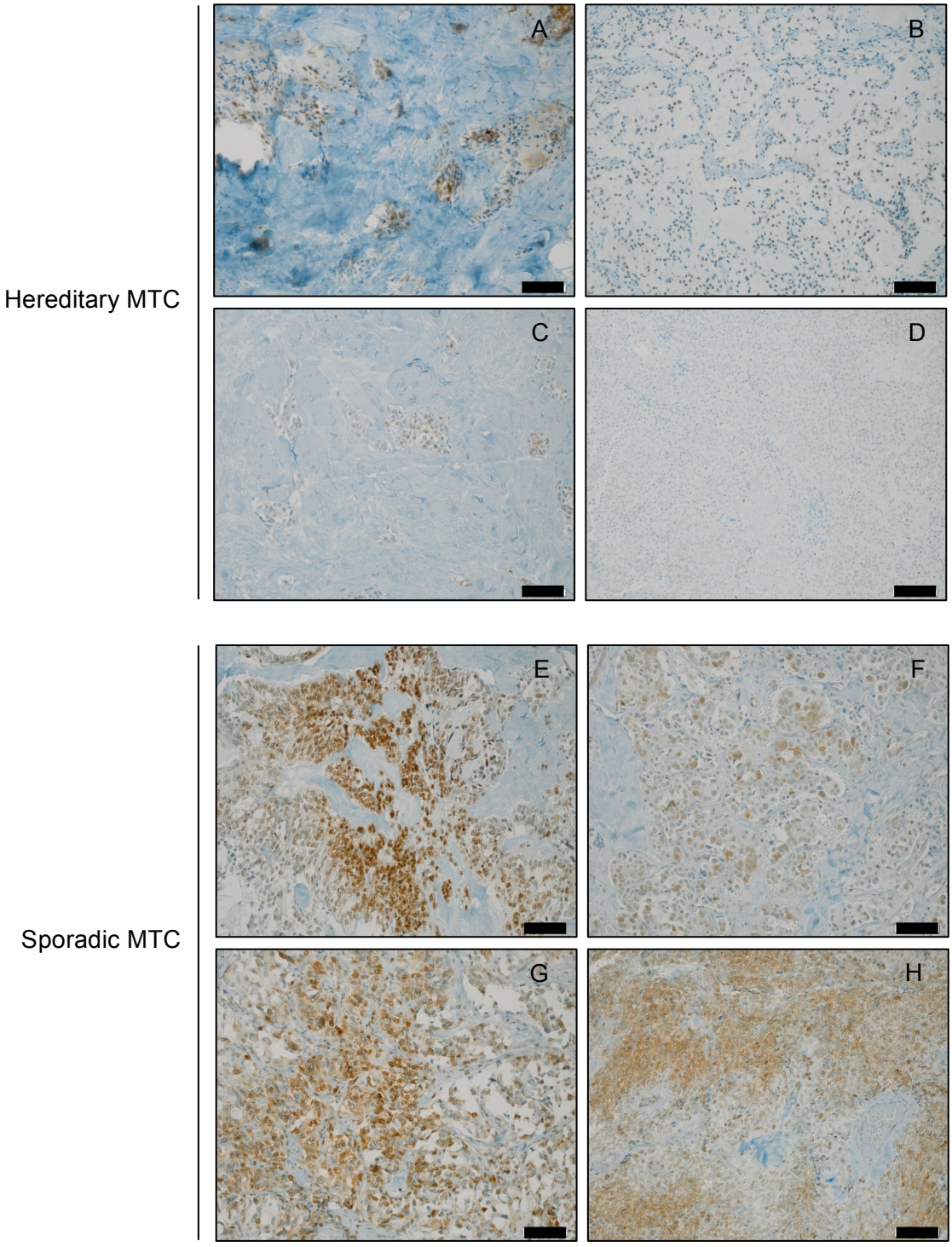

Figure 21: Staining of p27 in MTC specimens. The specific antibody bindings are localised through DAB staining (brown) and counterstained with haematoxylin (blue). **A-D:** p27 staining of hereditary MTC from patients Her_F_1, Her_F_2, Her_F_6 and Her_M_6. **E-H:** p27 staining of sporadic MTC from patients Spor_F_6, Spor_F_7, Spor_F_8 and Spor_M_7. The scale bar indicates a length of 50 microns. (Original Magnification: 200x).

4.4 Functional relevance of miRNAs in MTC

The profiling of thyroid tumours identified miRNAs that discriminate between hereditary and sporadic MTC. In addition, the miRNA expression signatures in thyroid tumours of MENX rats allow the discrimination between genotypes and between late and early stage tumours, with respect to progression. The deregulated expression of specific miRNAs in the more aggressive hereditary tumours in comparison to the less aggressive sporadic tumours, as well as the miRNA signatures of thyroid tumours of MENX rats prompted the investigation of the functional role of differentially expressed miRNAs in the development of MTC.

Among the miRNAs that seem to be involved in MTC we selected the miR-29 family and miR-124-3p for further investigations. The profiling of human MTC identified miR-124-3p as the most differentially expressed miRNA in hereditary *versus* sporadic human MTC (see Figure 17). Furthermore, differential expression of miR-124-3p was observed in the miRNA expression comparisons in tumours of MENX rats. MiRNA profiling identified miR-29 family members as the most differentially expression miRNA family among the significantly downregulated miRNAs in both human and MENX rat miRNA signatures (see Figure 20). The role of these miRNAs in the tumourigenesis of MTC was determined by *in vitro* functional analysis.

The causal analysis with the IPA Downstream Effects Analysis of miRNA signatures in both human and rat MTC shows the enrichment of miRNAs involved in cell growth and proliferation, as well as cell migration and cell invasion. Previous studies found a correlation between the downregulation of miR-29 family members with an increase in cell proliferation in malignancies such as gastric cancer (Gong *et al.* 2014, Jiang *et al.* 2014). Other studies have associated a differential expression of members of the miR-29 family with cell migration and invasion in prostate and lung cancer (Plaisier *et al.* 2012, Nishikawa *et al.* 2014). In addition, a change in miR-124-3p expression was also linked to an increase in cell proliferation in gastric cancer (Xie *et al.* 2014). Furthermore, the differential expression of miR-124-3p were linked to a change in cell migration and invasion in endometrial, breast and gastric cancers (Han *et al.* 2013, Li *et al.* 2014, Xie *et al.* 2014). Based on previous studies published in peer-reviewed literature and the high level information obtained by IPA, the influence of miR-29 family members and miR-124-3p on cell proliferation, cell migration and cell invasion was therefore investigated.

4.4.1 Downregulation of miRNAs in MTC cell lines

We decided to modulate the expression level of miR-29 family members and miR-124-3p in order to conduct functional analysis. Before conducting *in vitro* experiments, we assessed the expression of the members of the miR-29 family and miR-124-3p after transfection with specific miRNA inhibitors in order to determine the knockdown efficiency of endogenous miRNAs. According to the manufacturer, the miRNA inhibitors are small, chemically modified single-stranded RNA molecules designed to specifically bind and inhibit a selected endogenous miRNA molecule and enable miRNA functional analysis by downregulation of miRNA activity. The two MTC cell lines TT and 6-23 MTC were therefore transfected with a specific miRNA expression inhibitor directed towards the expression of members of the miR-29 family to determine the knockdown efficiency. Cells transfected with an unspecific control miRNA inhibitor were treated as control. The knockdown efficiency was determined by quantitative RT-PCR 48 h after transfection.

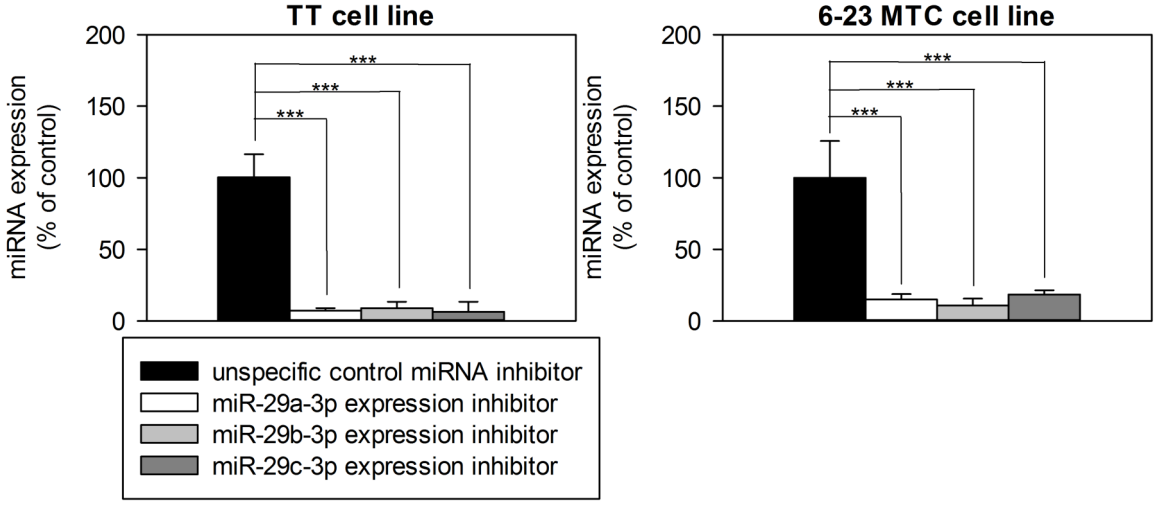

Figure 22: Downregulation efficiency of miR-29 family members in MTC cell lines. MTC cell lines TT and 6-23 MTC were transfected with specific miRNA inhibitors repressing the endogenous expression of miR-29 family members. Cells transfected with the unspecific control miRNA inhibitor were treated as control. The expression of transfected cells was analysed with quantitative RT-PCR and normalised with the corresponding U6 snRNA transcription levels using a comparative Ct method (Livak *et al.* 2001, Pfaffl 2001). The data of three independent experiments are summarised. Downregulation efficiencies (mean ±S.D.) are expressed as percentage of control (set as 100%) (**#**= not significant; *= p-value <0.05; **= p-value < 0.01; ***= p-value < 0.001).

Figure 22 shows that the expression of miR-29a-3p, miR-29b-3p and miR-29c-3p were reduced to 7.20%, 8.97% and 6.42% in TT cell line, respectively, and 14.88%, 10.77% and 18.53%, respectively, in the 6-23 MTC cell line, when compare to the control (set as 100%).

Prior to investigating the influence of miR-124-3p on the tumourigenesis of MTC cells, the efficacy of the miR-124-3p inhibitor mediated downregulation was determined. As described

above MTC cell lines were transfected with a specific miRNA inhibitor directed towards the endogenous miR-124-3p expression. Cells transfected with the unspecific miRNA inhibitor were treated as control.

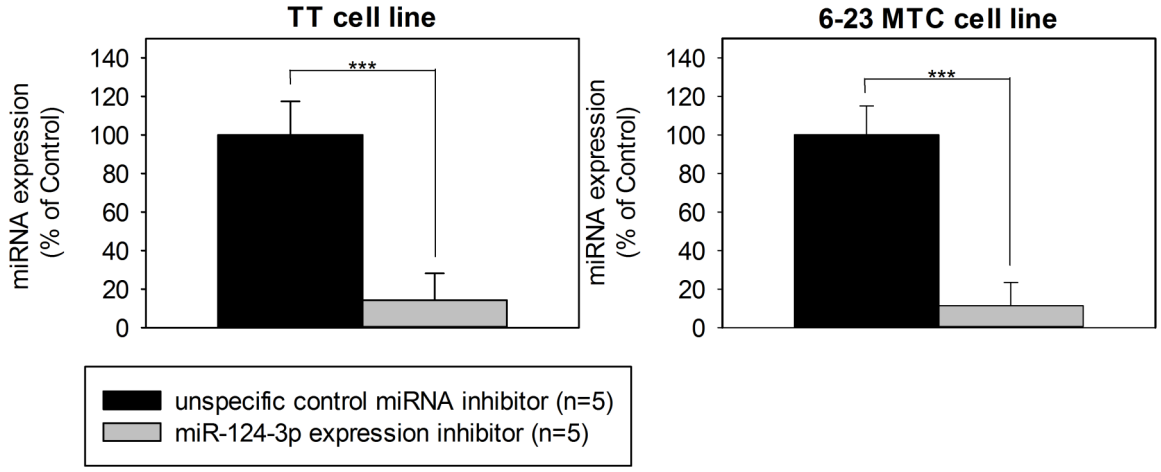

Figure 23: Downregulation of miR-124-3p in MTC cell lines. MTC cell lines TT and 6-23 MTC were transfected with specific miRNA inhibitors repressing the endogenous expression of miR-124-3p. Cells transfected with the unspecific control miRNA inhibitor were treated as control. The expression of transfected cells was analysed with quantitative RT-PCR and normalised with the corresponding U6 snRNA transcription levels using a comparative Ct method (Livak *et al.* 2001, Pfaffl 2001). The data of three independent experiments are summarised. Downregulation efficiencies (mean ±S.D.) are expressed as percentage of control (set as 100%) (#= not significant; *= p-value <0.05; **= p-value < 0.01; ***= p-value < 0.001).

Figure 23 shows that the endogenous expression of miR-124-3p was reduced to 14.24% in TT cells and 11.40% in 6-23 MTC cells, when compared to the control (set as 100%). In summary, the expression of miR-29 family members and miR-124-3p was reduced sufficiently by specific miRNA inhibitors in both MTC cell lines for use in the functional role analysis of differentially expressed miRNAs *in vitro*.

4.4.2 The influence of deregulated miRNAs on cell proliferation

An increase in proliferation is considered a hallmark of cancer (Hanahan *et al.* 2000). IPA Downstream Effects Analysis of miRNA array data, suggests extensive alteration of cell growth and proliferation during MTC pathogenesis. Therefore, the influence of the significantly differentially expressed miR-29 family members and miR-124-3p on cell proliferation was investigated.

The MTT assay measures cell viability by reducing MTT to its formazan salt through metabolic enzymes. An increase in cell viability is therefore accompanied with an increase in metabolic activity (Mosmann 1983, Berridge *et al.* 1993, Berridge *et al.* 2005). It is assumed that cell proliferation increases with cell viability and therefore the MTT assay helps to

determine the influence of the miR-29 family and miR-124-3p on the cell proliferation of MTC cells (Huyck *et al.* 2012). In order to conduct the MTT assay, the expression levels of miR-29 family members were downregulated through the transfection with specific miRNA inhibitors. Cells transfected with the unspecific control miRNA inhibitor were treated as control. After a 48 h incubation period, the MTT assay was conducted.

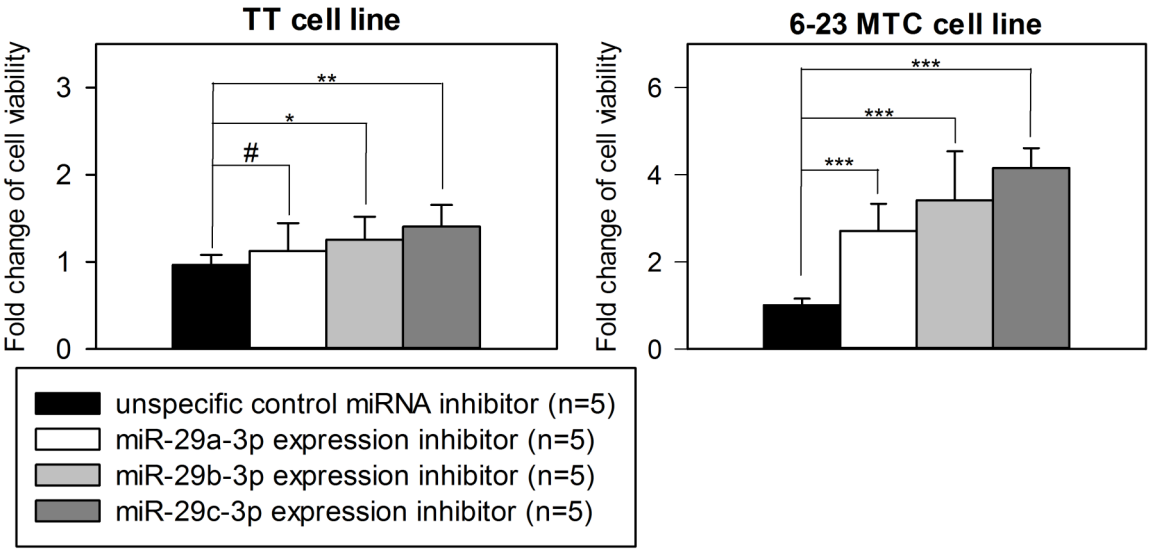

Figure 24: Cell viability of MTC cells after miR-29 family downregulation. In the MTC cell lines, TT and 6-23 MTC, the endogenous expression of miR-29 family members was downregulated. Cells transfected with the unspecific miRNA control inhibitor were treated as control. After a 48 h incubation period, transfected cells were treated with MTT and cell viability was measured optically after 4 h. Differences in cell viability are expressed as the fold change ±S.D. relative to the control and is representative of three different experiments performed (#= not significant; *= p-value <0.05; **= p-value < 0.01; ***= p-value < 0.001).

In TT cells, with exception of miR-29a-3p, the knockdown of members of the miR-29 family led increase in cell proliferation, when compared to the unspecific control (Figure 24). The increase in cell viability observed upon inhibiting the expression of miR-29b-3p (1.26 fold) and miR-29c-3p (1.40 fold) inhibition was significant. In 6-23 MTC cells, the increase in cell viability measured upon the downregulation of miR-29a-3p (2.71 fold), miR-29b-3p (3.41 fold) and miR-29c-3p (4.15 fold) was significant, when compared to control (Figure 24).

To complement the investigation of differentially expressed miRNAs on cell proliferation, the endogenous expression of miR-124-3p in MTC cell lines was downregulated with a specific miRNA expression inhibitor. Cells transfected with the unspecific control miRNA inhibitor were treated as control and the MTT assay was conducted as described above.

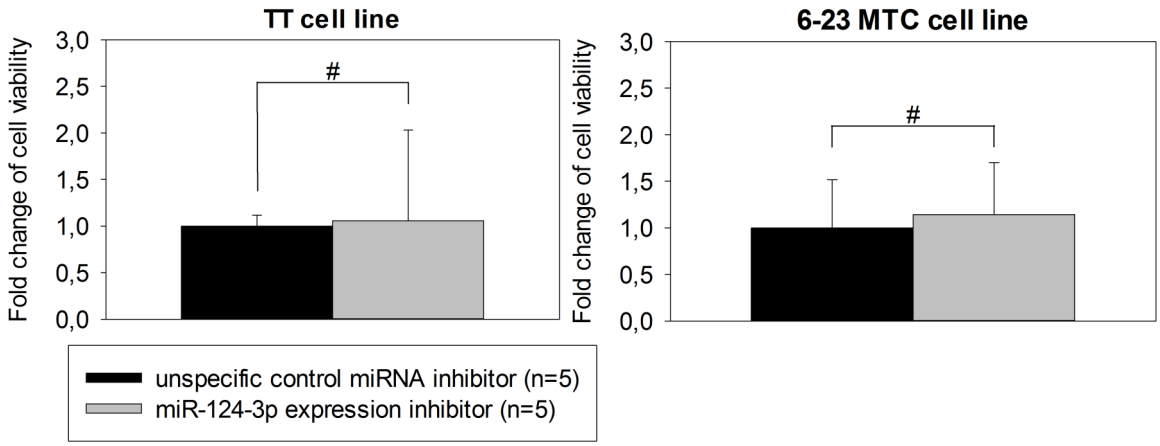

Figure 25: Cell viability of MTC cell lines after miR-124-3p downregulation. In the MTC cell lines, TT and 6-23 MTC, the endogenous expression of 124-3p was downregulated. Cells transfected with the unspecific miRNA control inhibitor were treated as control. After a 48 h incubation period, transfected cells were treated with MTT and cell viability was measured optically after 4 h. Differences in cell viability are expressed as the fold change ±S.D. relative to the control and is representative of three independent experiments performed (**#=** not significant; *= p-value <0.05; **= p-value < 0.01; ***= p-value < 0.001).

The downregulation of miR-124-3p induced no significant change in cell viability in both TT (1.06 fold) and 6-23 MTC (1.14 fold) cell lines, when compared to the control (Figure 25). Our studies revealed that only the modulation of miR-29 family members affects cell viability, therefore, based on the assumption that cell viability is related to cell proliferation, a change in expression of miR-29 family members affects MTC cell proliferation.

4.4.3 The influence of differentially expressed miRNAs on cell migration

Among the biological activities downstream of the differentially expressed miRNAs in rat and human MTC, cell migration was among the enriched high level functional categories, as determined by the IPA Downstream Effects Analysis. Any changes in cell migration may be measured with the migration assay, in which the hypoxic and nutrient-deficient conditions in the tumour are simulated. The migrations assay analyses the speed at which the cells migrate, as well as the chemotactic effects and therefore gives an accurate indication of the influence of the differentially expressed miRNAs of the miR-29 family or miR-124-3p on cell migration in MTC (Toetsch *et al.* 2009). In order to minimise the diffusion of nutrients between the two compartments, the cell migration was measured after 48 h.

For the purpose of conducting a migration assay, the endogenous expression of miR-29 family members in MTC cell lines was downregulated by transfection using specific miRNA expression inhibitors. In addition, cells were transfected with an unspecific control miRNA Inhibitor serving as control.

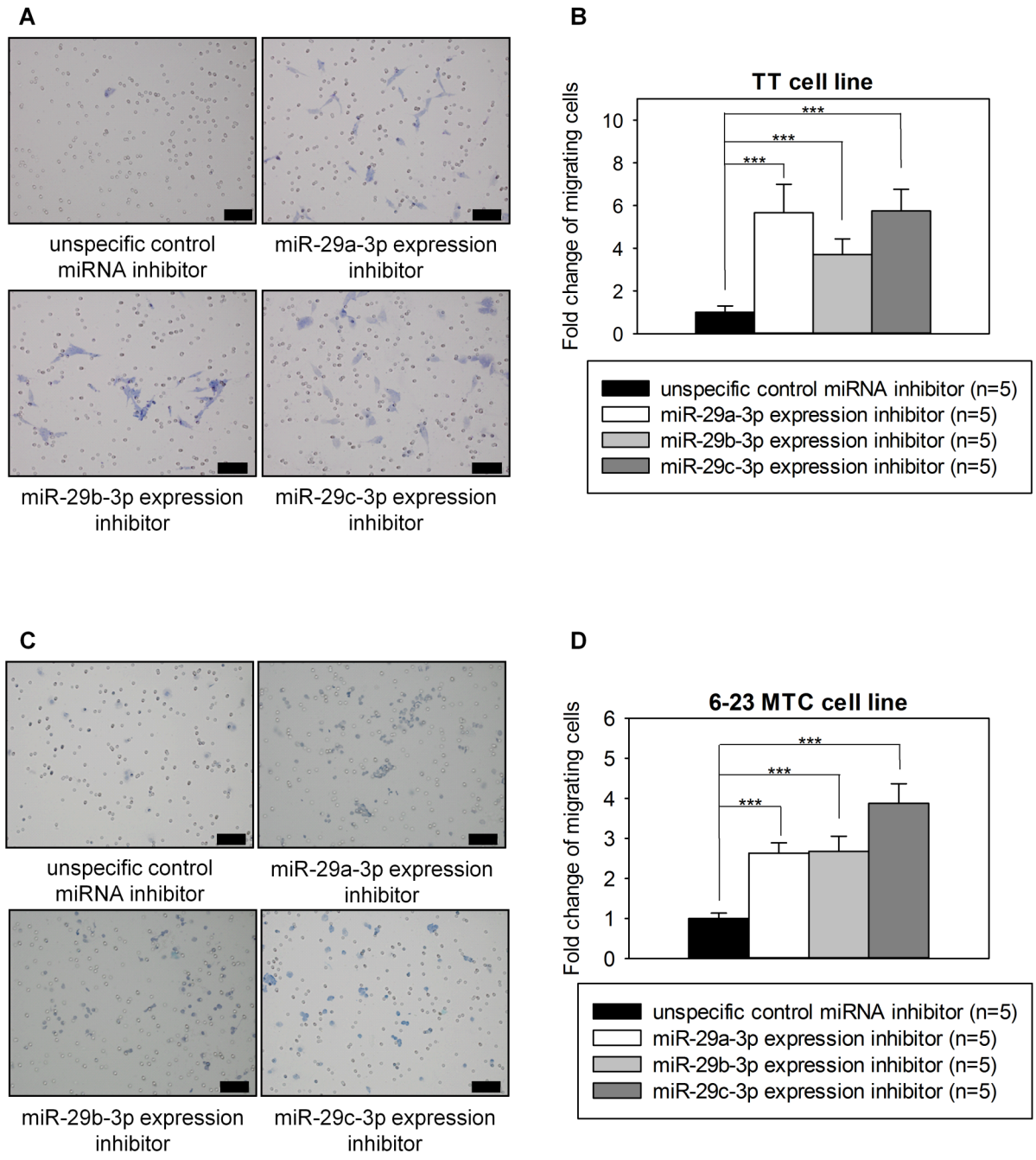

Figure 26: Cell migration of MTC cell lines after miR-29 family downregulation. MTC cell lines TT and 6-23 MTC were transfected with specific miRNA inhibitors repressing the endogenous expression of miR-29 family members. Cells transfected with the unspecific control miRNA inhibitor were treated as control. **A:** Images display the bottom of side of the filter inserts of TT cells (stained in blue) that migrated through the pores. **B:** Data of migrating TT cells summarised **C:** Images display the bottom of side of the filter inserts of 6-23 MTC cells (stained in blue) that migrated through the pores. **D:** Data of 6-23 MTC cells summarised. Differences in cell migration are expressed as the fold change ±S.D. relative to the control and is representative of three idenpendent experiments performed (#= not significant; *= p-value <0.05; **= p-value < 0.01; ***= p-value < 0.001). The scale bar indicates a length of 50 microns (Original Magnification: 200x).

After normalisation to the unspecific control miRNA inhibitor, the migrating TT cells were quantified. A significant increase was observed upon the downregulation of the endogenous

expression of miR-29a-3p (5.66 fold), miR-29b-3p (3.70 fold) and miR-29c-3p (5.74 fold), when compared to the control (Figure 26). A similar trend in the increase of migration upon the downregulation of miR-29a-3p (2.69 fold), miR-29b-3p (2.68 fold) and miR-29c-3p (3.78 fold) was observed in 6-23 MTC cells, when compared to the control (Figure 26).

Causal analysis implies that the differentially expressed miR-124-3p regulates cell migration in MTCs. To investigate the influence of migration, the endogenous expression of miR-124-3p was downregulated in MTC cell lines and a migration assay was conducted as described. Cells transfected with the unspecific control miRNA inhibitor served as control.

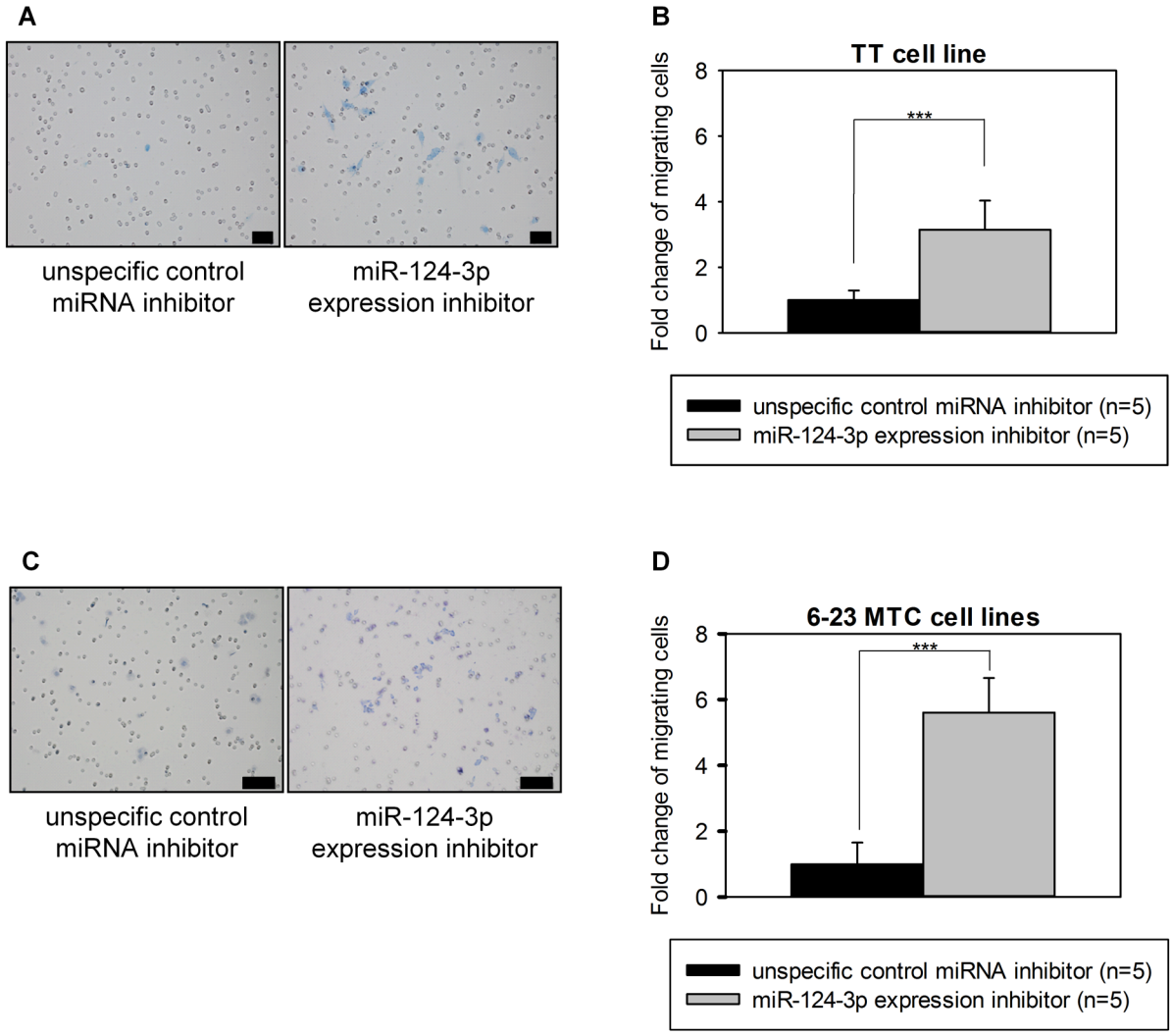

Figure 27: Cell migration of MTC cell lines after miR-124-3p downregulation. MTC cell lines TT and 6-23 MTC were transfected with a specific miRNA inhibitor repressing the endogenous expression of miR-124-3p. Cells transfected with the unspecific control miRNA inhibitor were treated as control. **A:** Images display the bottom of side of the filter inserts of TT cells (stained in blue) that migrated through the pores. **B:** Data of migrating TT cells summarised **C:** Images display the bottom of side of the filter inserts of 6-23 MTC cells (stained in blue) that migrated through the pores. **D:** Data of migrating 6-23 MTC cells summarised. Differences in cell migration are expressed as the fold change ±S.D. relative to the control and is representative of three different experiments performed (#= not significant; *= p-value <0.05; **= p-value < 0.01; ***= p-value < 0.001). The scale bar indicates a length of 50 microns (Original Magnification: 200x).

Following the knockdown of the endogenous miR-124-3p expression in the TT cell line, a significant increase in migration (3.15 fold), when compared to the control (Figure 27). Similar results were obtained in 6-23 MTC cells, where an increase in migration (5.61 fold) upon miR-124-3p knockdown was observed in relation to the control (Figure 27). Collectively, these results suggest that miR-29 family members and miR-124-3p participate in the regulation of MTC cells migration.

4.4.4 The influence of differentially expressed miRNAs on cell invasion

For cancer cells to successfully metastasise, an increase in cell motility has to be achieved through epidermal-mesenchymal-transition (EMT). During EMT epithelial cells are converted to migratory and invasive cells. This process is considered to be fundamental in the generation of tissues and organs during embryogenesis. A similar process happens during wound healing in adults (De Craene *et al.* 2013). More than 10 years ago, it was demonstrated that EMT is closely related to cancer progression (Thiery 2002). In addition to the transition to a migratory phenotype, the basal membrane needs to be penetrated. Invading cells overcome the basal membrane by secreting a wide array of proteases that degrade the ECM (Nguyen *et al.* 2007).

To investigate the influence of differentially expressed miRNAs on invasion, an invasion assay was conducted. The experimental setup is very similar to the migration assay with the exception that the porous membranes of the Boyden chamber are obstructed by Matrigel®. Matrigel® is composed of materials such as collagens, laminins, fibronectin that simulates key components of the ECM (Toetsch *et al.* 2009).

Similar to the migration assay, a diffusion of nutrients is also observed in the invasion assay. This diffusion flattens the gradient of nutrients established between the two compartments of the chamber (Toetsch *et al.* 2009). In order to minimise the diffusion of nutrients between the two compartments, the cell migration was measured after 48 h.

For the purpose of conducting an invasion assay, the endogenous expression of miR-29 family members in MTC cell lines was downregulated by transfection using specific miRNA expression inhibitors. In addition, cells transfected with an unspecific control miRNA inhibitor served as control. The invasion assay was conducted 48 h post transfection and evaluated after 48 h.

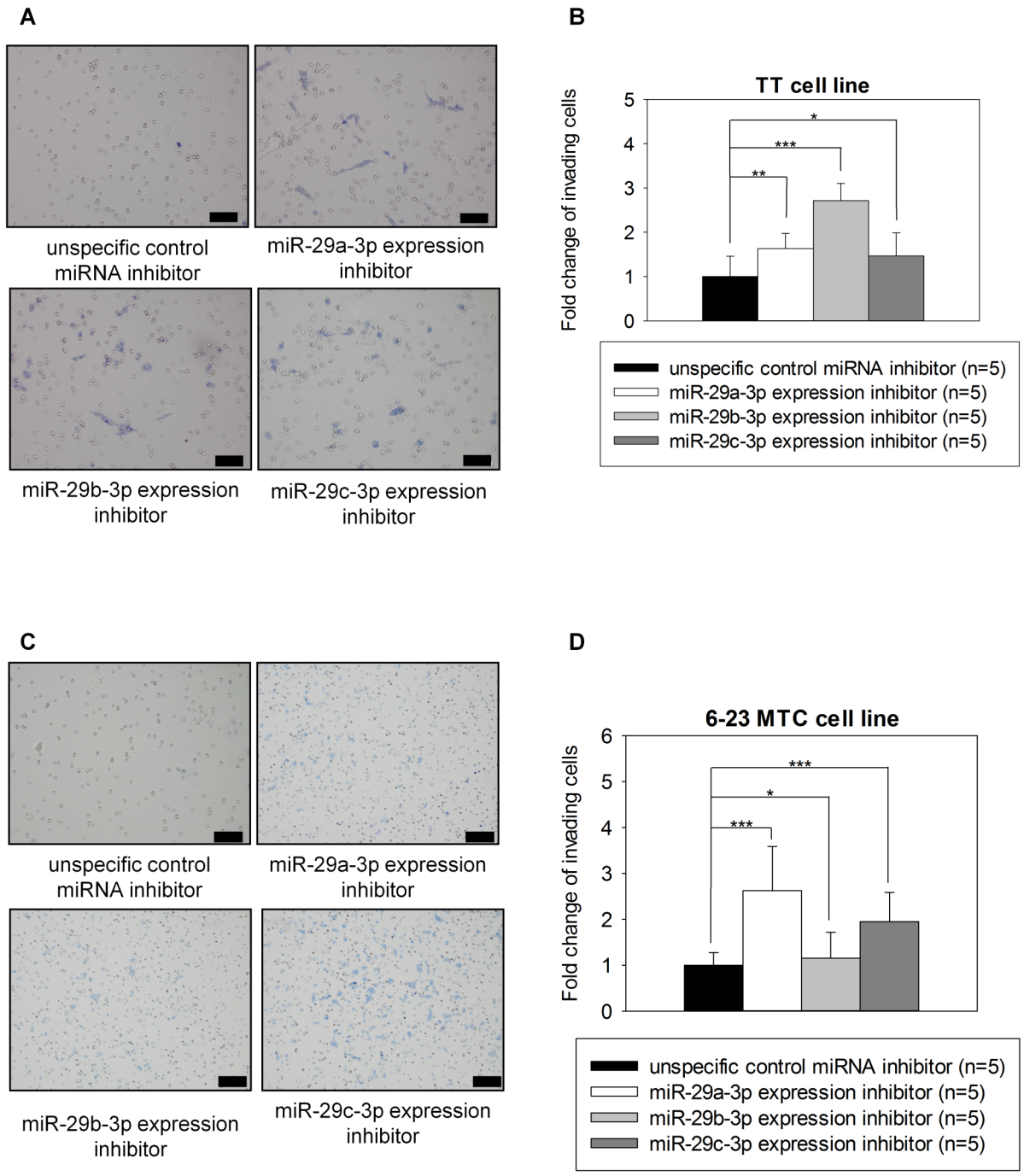

Figure 28: Cell invasion of MTC cell lines after miR-29 family downregulation. MTC cell lines TT and 6-23 MTC were transfected with specific miRNA inhibitors repressing the endogenous expression of miR-29 family members. Cells transfected with the unspecific control miRNA inhibitor were treated as control. **A:** Images display the bottom of side of the filter inserts of TT cells (stained in blue) that invaded and migrated through the pores. **B:** Data of invading TT cells summarised **C:** Images display the bottom of side of the filter inserts of 6-23 MTC cells (stained in blue) that invaded and migrated through the pores. **D:** Data of invading 6-23 MTC cells summarised. Differences in cell invasion are expressed as the fold change ±S.D. relative to the control and is representative of three different experiments performed (#= not significant; *= p-value <0.05; **= p-value < 0.01; ***= p-value < 0.001). The scale bar indicates a length of 50 microns (Original Magnification: 200x).

A significant increase in invading cells was observed upon the downregulation of miR-29a-3p (1.63 fold), miR-29b-3p (2.71 fold) and miR-29c-3p (1.46 fold), in comparison to the control in

the TT cell line (Figure 28). A similar trend was observed in 6-23 MTC cells, where the downregulation of the endogenous expression of miR-29a-3p (2.62 fold), miR-29b-3p (1.16 fold) and miR-29c-3p (1.95 fold) led to significant increase in invasion, when compared to the control (Figure 28).

To investigate the effect of miR-124-3p on invasion, the TT and the 6-23 MTC cell lines were transfected with the specific inhibitor against the expression of miR-124-3p, while cells transfected with unspecific control miRNA inhibitor served as control

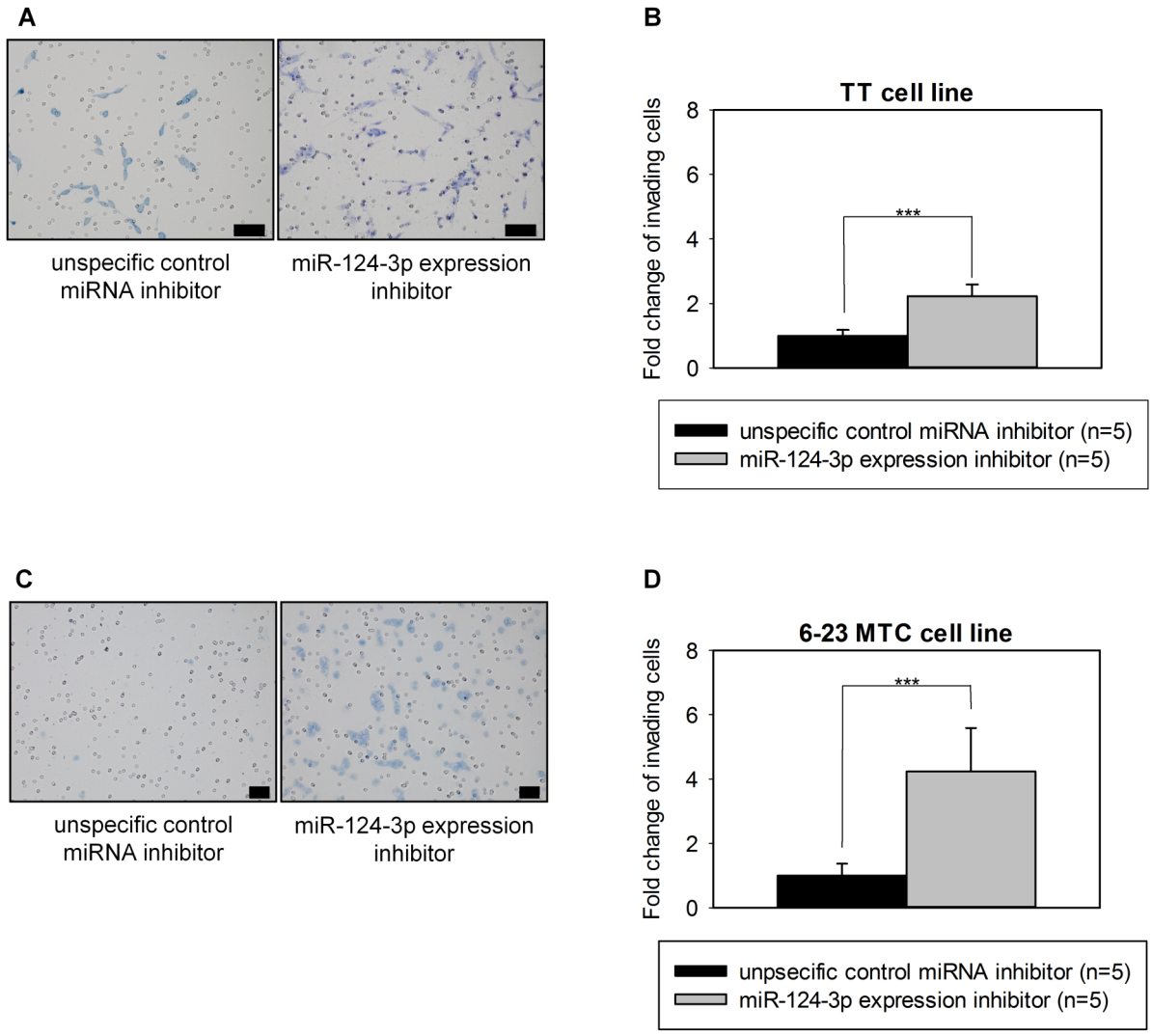

Figure 29: Cell invasion of MTC cell lines after miR-124-3p downregulation. MTC cell lines TT and 6-23 MTC were transfected with a specific miRNA inhibitor repressing the endogenous expression of miR-124-3p. Cells transfected with the unspecific control miRNA inhibitor were treated as control. **A:** Images display the bottom of side of the filter inserts of TT cells (stained in blue) that migrated through the pores. **B:** Data of invading TT cells summarised **C:** Images display the bottom of side of the filter inserts of 6-23 MTC cells (stained in blue) that invaded and migrated through the pores. **D:** Data of invading 6-23 MTC cells summarised. Differences in cell invasion are expressed as the fold change ±S.D. relative to the control and is representative of three different experiments performed (#= not significant; *= p-value <0.05; **= p-value < 0.01; ***= p-value < 0.001). The scale bar indicates a length of 50 microns (Original Magnification: 200x).

A significant increase in invading cells (2.22 fold) was observed in TT cells upon transfection with a miR-124-3p expression inhibitor, when compared to the control (Figure 29). This trend was also observed in 6-23 MTC cells after the transfection with a miR-124-3p specific inhibitor, where a significant increase (4.23 fold) was observed in relation to the control.

Altogether, the downregulation of miR-29 expression corresponds to an increase in cell invasion in both cell lines. Upon downregulation of miR-124-3p a significant increase in cell invasion was observed in TT and 6-23 MTC cells. Collectively, the data suggests that both miR-124-3p and members of the miR-29 family are involved in the regulation of cell migration and invasion.

4.5 Identification of target genes of differentially expressed miRNAs

4.5.1 *In silico* identification of target genes

The miRNA expression analysis of both human and rat MTC revealed a significant differential expression of the miR-29 family and miR-124-3p. Functional assays *in vitro* showed that downregulation of miR-29 family members and miR-124-3p promotes invasion and migration of MTC cells.

To fully understand the role of miR-29 family in the tumourigenesis of MTC, the biological targets of these miRNAs have to be determined. Initially, the prediction software PicTar, miRanda and TargetScan were used to predict the mRNA targets of miR-29 family members. To strengthen the search, the common target genes were cross-referenced with the target prediction algorithm of IPA. Only target genes identified by all four prediction algorithms were considered.

Table 37: Predicted biological targets of miR-29a-3p. Common human target genes of miR-29a-3p using prediction algorithms PicTar, miRanda, TargetScan and IPA.

ABCB6	*BCL2L2*	*BMF*	*CALCR*	*CX3CL1*	*EIF4E2*
ELF2	*EMP1*	*FSTL1*	*GOLGA7*	*GPR37*	*HAS3*
IREB2	*KIFC2*	*LAMC1*	*LASP1*	*LPL*	*NAP1L3*
PALM	*PCDHA1*	*PCDHA10*	*PCDHA11*	*PCDHA12*	*PCDHA13*
PCDHA2	*PCDHA3*	*PCDHA4*	*PCDHA6*	*PCDHA8*	*PCDHAC1*
PCDHAC2	*PMP22*	*RAB30*	*RNF39*	*SGK*	*SYT7*
TFEB	*TNFRSF1A*				

Table 38: Predicted biological targets of miR-29b-3p. Common human target genes of miR-29b-3p using prediction algorithms PicTar, miRanda, TargetScan and IPA.

AQP4	*BLMH*	*BTG2*	*CBX6*	*COL3A1*	*COL4A4*
DRD1	*DUSP2*	*GPR85*	*HBP1*	*HMGCS1*	*HNRPF*
IFI30	*INA*	*LAMC1*	*MAP2K6*	*MMP2*	*PAIP2*
RERE	*SPARC*	*TDG*			

Table 39: Predicted biological targets of miR-29c. Common human target genes of miR-29c using prediction algorithms PicTar, miRanda, TargetScan and IPA.

ABCB6	*AGPAT4*	*AHR*	*ARF5*	*ATP1B1*	*ATRN*
BAIAP2	*BCL2L2*	*BLMH*	*BMF*	*BTG2*	*CALCR*
CAPN7	*CBX6*	*COL3A1*	*COL4A4*	*CORO6*	*CX3CL1*
DAB2IP	*DIABLO*	*DNAJB11*	*DRD1*	*DUSP2*	*EIF4E*
ELF2	*EMP1*	*FOS*	*FSTL1*	*GOLGA7*	*GPR37*
GPR85	*HBP1*	*HMGCR*	*HMGCS1*	*HMGN3*	*HNRNPF*
IFI30	*INA*	*INSIG1*	*IREB2*	*ITGB1*	*KCNIP2*
KIFC2	*KLF4*	*KLHDC3*	*LAMB2*	*LASP1*	*LPL*
LUZP1	*MAP2K6*	*MMP2*	*MYCN*	*NAP1L3*	*NCOA4*
NFIA	*PAIP2*	*PALM*	*PARG*	*PCDHA1*	*PCDHA11*
PCDHA12	*PCDHA10*	*PCDHA13*	*PCDHA2*	*PCDHA3*	*PCDHA4*
PCDHA6	*PCDHA8*	*PCDHAC1*	*PCDHAC2*	*PDGFRB*	*PER1*
PLAG1	*PLP1*	*PMP22*	*PPIC*	*PRKRA*	*PRR3*
RAB15	*RAB30*	*RERE*	*SGK1*	*SLC16A1*	*SLC30A3*
SMPD3	*SNX24*	*SPARC*	*STRN3*	*SYT7*	*TDG*
TNFAIP1	*TNFRSF1A*	*YBX3*	*ZFP36*		

Using this approach we identified a total of 38 target genes for miR-29a-3p (Table 37), 21 target genes for miR-29b-3p (Table 38) and 94 target genes for miR-29c-3p (Table 39). To obtain an overview of the biological functions of the predicted target genes, a high level functional analysis was conducted using IPA Downstream Effects Analysis, where the area “Molecular and Cellular Functions” was chosen for investigation. The study of functional categories gives a high level overview of the biological processes of the miR-29 family putative target genes and provides a more robust analysis, rather than analysing individual target genes.

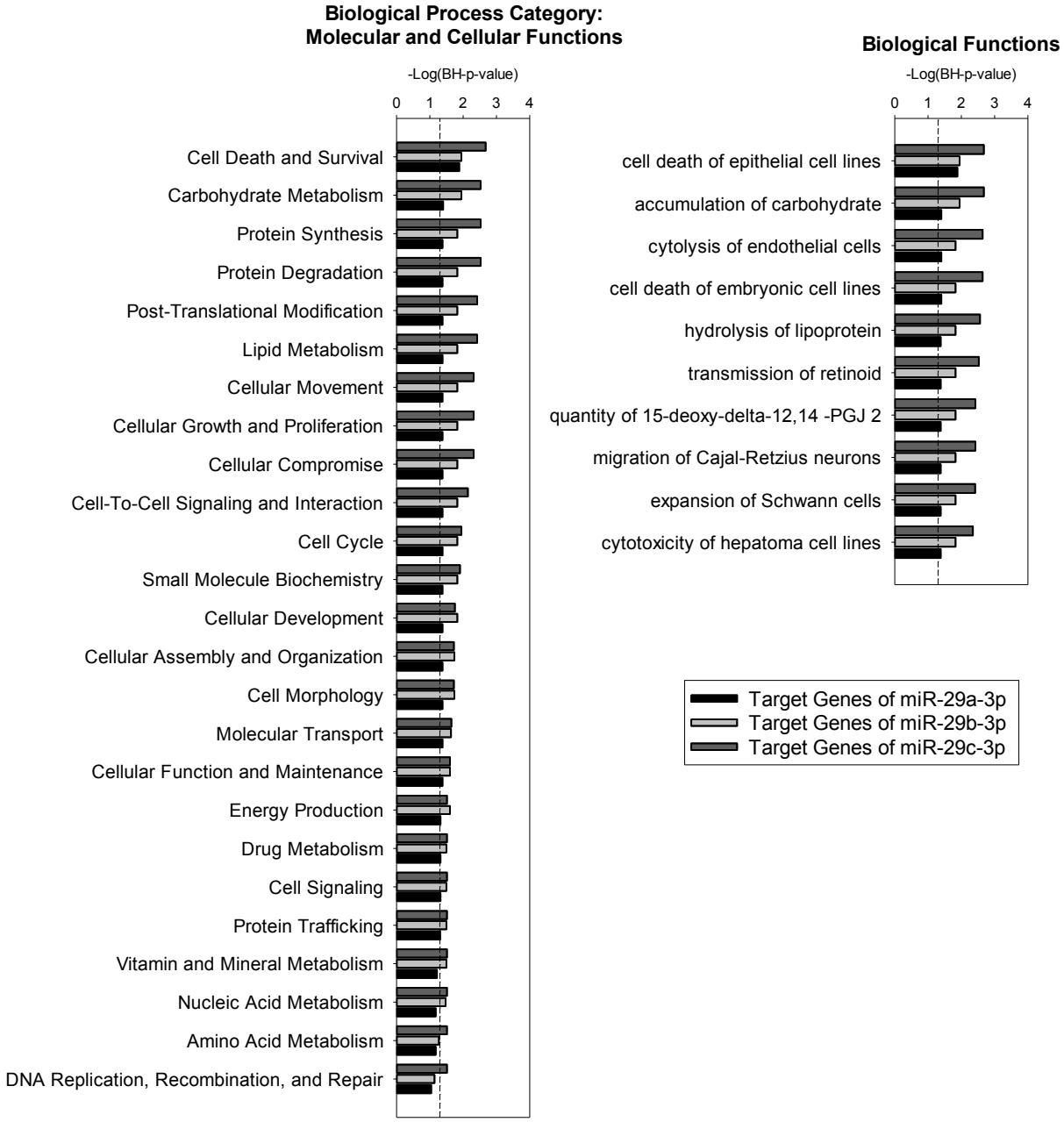

Figure 30: IPA high level function categories and biological functions of target genes of miR-29 family members. The histogram displays IPA functional categories. The y-axis reports the significance of enrichment and is plotted as log of the BH multiple testing corrected p-value calculated by IPA based on the specific data set. The dotted line is the threshold BH-p-value of 0.05.

Figure 30 shows the high level functional analysis above the threshold of a BH-p-value of <0.05, which are considered significantly enriched using the IPA Downstream Effects Analysis. Most biological targets of miR-29 family members belong to the category “Cell Death and Survival”. Other cancer relevant enriched categories are “Cellular Movement”, “Cellular Growth and Proliferation” “Cell-to-Cell Signalling and Interaction” and “Cell Cycle”. Target genes of miR-29c-3p show the strongest enrichment within the above mentioned

categories, as the sum of ascertained target genes was higher, when compared to miR-29a-3p and miR-29b-3p.

High level functional categories in the area “Molecular and Cellular Functions” were broken down into specific biological functions using the IPA Downstream Effects Analysis of miR-29 family target genes. The highest degree of enrichment was observed for the biological process “cell death of epithelial cell lines” followed by the biological functions “cell death of embryonic cell lines” (Figure 30).

Causal analysis of miR-29 family target genes using IPA Downstream Effects Analysis suggests an important role in the regulation of cell death and apoptosis. This category was also enriched in IPA Downstream Effects analysis of hereditary *versus* sporadic MTC. Our functional investigation revealed a significant increase in cell proliferation, cell migration and invasion upon the downregulation of endogenous miR-29 family members. Therefore, our functional analysis is in agreement with the causal analysis of the miR-29 family target genes, showed that the categories “Cell Growth and Proliferation” and “Cell Migration” were significantly enriched.

Our experimental analysis revealed an increase in cell migration and invasion coinciding with the downregulation of endogenous miR-124-3p expression in MTC cell lines. To fully comprehend the functional role of miR-124-3p in MTC, the biological targets were determined *in silico*. Similarly to the analysis of putative miR-29 family target genes, common target genes for miR-124-3p were obtained by employing the prediction algorithms PicTar, miRanda, TargetScan and IPA.

Table 40: Predicted biological targets of miR-124-3p. Common human target genes of miR-124-3p as determined by the prediction algorithms TargetScan, miRanda and Pictar. The target genes were cross-referenced with IPA.

AHR	*ANXA11*	*ATF7IP*	*B4GALT1*	*BMP6*	*CGN*
COL4A1	*DHCR24*	*DMRT1*	*EDNRB*	*EYA4*	*FOXQ1*
GLRB	*GRIA3*	*IQGAP1*	*KCNK10*	*KCNK2*	*KIAA1244*
LAMC1	*LEMD3*	*LHX2*	*LRRC1*	*MAPK14*	*MITF*
MYH10	*MYH9*	*P4HA1*	*PARP16*	*PCDH8*	*PDCD6*
PHF6	*PRRX1*	*PTBP2*	*PTPN9*	*PTTG1IP*	*QKI*
RAB27A	*RAD17*	*RHOA*	*RHOG*	*RNF128*	*ROCK1*
RYR2	*RYR3*	*SEMA6A*	*SEMA6D*	*SERTAD4*	*SLITRK6*
SMARCAD1	*SORD*	*SOX9*	*SPHK1*	*STAT3*	*TARBP1*
TOR3A	*TPD52L2*	*YEATS2*			

A total of 57 target genes for miR-124-3p were identified, which are shown in Table 40. A causal analysis of the biological targets of miR-124-3p was conducted using IPA Downstream Effects Analysis, where high level functional categories and biological functions were investigated.

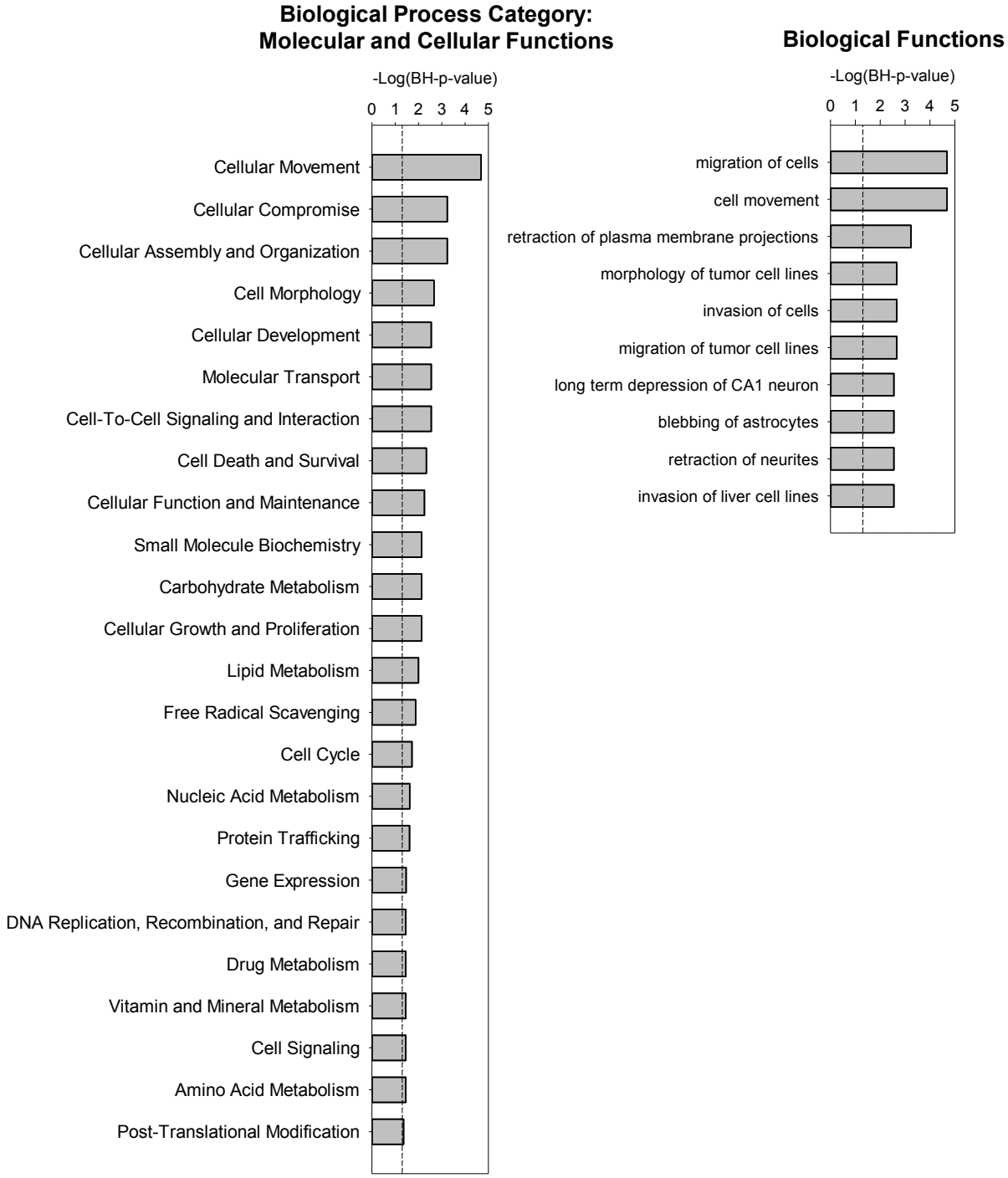

Figure 31: IPA high level functional categories and biological functions of miR-124-3p target genes. The histogram displays IPA categories and functions. The y-axis reports the significance of enrichment and is plotted as log of the BH multiple testing corrected p-value calculated by IPA based on the specific data set. The dotted line is the threshold BH-p-value of 0.05.

The target genes were analysed in the area “Molecular and Cellular Functions”. Figure 31 shows the significantly enriched high level functional categories of miR-124-3p target genes above the threshold of BH-p-value of <0.05 (indicated in the figure by the dotted line). Most target genes of miR-124-3p fall into the category “Cellular Movement”. Further enriched cancer relevant functional analysis categories include “Cell-to-Cell Signalling and Interaction”, “Cell Death and Survival” as well as “Cellular Growth and Proliferation”.

Further analysis into the biological functions of target genes of miR-124-3p identified “migration of cells” and “cell movement” as highly enriched using the IPA Downstream Effects Analysis. Furthermore, the functions “invasion of cells”, “migration of tumour cell lines” and “invasion of liver cell lines” were identified as downstream functions of the target genes of miR-124-3p.

Experimental data revealed an increase in cell migration and invasion, upon inhibition of endogenous miR-124-3p expression in MTC cell lines. In agreement with these experimental data, the IPA Downstream Analysis of target genes showed that the predicted target genes of miR-124-3p are involved in cell motility and invasion.

4.5.2 Experimental validation of target genes of miR-124-3p

MiR-124-3p displayed the highest differential expression between hereditary and sporadic MTC in humans. In addition, a differential expression of this miRNA was also observed in MTC of MENX rats, suggesting the importance of miR-124-3p in the pathogenesis of MTC.

Potential target genes of miR-124-3p were identified using four different prediction algorithms as described above. Functional analysis of the predicted biological targets with IPA identified “Cellular Movement” as the most enriched functional category in the area “Molecular and Cellular Functions”. Our experimental investigations revealed an increase in cell migration upon downregulation of endogenous miR-124-3p expression in MTC cell lines, further implying that biological targets of miR-124-3p may function in the regulation of cell migration. Table 41 shows the individual predicted biological targets in the category “Cellular Movement”.

Table 41: Target genes of miR-124-3p regulating cell motillity. Human target genes of miR-124-3p obtained by prediction algorithms PicTar, miRanda, TargetScan and IPA enriched within the high level functional category “Cellular Movement”.

ABCC4	*AHR*	*B4GALT1*	*BMP6*	*CHST1*	*COL4A1*
DMRT1	*EDNRB*	*FOXQ1*	*GLRB*	*GRIA2*	*GRIA3*
IQGAP1	*KCNK2*	*LAMC1*	*LHX2*	*MAPK14*	*MITF*
MYH9	*MYH10*	*MYRF*	*PPM1F*	*PRRX1*	*RAB27A*
RHOA	*RHOG*	*ROCK1*	*SEMA6A*	*SEMA6D*	*SERP1*
SORD	*SPHK1*	*STAT3*	*USP14*		

A direct interaction between miR-124-3p and its predicted target genes can be validated by cloning the 3’-UTR sequence of a target into a vector containing a dual-luciferase reporter gene, where a change in luciferase activity is detected upon direct interaction of the miRNA of interest with the cloned 3’-UTR. In order to verify whether selected target genes of miR-124-3p are indeed directly regulated by this miRNA, a luciferase reporter assay was conducted.

For the regulation of the target mRNA expression, the pairing of seven consecutive bases to the 5’ end of the miRNA is sufficient. This interaction is termed a 7mer seed match. A stronger regulation is observed with a 8mer seed match, where eight consecutive bases pair with the 3’-UTR of a target gene. The magnitude of regulation for 7mer and 8mer seed matches strongly increases when multiple copies of the seed matches are present in the 3’-UTR (Brennecke *et al.* 2005, Bartel 2009). Unfortunately, predicted interactions of 3’-UTR of target genes with the miRNA seed region are frequently false positive (Lewis *et al.* 2005, Bartel 2009). In order to validate an interaction between miR-124-3p and the target genes, target genes not previously listed in Table 41 were selected for the presence of either 7mer or 8mer seed matches. The target gene ras-related protein 27A *(RAB27A*) was chosen from the candidates since it contained multiple 7mer or 8mer seed matches in its 3’-UTR for miR-124-3p. In addition, the target genes *MAPK14* and sphingosine kinase 1 (*SPHK1*) were chosen for further validation since these genes have been previously reported in association with MTC and the MEN2 syndrome, respectively (Murakami *et al.* 2007, Ruiz-Llorente *et al.* 2007).

In order to validate the candidate target genes of miR-124-3p, a co-transfection of the pmiRGLO vector containing the 3’-UTR of the miRNA targets, with a specific miR-124-3p inhibitor was conducted in the TT cells. Reporter plasmids co-transfected with the unspecific control miRNA inhibitor were used as controls. The reporter gene activity was measured 48 h after transfection.

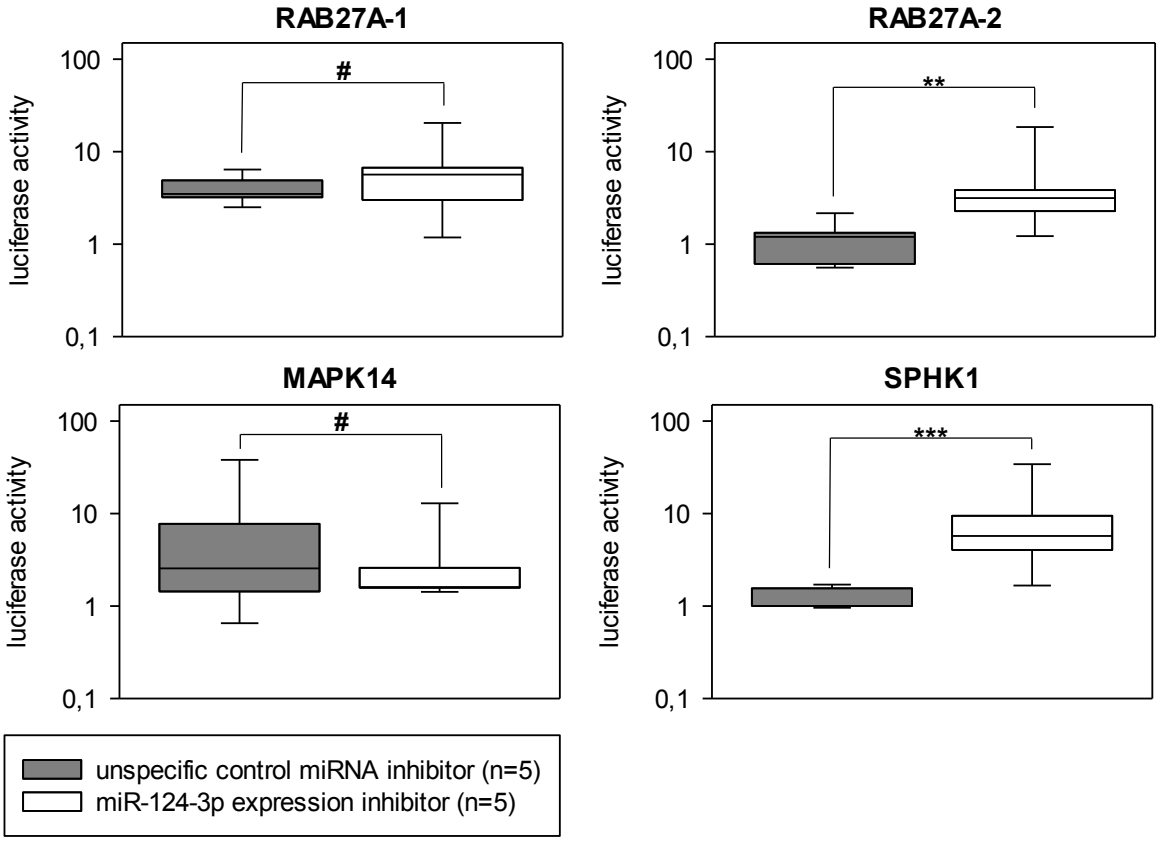

Figure 32: Validation of miR-124-3p target genes. Relative luciferase activities after a co-transfection of luciferase constructs and a specific miR-124-3p expression inhibitor in TT cells. The relative luciferase activites of cells co-transfected with the luciferase contruct and the unspecific control miRNA inhibitor served as control. Data of three independent experiments are summarised as box plots. All box plots show 25th to 75th percentiles (box) and 5th and 95th percentiles (whiskers). Solid dots are outliers below 5% and above 95%. The line in the box represents the median (#= not significant; *= p-value <0.05, **= p-value <0.01, ***= p-value <0.001).

Using luciferase reporter assays, three candidate target genes of miR-124-3p were measured. Due to the length of the 3'-UTR of *RAB27A* and the difficulties presented by cloning large DNA fragments into plasmids, the 3'-UTR was divided into two fragment named RAB27A-1 and RAB27A-2. Each of the *RAB27A* 3'-UTR fragments contain a predicted target sites for miR-124-3p. We were able to confirm the direct repression of reporter gene expression for two out of four miR-124-3p candidate target gene constructs. Figure 32 shows a significant increase in luciferase activity after the inhibition of endogenous miR-124-3p expression for constructs containing the 3'-UTR of *RAB27A* and *SPHK1*, thereby establishing these genes as direct miR-124-3p targets in TT cells.

4.6 Expression of *RAB27A* and *SPHK1* in human MTC

The miRNA profiling of human MTC identified miR-124-3p as the most significantly downregulated miRNA in the expression profile between hereditary and sporadic MTC. The *in silico* analysis predicted *RAB27A* and *SPHK1* as putative targets of miR-124-3p, which

were subsequently validated as target genes by luciferase reporter assays. In order to determine the relevance of *RAB27A* and *SPHK1* as potential biomarkers of MTC, their expression was measured in hereditary and sporadic tumours using quantitative RT-PCR.

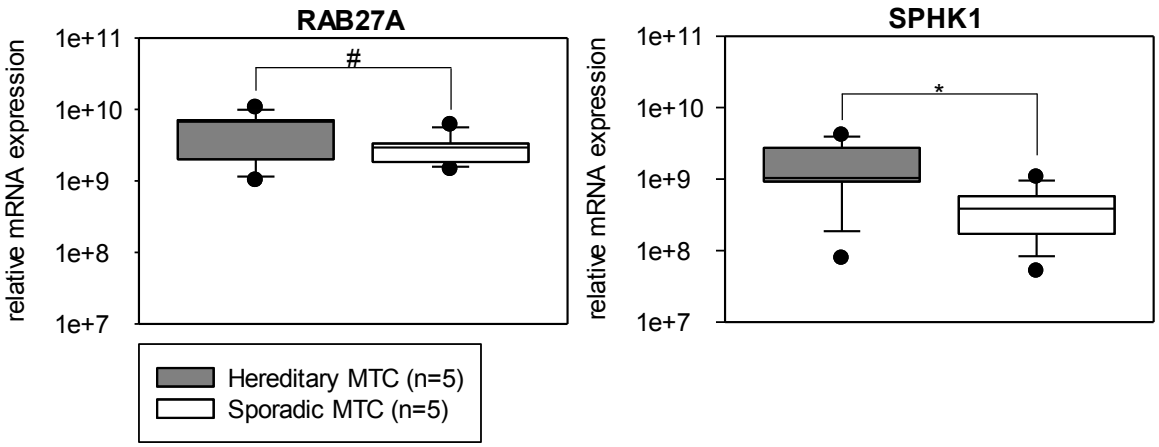

Figure 33: The expression of *RAB27A* and *SPHK1* in human MTC. All data was normalised to TBP transcription levels using a comparative Ct method (Livak *et al.* 2001, Pfaffl 2001). All box plots show 25th to 75th percentiles (box) and 5th and 95th percentiles (whiskers). Solid dots are outliers below 5% and above 95%. The line in the box represents the median (#= not significant; *= p-value <0.05, **= p-value <0.01, ***= p-value <0.001).

The analysis of the *RAB27A* and *SPHK1* expression in human MTC revealed a significant higher expression of *SPHK1* in hereditary MTC, when compared to sporadic MTC patients (Figure 33). This suggests that the expression of *SPHK1* can be used to distinguish between sporadic and hereditary MTC. Unfortunately, without the comparison of C-cell tumours to normal C-cells, it is not possible to determine if *SPHK1* is a biomarker for tumour progression. However, *SPHK1* represents a novel gene potentially involved in hereditary MTC.

5 Discussion

MTC is a rare subtype among thyroid cancers, but despite its low incidence, there is a disproportionate number of MTC related deaths, in comparison to other thyroid cancer subtypes (David *et al.* 2010, Kaatsch *et al.* 2013, Santarpia *et al.* 2013). In 25% of patients MTC occurs in a hereditary form as part of the MEN2 syndrome, caused by germline *RET* mutations. With the exception of *RET*, the genetic changes leading to MTC are still not well understood, especially in a metastatic context (Santarpia *et al.* 2013). Another challenge in studying MTC is presented by the extreme paucity of MTC animal models. Despite previous efforts, only one mouse model of MTC is currently listed in the Mouse Genome Information database (Kedzia *et al.* 2005, Begley *et al.* 2012, Laulederkind *et al.* 2013, Blake *et al.* 2014, Smith *et al.* 2014).

The differential expression of miRNA expression is known to be involved in cancer initiation and progression. Specific subsets of miRNAs exert their effect on the tumourigenetic process through the regulation of target genes (He *et al.* 2005, Lu *et al.* 2005, Croce 2009, Iorio *et al.* 2012). A handful of studies assessing miRNA expression in thyroid cancer have been previously published (Nikiforova *et al.* 2008, Abraham *et al.* 2011, Ciampi *et al.* 2013, Santarpia *et al.* 2013).

One of the main challenges in investigating MTC in rats and humans is that the C-cell population makes up approximately 1% of the thyroid cell mass. In addition, the C-cells do not form a coherent tissue within the organ and their isolation is very labour intensive (Figure 2 and Figure 9). As a consequence, the investigation of a normal thyroid tissue in its use as a representative normal tissue is not possible and only different tumour tissues can be investigated (Leboulleux *et al.* 2004, Lodish *et al.* 2008, Maliszewska *et al.* 2013). Most studies compare hereditary with sporadic MTC tissues as demonstrated by Abraham *et al* (Abraham *et al.* 2011). Another approach was to compare the primary tumours with corresponding metastatic tumours (Santarpia *et al.* 2013).

The difficulty in obtaining and isolating RNA from individual C-cells from healthy thyroids represents the main bottleneck in investigating MTC. Advances in technology made it possible to investigate the miRNA expression of single cells via quantitative RT-PCR and fluorescence-activated cell sorting (FACS). An attempt in isolating healthy C-cells from wild-type Wistar rats using FACS was conducted in 2007. C-cells were identified by utilising fluorescent-labelled antibodies against calcitonin from isolated thyroid glands using 40 to 45 animals. This generated approximately 1 µg of total RNA that was employed for quantitative

RT-PCR experiments (Moerch *et al.* 2007, Wu *et al.* 2013). Unfortunately, this procedure is very complicated and involves the dissociation of C-cells from the thyroid. In addition, the C-cell marker calcitonin is intracellular and cells have to permeabilised before sorting. As a consequence, the RNA isolated was of a bad quality and suited for only some experiments. Further research is required in order to explore the single cell miRNA profiling from C-cells isolated from the thyroid gland.

In our study, the miRNA expression of MTC in MENX rats was compared with the miRNA signature of human MTC. After determining the similarities between rat and human MTC at the molecular level, the functional role of the most differentially expressed miRNAs was investigated. As miRNAs potentially regulate multiple biological targets, a screening of target genes was conducted followed by the validation of the selected candidates using a luciferase assay.

For the MENX rat tumours, we compared MTC arising in homozygous mutants rats with those from heterozygous mutant animals. The prolonged lifespan of heterozygous mutants rats enables the comparison between late and early stage MTCs.

5.1 MiRNA expression of MENX rat MTC

In this investigation, RNA was isolated from thyroid tumours of 9 month-old homozygous and age-matched heterozygous mutant rats. Histological evaluation identified thyroid tumours at a pre-metastatic stage in rats of the named genotypes and therefore the investigation was focused on the influence of the p27 levels on MTC tumourigenesis in MENX rats.

Profiling of rat MTC identified a total of 139 significantly differentially expressed miRNAs between homozygous and age-matched heterozygous mutant rats, suggesting that the p27 levels affects the miRNA expression. Specifically, reduction of p27 levels leads to the downregulation of many miRNAs in homozygous mutant rats.

According to IPA Downstream Effects Analysis, the most differentially expressed miRNAs between 9 month-old homozygous and age-matched heterozygous mutant rats have been previously linked to other cancer types. Furthermore, the causal analysis *in vitro* suggests that differentially expressed miRNAs were linked to cancer relevant cellular processes such as cell proliferation, survival and cell death as well as migration and invasion. Therefore, it is highly probable that differentially expressed miRNAs play a role also in MTC tumourigenesis of MENX rats.

The strongest downregulation in homozygous *versus* age-matched heterozygous mutant rats was observed for miR-449c-5p, miR-203a-3p and miR-27b-3p. The chromosomal region 2q16, from which miR-449-5p is transcribed, is known to be unstable in rat mammalian cancer (Qiu *et al.* 2003). Unfortunately, the exact function in rats still remains illusive. Previous studies demonstrated tumour-suppressive functions of miR-449c-5p in non small cell lung carcinoma in humans by targeting c-Myc (Miao *et al.* 2013). This suggests that miR-449-5p may participate in the oncogenesis of MTC in MENX rats. The role of miR-203a-3p, which is located on chromosome 6q32, has been examined more thoroughly in different cancer types, when compared with that of miR-449c-5p. In rat hepatocellular carcinomas, miR-203a-3p was downregulated and correlated with tumour-suppressive functions (Wang, C. *et al.* 2014). A differential expression of miR-203a-3p was identified in human hepatocellular carcinoma and aberrant expression of miR-203a-3p inhibits cell growth and suggests a tumour-suppressive function (Furuta *et al.* 2010). Tumour-suppressive functions of miR-203-3p have been described in leukaemias, basal cell carcinomas and squamous carcinoma cell lines, where a differential expression of miR-203a-3p was correlated with cell proliferation, differentiation and apoptosis (Bueno *et al.* 2008, Lena *et al.* 2008, Sonkoly *et al.* 2012).

The differential expression of the miR-27 family, located on the chromosomal regions 17p14 and 19q11, was downregulated in MTC of homozygous *versus* age-matched heterozygous mutant rats. In rat hepatocellular carcinomas an upregulation of miR-27 family members was identified that suggests an oncogenic role, promoting tumour formation (Wang, C. *et al.* 2014). In humans, miR-27 family members were shown to be involved in various cancer types such as breast and endometrial carcinomas (Guttilla *et al.* 2009, Li *et al.* 2010, Myatt *et al.* 2010). Functional roles of miR-27 have been classified as either oncogenic, by regulating cell proliferation, or as tumour-suppressive, through the regulation of the cell cycle. The functional role of miR-27 is closely regulated by other miRNAs (Mertens-Talcott *et al.* 2007, Guttilla *et al.* 2009).

Members of the miR-29 family were among the most significantly downregulated miRNAs in homozygous *versus* age-matched heterozygous mutant MENX rats. The miR-29 family members are transcribed from the chromosomal regions 1p11, 4q21 and 13q27 and share a common seed region sequence, predicted to target largely overlapping sets of genes (Kriegel *et al.* 2012). In rats, miR-29 family members regulate the cell cycle of cardiomyocytes during ventricular maturation (Cao *et al.* 2013). In human kidneys, the downregulation of miR-29 correlates with the impaired regulation of cell differentiation and apoptosis (Kriegel *et al.* 2012).

In addition to the investigation of the influence of the p27 levels on the miRNA expression in MTC of MENX rats, the change in miRNA expression associated with tumour progression in heterozygous mutant rats was also investigated. The prolonged life span of heterozygous mutant rats of 18 months, where distant metastases are observed, allows the investigation of MTC from a pre-metastatic to a progressed stage, with equal p27 levels. Interestingly, the most differentially expressed miRNAs in the comparisons of miRNA expression profiles (9 month-old homozygous *versus* age-matched heterozygous mutant rats; 18 month-old *versus* 9 month-old heterozygous mutants rats) are almost identical with miR-449c-5p, miR-203a-3p and miR-27b-3p showing similar patterns of downregulation.

The expression of miR-124-3p increased with tumour progression in heterozygous mutant rats, suggesting an oncogenic role in the generation of MTC. Interestingly, miR-124-3p is a highly conserved and predominately neuronal miRNA, showing an extensive involvement in the embryonic development of rat neurons. Specifically, an increased expression of miR-124-3p repressed neuronal phenotypes (Jeyaseelan *et al.* 2008). In contrast to the increase in miR-124-3p expression observed with tumour progression in heterozygous mutant rats, a p27-dependent downregulation of miR-124-3p was observed in the tumours of homozygous mutant rats. These results suggest that expression of miR-124-3p correlates with the p27 levels and the downregulation of miR-124-3p suggests tumour-suppressive rather than oncogenic functions. Further investigations have to be conducted in order to comprehend the relationship between p27 levels and miR-124-3p expression.

A study in 2009 revealed the presence of dividing precursors upon downregulation of miR-124-3p expression in the subventricular zone of the mammalian brain. Furthermore, the blocking of miR-124-3p led to the generation of hyperplasias in the mammalian brain (Cheng, L. C. *et al.* 2009). The differential expression of the neuronal miR-124-3p suggests a deregulation of development of neuroendocrine thyroid cells in MENX rats. The miRNA signature of thyroid tumours associated with p27 loss suggests that these tumours derive from cells with precursor-like features. This assumption is enforced by the downregulation of let-7, miR-17-1-3p, miR-324-5p and miR-326-3p in MTC of 9 month-old homozygous *versus* age-matched heterozygous mutant rats. The expression of these miRNAs promotes the differentiation of neuronal stem cells (Fineberg *et al.* 2009). Previous investigations on pheochromocytomas of MENX rats noticed an increase in expression of precursor cell markers in homozygous mutant rats, suggesting that these tumours originate from cells having features of neuronal precursors, present in higher numbers due to the lack of functional p27 (Molatore *et al.* 2010). The IPA Downstream Effects Analysis identified the functional categories “Psychological Disease”, “Neurological Disease” and “Developmental

Disorder" as significantly enriched, strengthening the assumption that MTC arises from dividing precursor cells in rats.

The similarity between the rat expression profiles validates the assumption that the reduction of p27 levels initiates MTC tumour formation. This is further supported by the earlier onset of MTC in homozygous mutant rats when compared to heterozygous mutant rats. The noticeable increase of C-cell numbers in thyroid glands of 2 month-old homozygous mutant rats, in comparison to heterozygous mutant and wild-type rats suggests a correlation between the p27 levels and C-cell differentiation (Pellegata *et al.* 2006). The differential expression of miRNAs regulating the differentiation of neuronal precursor cells indicates the development of MTC from an expanded pool of cells with neuronal precursor features likely generated by the reduction of p27.

5.2 Deregulation of miRNA expression in human MTC

To determine the validity of MENX rats as an animal model of human MTC, the miRNA expression of human hereditary *versus* sporadic MTC was established. For this investigation, fresh frozen human MTC tissues, identified as either hereditary or sporadic were collected. A feature of the collected MTC specimens is that most hereditary patients carry the *RET* mutation C620R, giving a unique opportunity to investigate the effect of a specific *RET* mutation on miRNA expression. In addition, the majority of sporadic MTC specimens profiled were *RET* mutation negative allowing a comparison between *RET* mutation positive hereditary MTC and RET mutation negative sporadic MTC.

As described previously, hereditary MTC is historically and clinically defined through the presence of germinal mutations present in the *RET* proto-oncogene and is characterised by an early onset of disease. In contrast, sporadic MTC can arise clinically at any age and the presence of germline *RET* mutations can be excluded (Leboulleux *et al.* 2004, Lodish *et al.* 2008, Ameur *et al.* 2009).

Analysis of the miRNA expression between hereditary and sporadic MTC identified many differentially expressed miRNAs. This suggests that hereditary *RET* mutations associated with MEN2A influence the miRNA expression, as also observed by Abraham *et al.* (Abraham *et al.* 2011).

In our study, a total of 30 differentially expressed miRNAs were quantified by miRNA array analysis. The expression of the differentially expressed miR-29 family members, miRNA-124-3p, miR-148b-3p, miR-183-5p, miR-192-5p and miR-335-5p were validated with quantitative RT-PCR in the same samples used for the arrays. Validation of the expression of the

selected differentially expressed miRNAs indicates that the expression profiles obtained by miRNA arrays are reliable. Furthermore, the validated differentially expressed miRNAs may have functional roles in the generation of MTC.

The highest downregulation in hereditary *versus* sporadic MTC was observed for miR-124-3p, miR-335-5p and miR-183-5p. The differentially expressed miR-124-3p is derived from pre-miR-124-3p located on chromosome 8p23.1. This chromosomal region is associated with mutations, deletions or duplications in neuropsychiatric disorders as well as in many cancer types (Emi *et al.* 1992, Liao *et al.* 2000, Sanuki *et al.* 2011). In addition, the differential expression of miR-124-3p was also linked to hepatocellular and bladder cancers and was associated with the regulation of migration and invasion (Lang *et al.* 2012, Xu *et al.* 2013). A differential expression of miR-124-3p similar to our investigation was described in a paper by Nikiforova *et al.*, which analysed few cases of hereditary MTC (Nikiforova *et al.* 2008). Our results, together with previously published data, suggest the importance of miR-124-3p in tumour development, where its downregulation seems to promotes MTC tumourigenesis.

Further analysis revealed a significant downregulation of miR-335-5p in hereditary *versus* sporadic MTC. Previous investigations showed that miR-335-5p is transcribed from the genomic region of chromosome 7p32.2 and was identified as a tumour suppressor in breast cancer, where the loss of expression correlates with tumour progression (Tavazoie *et al.* 2008, Png *et al.* 2011). Additionally, miR-335-5p has been reported to orchestrate cell proliferation, migration and differentiation in human mesenchymal stem cells (Shu *et al.* 2011, Tome *et al.* 2011). It was demonstrated that miR-335-5p targets pRb and controls cell proliferation by inducing cell cycle arrest (Scarola *et al.* 2010). To date, a differential expression of miR-335-5p has not been linked to MTC.

Amongst the most downregulated miRNAs in hereditary *versus* sporadic MTC, miR-183-5p, which is located on the genomic region of chromosome 7q32.2, was identified. The differential expression of miR-183-5p was previously described in MTC, where a reduced expression of this miRNA was detected in hereditary *versus* sporadic MTC, emphasising its importance in MTC pathogenesis. The downregulation of miR-183-5p was correlated with an increased expression of MAP1LC3B, a protein associated with autophagy (Bastian *et al.* 1998, Abraham *et al.* 2011). The downregulation of miR-183-5p we observed is in agreement with the results obtained by Abraham *et al.* and further underlines the relevance of miR-183-5p in the development of MTC.

The members of the differentially expressed miR-29 family are transcribed from the genomic regions of chromosome 1q32.2 and chromosome 7q32.3. As described in section 5.1, the downregulation of the miR-29 family had been previously identified in cancer. Recently, an

investigation focussing on the miRNA signature of primary MTCs and the respective metastases identified the downregulation of miR-29c-3p accompanying metastasis formation. The expression of members of the miR-29 family in our comparisons of human expression signatures is downregulated in hereditary *versus* sporadic MTC. The differential expression of members of the miR-29 family identified in our comparisons indicates the importance of this miRNA family in the development of MTC.

IPA Downstream Effects Analysis of human MTC expression profiles showed that the differentially expressed miRNAs regulate cell proliferation, migration, invasion as well as apoptosis in hereditary *versus* sporadic MTC. The enriched high level functional categories correlate with patient data, where hereditary MTC patients showed signs of local and distant metastasis in 10 out of 15 cases and residual disease in 6 out of 15 cases.

In summary, the differentially expressed miRNAs in hereditary *versus* sporadic MTC were previously linked to cancer, implying that a change in expression of these miRNAs influences the development of MTC. Interestingly, the loss of expression of miR-29c-3p, miR-124-3p and miR-183-5p were linked to MTC pathogenesis in previous investigations, therefore further emphasising the importance of these miRNAs in MTC tumour development.

5.3 The MENX rats as an animal model for human MTC

The deregulation of miRNAs is a frequent event observed in human cancers and therefore many investigations focussed on the suitability of miRNAs as markers for cancer diagnosis and prognosis (Lu *et al.* 2005, Cheng, S. Y. *et al.* 2009, Croce 2009, Iorio *et al.* 2012). Based on previous investigations regarding the use of miRNAs as tumour markers, the global changes in miRNA expression were studied in thyroid tumours of rats and of human patients to identify differentially expressed miRNAs and thus explore the suitability of the rats as an animal model of human MTC.

During the course of this investigation, we generated five data sets and conducted a comparison as follows: 9 month-old homozygous *versus* age-matched heterozygous mutant rats; 18 month-old heterozygous *versus* 9 month-old heterozygous mutant rats; human hereditary MTC *versus* human sporadic MTC. These data sets were compared to determine similarities in miRNA expression.

The highest degree of similarity was observed in the comparison “9 month-old homozygous with age-matched heterozygous mutant rats” with that of MTC from “18 month-old heterozygous with 9 month-old heterozygous mutant rats”. High identity between rat genotypes was expected from our inbred rat colony.

Approximately 35% of differentially expressed miRNAs in hereditary *versus* sporadic MTC were found in the miRNA expression profiles of MENX rats. The similarity between MENX rats and human MTC demonstrates that MENX rats model quite faithfully the human disease on a molecular level. Indeed, the similarities between the three comparisons investigating the miRNA expression of MTC revealed a common differential expression of let-7a-5p, let-7f-5p, miR-21-5p, miR-27b-3p, miR-29a-3p, miR-29b-3p, miR-30b-5p miR-124-3p as well as miR-335-5p. These miRNAs belong to conserved miRNA families, further underlying molecular similarities between rat and human MTC.

Based on miRNA expression, a high similarity in miRNA expression signatures between human and MENX rat MTC was established. Given the initiating role of p27 in rat tumours, human MTC tumours were stained for p27 and a reduced expression of p27 was detected in hereditary *versus* sporadic MTC tumour tissues. This therefore further underlines the similarities between human and rat MTC. Previous studies showed that p27 is regulated by RET and a loss of p27 is critical for developing MTC, thereby demonstrating that RET and p27 are part of the same signalling cascade (Sheaff *et al.* 1997, Joshi *et al.* 2007, van Veelen *et al.* 2008, van Veelen *et al.* 2009, Knight *et al.* 2011). High similarities between the comparison of miRNA signatures of rat and human data sets imply that the reduction of p27 is a key event in the generation of MTC.

In conclusion, MTC of MENX rats models the human disease at the molecular level based on the differential miRNA expressions obtained. Specifically, homozygous MENX rats model more closely human hereditary than sporadic MTC. In addition, the prolonged life-span of heterozygous in comparison to homozygous mutant rats enables the study of MTC tumour progression. This *in vivo* model of advanced MTC is especially useful in determining the efficacy of targeted therapies against MTC, especially when investigating the effects against metastasis.

5.4 Functional roles of deregulated miRNAs in MTC generation

Causal analysis of rat miRNA signatures with IPA identified the enrichment of the high level functional categories “Cell Proliferation”, “Cell Migration” and “Cell Invasion” in tumours associated with p27-deficiency in homozygous mutant rats as well as with tumour progression in heterozygous mutant rats. The differentially expressed miR-29 family members and miR-124-3p identified in human and rat miRNA signatures were chosen among the candidates for further functional studies *in vitro*. Their differential expression validated in rat and human MTC by quantitative RT-PCR suggests that miR-29 family members and miR-124-3p serve important biological roles in the development of MTC.

Therefore, MTC cell lines were transfected with specific miRNA inhibitors blocking the expression of our selected endogenous miRNAs and then investigated for effects on cell viability, migration and invasion.

Inhibition of miR-29b-3p and miR-29c-3p showed the strongest effect on 6-23 MTC and TT cell proliferation, which was significantly increased upon their donwregulation. Studies investigating the oncogenic properties of the miR-29 family members, suggest that a loss of expression correlates with increased cell proliferation in gastric cancers and other malignancies (Gong *et al.* 2014, Jiang *et al.* 2014). Our experimental evidence on the influence of miR-29 family members on cell proliferation is in agreement with previous studies. This therefore strongly suggests that the differential expression of miR-29 family members observed in human and MENX rat miRNA expression signatures leads to elevated cell proliferation.

The differential expression of miR-124-3p observed in human and MENX rat expression signatures suggests that this miRNA may regulate cell proliferation, as it was the most significantly downregulated miRNA in the human MTC profile. We did not observe a change in cell proliferation upon miR-124-3p downregulation in MTC cell lines. This is in contrast to investigations reporting an increase in cell proliferation after the inhibition of miR-124-3p in gastric cancer (Xie *et al.* 2014). Therefore, the downregulation of miR-124-3p observed in human and rat MTC did not influence the proliferation of MTC tumour cells.

In MTC, the presence of metastases correlates with poor prognosis and outcome, ultimately leading to cancer-related deaths (Santarpia *et al.* 2013). The metastatic spread of tumours is a complex, multistep process, where cells from the original tumour site leave, migrate locally and eventually reach blood and lymph vessels, where they are transported to other parts of the body (Nguyen *et al.* 2007). Among the features associated with the formation of metastases is an increase in cell migration. Proteases are secreted by invasive tumour cells to degrade the ECM, thereby allowing cells access to neighbouring tissues and vessel structures (Klein 2008). The influence of miR-29 family and miR-124-3p on cell migration and invasion was investigated to determine how these differentially expressed miRNAs promote a metastatic phenotype in MTC.

The transfection of MTC cell lines with specific inhibitors against members of the miR-29 family and miR-124-3p significantly increased cell migration and invasion in both 6-23 MTC and TT cell lines. This experimental evidence suggests that the loss of these differentially expressed miRNAs promotes MTC tumourigenesis by enhancing migration and invasion of the tumour cells. A downregulation of the miR-29 family seems to have tumour-suppressive functions in many cancers, such as prostate and lung cancer, where its members regulate

cell migration and invasion (Plaisier *et al.* 2012, Nishikawa *et al.* 2014). The tumourigenetic effect observed upon the downregulation of miR-29 family members strongly indicates that these miRNAs promote migration and invasion in rat and human MTC. Recently, miR-29 family members were identified in a miRNA signature associated with metastatic MTC, where a downregulation of miR-29 family members was observed in the metastasis, when compared to the corresponding primary tumours (Santarpia *et al.* 2013). In agreement with findings from previous studies, our array and *in vitro* data further supports a role of miR-29 family members in regulating invasion and migration in MTC.

A downregulation of miR-124-3p plays a crucial role in metastatic processes and it has been directly correlated with increased invasion in endometrial, breast and gastric cancers (Han *et al.* 2013, Li *et al.* 2014, Xie *et al.* 2014). The tumour-suppressive functions of miR-124-3p, as determined by our *in vitro* studies, are in agreement with the study conducted by Cheng *et al.*, who discovered that the downregulation of miR-124-3p leads to the generation of hyperplasias from dividing precursor cells in the mammalian brain (Papagiannakopoulos *et al.* 2008, Cheng, L. C. *et al.* 2009). The metastasis-promoting properties accompanying miR-124-3p downregulation suggest that the downregulation observed in human and rat comparisons of miRNA expression signatures promotes invasion.

In summary, experimental evidence suggests that the miR-29 family members and miR-124-3p differentially expressed in both rat and human MTC tumours contribute to the development of MTC, as their downregulation correlates with increased migration and invasion. The downregulation of miR-29 family members also correlates with an increase in cell proliferation.

5.5 Identifying biological targets of selected miRNAs

Expressed miRNAs regulate approximately one third of the human genome, where each individual miRNA has numerous targets (Menon *et al.* 2009). Base pairing of the miRNAs seed region with the 3'-UTR of mRNAs is required for targeting (Filipowicz *et al.* 2008). Determination of biological targets is therefore essential in determining the specific functions of differentially expressed miRNAs in MTC.

In order to identify miRNA targets, prediction algorithms were utilised. One such algorithm is TargetScan, that employs seed match 3'-complementarity and the contribution of local AU content and position. The disadvantage of this method is that sites with poor seed pairing are omitted (Lewis *et al.* 2005, Grimson *et al.* 2007, Garcia *et al.* 2011, Witkos *et al.* 2011). The miRanda target prediction algorithm makes use of complementarity and free energy binding to compute target genes. Unfortunately, miRanda has low precision and provides many false

positive results (John *et al.* 2004, Witkos *et al.* 2011). PicTar is a prediction algorithm based on binding energy, complementarity and conservation of sites. Non-conserved sites are not predicted (Krek *et al.* 2005, Witkos *et al.* 2011). It has to be taken into consideration that miRNA-mRNA duplexes contains mismatches and bulges (Filipowicz *et al.* 2008). As a consequence, a combination of three prediction algorithms as well as the prediction algorithm by IPA was used. Genes only detected by all four prediction algorithms were considered as targets in order minimise the prediction of any false positive target genes.

A total of 57 target mRNAs were identified for miR-124-3p. Subsequent functional analysis with the IPA Downstream Effects Analysis identified in the area “Cellular Movement” as the most enriched high level functional category of miR-124-3p target genes. The results of our experimental analysis overlaps with the causal analysis conducted with IPA. As a consequence the search for miR-124-3p target genes was focussed on those known to regulate cell migration.

Among the target genes of miR-124-3p that regulate cell migration *RAB27A* was chosen for further analysis as it contained the highest number of predicted seed matches according to the TargetScan prediction algorithm. In addition, two predicted targets, *MAPK14* and *SPHK1*, which were previously associated with MTC and MEN2A, respectively, were also chosen for further study (Murakami *et al.* 2007, Ruiz-Llorente *et al.* 2007).

We were able to confirm the direct interaction of miR-124-3p with *RAB27A* and *SPHK1* and therefore these genes are direct target genes of this miRNA in MTC cells. This suggests that *RAB27A* and *SPHK1* may regulate cell migration as a response to the downregulation of miR-124-3p. Interestingly, increased expression of *RAB27A* was identified in human gliomas, where it correlates with malignant progression (Wang, H. *et al.* 2014). RAB27A protein is a member of the small GTPase superfamily and plays an important role in cell secretion, endocytosis, signal transduction and in development (Recchi *et al.* 2012). Unfortunately, a differential expression of RAB27A between hereditary and sporadic MTC could not be established.

The second confirmed target gene regulated by miR-124-3p was *SPHK1*. Following the validation as a target gene, the expression of *SPHK1* was investigated in human MTC using quantitative RT-PCR. The analysis showed a significant upregulation of *SPHK1* in hereditary *versus* sporadic MTC, suggesting a potential role of *SPHK1* as a biomarker for MTC. Recently, an upregulation of *SPHK1* was associated with enhanced migration and invasion in glioblastoma, oesophageal and colon cancer (Young *et al.* 2009, Pan *et al.* 2011, Liu *et al.* 2013). These results suggest that increased *SPHK1* expression upon loss of miR-124-3p expression promotes migration and invasion in MTC. Interestingly, a recent study

demonstrated an induction of *SPHK1* by MEN2A-associated *RET* mutations in glioblastoma cells (Murakami *et al.* 2007). In order to validate the role of SPHK1 in the oncogenesis of MTC, a downregulation in MTC cells lines followed by the functional analysis to investigate the effects on cell migration and invasion should be conducted.

6 Conclusion

In conclusion, we were able to demonstrate that the miRNA expression of MTC in MENX rats is dependent on p27 levels, as well as tumour progression. The rat tumours miRNA profiles suggest that MTC is generated from a p27-deficient proliferating precursor cell type. The miRNA profile of hereditary *versus* sporadic MTC in humans identified differentially expressed miRNAs that regulate neuronal differentiation but also other features such as invasion and migration, suggesting that MTC in humans is generated from proliferating neuronal precursor cells.

Over 35% of the differentially expressed miRNAs in human MTC were also identified in the miRNA expression profiles of MENX rats including miR-29 family members and miR-124-3p. These results suggest that MENX rats can be used to model the human disease and offer the possibility to study the progression of MTC toward a metastatic phenotype.

Members of the miR-29 family and miR-124-3p were selected for further functional studies. The downregulation of both the miR-29 family members and of miR-124-3p was correlated with an increase in cell migration and proliferation. Furthermore, the downregulation of the miR-29 family was also correlated with an increase in cell proliferation. In agreement with previously published data, the downregulation of the miR-29 family and of miR-124-3p promotes MTC tumourigenesis by enhancing migration and invasion. Further studies will reveal if these differentially expressed miRNAs have prognostic or therapeutic value.

Investigating the biological targets of miR-124-3p identified *RAB27A* and *SPHK1* as bona fide targets. *SPHK1*, previously associated with increased migration and invasion in other cancers, showed a differential expression in human MTC and may represent a novel putative marker of hereditary MTC.

7 Literature

Abraham, D., Jackson, N., Gundara, J. S., Zhao, J., Gill, A. J., Delbridge, L., Robinson, B. G. and Sidhu, S. B. (2011). "MicroRNA profiling of sporadic and hereditary medullary thyroid cancer identifies predictors of nodal metastasis, prognosis, and potential therapeutic targets." Clin Cancer Res **17**: 4772-4781.

Acton, D. S., Velthuyzen, D., Lips, C. J. and Hoppener, J. W. (2000). "Multiple endocrine neoplasia type 2B mutation in human RET oncogene induces medullary thyroid carcinoma in transgenic mice." Oncogene **19**: 3121-3125.

Adams, B. D., Claffey, K. P. and White, B. A. (2009). "Argonaute-2 expression is regulated by epidermal growth factor receptor and mitogen-activated protein kinase signaling and correlates with a transformed phenotype in breast cancer cells." Endocrinology **150**: 14-23.

Ahmed, M., Barbachano, Y., Riddell, A., Hickey, J., Newbold, K. L., Viros, A., Harrington, K. J., Marais, R. and Nutting, C. M. (2011). "Analysis of the efficacy and toxicity of sorafenib in thyroid cancer: a phase II study in a UK based population." Eur J Endocrinol **165**: 315-322.

Airaksinen, M. S. and Saarma, M. (2002). "The GDNF family: signalling, biological functions and therapeutic value." Nat Rev Neurosci **3**: 383-394.

Ambros, V., Bartel, B., Bartel, D. P., Burge, C. B., Carrington, J. C., Chen, X., Dreyfuss, G., Eddy, S. R., Griffiths-Jones, S., Marshall, M., Matzke, M., Ruvkun, G. and Tuschl, T. (2003). "A uniform system for microRNA annotation." RNA **9**: 277-279.

Ameur, N., Lacroix, L., Roucan, S., Roux, V., Broutin, S., Talbot, M., Dupuy, C., Caillou, B., Schlumberger, M. and Bidart, J. M. (2009). "Aggressive inherited and sporadic medullary thyroid carcinomas display similar oncogenic pathways." Endocr Relat Cancer **16**: 1261-1272.

Asai, N., Iwashita, T., Matsuyama, M. and Takahashi, M. (1995). "Mechanism of activation of the ret proto-oncogene by multiple endocrine neoplasia 2A mutations." Mol Cell Biol **15**: 1613-1619.

Bai, F., Pei, X. H., Nishikawa, T., Smith, M. D. and Xiong, Y. (2007). "p18Ink4c, but not p27Kip1, collaborates with Men1 to suppress neuroendocrine organ tumors." Mol Cell Biol **27**: 1495-1504.

Ball, D. W. (2007). "Medullary thyroid cancer: monitoring and therapy." Endocrinol Metab Clin North Am **36**: 823-837.

Barbet, J., Campion, L., Kraeber-Bodere, F. and Chatal, J. F. (2005). "Prognostic impact of serum calcitonin and carcinoembryonic antigen doubling-times in patients with medullary thyroid carcinoma." J Clin Endocrinol Metab **90**: 6077-6084.

Bartek, J., Lukas, C. and Lukas, J. (2004). "Checking on DNA damage in S phase." Nat Rev Mol Cell Biol **5**: 792-804.

Bartel, D. P. (2009). "MicroRNA Target Recognition and Regulatory Functions." Cell **136**: 215-233.

Baskerville, S. and Bartel, D. P. (2005). "Microarray profiling of microRNAs reveals frequent coexpression with neighboring miRNAs and host genes." RNA **11**: 241-247.

Bastian, B. C., LeBoit, P. E., Hamm, H., Brocker, E. B. and Pinkel, D. (1998). "Chromosomal gains and losses in primary cutaneous melanomas detected by comparative genomic hybridization." Cancer Res **58**: 2170-2175.

Begley, D. A., Krupke, D. M., Neuhauser, S. B., Richardson, J. E., Bult, C. J., Eppig, J. T. and Sundberg, J. P. (2012). "The Mouse Tumor Biology Database (MTB): a central electronic resource for locating and integrating mouse tumor pathology data." Vet Pathol **49**: 218-223.

Benjamini, Y. and Hochberg, Y. (1995). "Controlling the False Discovery Rate: A Practical and Powerful Approach to Multiple Testing." Journal of the Royal Statistical Society. Series B (Methodological) **57**: 289-300.

Berindan-Neagoe, I., Monroig Pdel, C., Pasculli B. and Calin, G. A. (2014). "MicroRNAome genome: a treasure for cancer diagnosis and therapy." CA Cancer J Clin **64**: 311-336.

Berridge, M. V., Herst, P. M. and Tan, A. S. (2005). "Tetrazolium dyes as tools in cell biology: new insights into their cellular reduction." Biotechnol Annu Rev **11**: 127-152.

Berridge, M. V. and Tan, A. S. (1993). "Characterization of the cellular reduction of 3-(4,5-dimethylthiazol-2-yl)-2,5-diphenyltetrazolium bromide (MTT): subcellular localization, substrate dependence, and involvement of mitochondrial electron transport in MTT reduction." Arch Biochem Biophys **303**: 474-482.

Blahna, M. T. and Hata, A. (2012). "Smad-mediated regulation of microRNA biosynthesis." FEBS Lett **586**: 1906-1912.

Blake, J. A., Bult, C. J., Eppig, J. T., Kadin, J. A., Richardson, J. E. and the Mouse Genome Database Group (2014). "The Mouse Genome Database: integration of and access to knowledge about the laboratory mouse." Nucleic Acids Res **42**: 810-817.

Brandi, M. L., Gagel, R. F., Angeli, A., Bilezikian, J. P., Beck-Peccoz, P., Bordi, C., Conte-Devolx, B., Falchetti, A., Gheri, R. G., Libroia, A., Lips, C. J., Lombardi, G., Mannelli, M., Pacini, F., Ponder, B. A., Raue, F., Skogseid, B., Tamburrano, G., Thakker, R. V., Thompson, N. W., Tomassetti, P., Tonelli, F., Wells, S. A. Jr. and Marx, S. J. (2001). "Guidelines for diagnosis and therapy of MEN type 1 and type 2." J Clin Endocrinol Metab **86**: 5658-5671.

Brennecke, J., Stark, A., Russell, R. B. and Cohen, S. M. (2005). "Principles of microRNA-target recognition." PLoS Biol **3**: p. e85.

Bueno, M. J., Perez de Castro, I., Gomez de Cedron, M., Santos, J., Calin, G. A., Cigudosa, J. C., Croce, C. M., Fernandez-Piqueras, J. and Malumbres, M. (2008). "Genetic and epigenetic silencing of microRNA-203 enhances ABL1 and BCR-ABL1 oncogene expression." Cancer Cell **13**: 496-506.

Calender, A. (2000). "Molecular genetics of neuroendocrine tumors." Digestion **62 Suppl 1**: 3-18.

Canepa, E. T., Scassa, M. E., Ceruti, J. M., Marazita, M. C., Carcagno, A. L., Sirkin, P. F. and Ogara, M. F. (2007). "INK4 proteins, a family of mammalian CDK inhibitors with novel biological functions." IUBMB Life **59**: 419-426.

Cao, X., Wang, J., Wang, Z., Du, J., Yuan, X., Huang, W., Meng, J., Gu, H., Nie, Y., Ji, B., Hu, S. and Zheng, Z. (2013). "MicroRNA profiling during rat ventricular maturation: A role for miR-29a in regulating cardiomyocyte cell cycle re-entry." FEBS Lett **587**: 1548-1555.

Capp, C., Wajner, S. M., Siqueira, D. R., Brasil, B. A., Meurer, L. and Maia, A. L. (2010). "Increased expression of vascular endothelial growth factor and its receptors, VEGFR-1 and VEGFR-2, in medullary thyroid carcinoma." Thyroid **20**: 863-871.

Carlomagno, F., Anaganti, S., Guida, T., Salvatore, G., Troncone, G., Wilhelm, S. M. and Santoro, M. (2006). "BAY 43-9006 inhibition of oncogenic RET mutants." J Natl Cancer Inst **98**: 326-334.

Carlomagno, F., Guida, T., Anaganti, S., Vecchio, G., Fusco, A., Ryan, A. J., Billaud, M. and Santoro, M. (2004). "Disease associated mutations at valine 804 in the RET receptor tyrosine kinase confer resistance to selective kinase inhibitors." Oncogene **23**: 6056-6063.

Ceccherini, I., Bocciardi, R., Luo, Y., Pasini, B., Hofstra, R., Takahashi, M. and Romeo, G. (1993). "Exon structure and flanking intronic sequences of the human RET proto-oncogene." Biochem Biophys Res Commun **196**: 1288-1295.

Cenik, E. S. and Zamore, P. D. (2011). "Argonaute proteins." Curr Biol **21**: R446-449.

Cerrato, A., De Falco, V. and Santoro, M. (2009). "Molecular genetics of medullary thyroid carcinoma: the quest for novel therapeutic targets." J Mol Endocrinol **43**: 143-155.

Chang, E. H., Gonda, M. A., Ellis, R. W., Scolnick, E. M. and Lowy, D. R. (1982). "Human genome contains four genes homologous to transforming genes of Harvey and Kirsten murine sarcoma viruses." Proc Natl Acad Sci U S A **79**: 4848-4852.

Chen, Y. T., Kitabayashi, N., Zhou, X. K., Fahey, T. J. 3rd and Scognamiglio, T. (2008). "MicroRNA analysis as a potential diagnostic tool for papillary thyroid carcinoma." Mod Pathol **21**: 1139-1146.

Cheng, L. C., Pastrana, E., Tavazoie, M. and Doetsch, F. (2009). "miR-124 regulates adult neurogenesis in the subventricular zone stem cell niche." Nat Neurosci **12**: 399-408.

Cheng, S. Y. and Ringel, M. D. (2009). "Frontiers in thyroid cancer: December 2009." Thyroid **19**: 1297-1298.

Choudhry, H. and Catto, J. W. (2011). "Epigenetic regulation of microRNA expression in cancer." Methods Mol Biol **676**: 165-184.

Ciampi, R., Mian, C., Fugazzola, L., Cosci, B., Romei, C., Barollo, S., Cirello, V., Bottici, V., Marconcini, G., Rosa, P. M., Borrello, M. G., Basolo, F., Ugolini, C., Materazzi, G., Pinchera, A. and Elisei, R. (2013). "Evidence of a low prevalence of RAS mutations in a large medullary thyroid cancer series." Thyroid **23**: 50-57.

Cote, G. J., Wohllk, N., Evans, D., Goepfert, H. and Gagel, R. F. (1995). "RET proto-oncogene mutations in multiple endocrine neoplasia type 2 and medullary thyroid carcinoma." Baillieres Clin Endocrinol Metab **9**: 609-630.

Croce, C. M. (2009). "Causes and consequences of microRNA dysregulation in cancer." Nat Rev Genet **10**: 704-714.

Croyle, M., Akeno, N., Knauf, J. A., Fabbro, D., Chen, X., Baumgartner, J. E., Lane, H. A. and Fagin, J. A. (2008). "RET/PTC-induced cell growth is mediated in part by epidermal growth factor receptor (EGFR) activation: evidence for molecular and functional interactions between RET and EGFR." Cancer Res **68**: 4183-4191.

David, A. R. and Zimmerman, M. R. (2010). "Cancer: an old disease, a new disease or something in between?" Nat Rev Cancer **10**: 728-733.

De Craene, B. and Berx, G. (2013). "Regulatory networks defining EMT during cancer initiation and progression." Nat Rev Cancer **13**: 97-110.

De Felice, M. and Di Lauro, R. (2004). "Thyroid development and its disorders: genetics and molecular mechanisms." Endocr Rev **25**: 722-746.

Diederichs, S. and Haber, D. A. (2007). "Dual role for argonautes in microRNA processing and posttranscriptional regulation of microRNA expression." Cell **131**: 1097-1108.

Ding, J., Zhou S. and Guan, J. (2011). "miRFam: an effective automatic miRNA classification method based on n-grams and a multiclass SVM." BMC Bioinformatics **12**: 216.

Doench, J. G. and Sharp, P. A. (2004). "Specificity of microRNA target selection in translational repression." Genes Dev **18**: 504-511.

Downward, J. (2003). "Targeting RAS signalling pathways in cancer therapy." Nat Rev Cancer **3**: 11-22.

Du, T. and Zamore, P. D. (2005). "microPrimer: the biogenesis and function of microRNA." Development **132**: 4645-4652.

Dvorakova, S., Vaclavikova, E., Sykorova, V., Vcelak, J., Novak, Z., Duskova, J., Ryska, A., Laco, J., Cap, J., Kodetova, D., Kodet, R., Krskova, L., Vlcek, P., Astl, J., Vesely, D. and Bendlova, B. (2008). "Somatic mutations in the RET proto-oncogene in sporadic medullary thyroid carcinomas." Mol Cell Endocrinol **284**: 21-27.

Elisei, R., Cosci, B., Romei, C., Bottici, V., Renzini, G., Molinaro, E., Agate, L., Vivaldi, A., Faviana, P., Basolo, F., Miccoli, P., Berti, P., Pacini, F. and Pinchera, A. (2008). "Prognostic significance of somatic RET oncogene mutations in sporadic medullary thyroid cancer: a 10-year follow-up study." J Clin Endocrinol Metab **93**: 682-687.

Elisei, R., Schlumberger, M. J., Muller, S. P., Schoffski, P., Brose, M. S., Shah, M. H., Licitra, L., Jarzab, B., Medvedev, V., Kreissl, M. C., Niederle, B., Cohen, E. E., Wirth, L. J., Ali, H., Hessel, C., Yaron, Y., Ball, D., Nelkin, B. and Sherman, S. I. (2013). "Cabozantinib in progressive medullary thyroid cancer." J Clin Oncol **31**: 3639-3646.

Emi, M., Fujiwara, Y., Nakajima, T., Tsuchiya, E., Tsuda, H., Hirohashi, S., Maeda, Y., Tsuruta, K., Miyaki, M. and Nakamura, Y. (1992). "Frequent loss of heterozygosity for loci on chromosome 8p in hepatocellular carcinoma, colorectal cancer, and lung cancer." Cancer Res **52**: 5368-5372.

Eng, C., Clayton, D., Schuffenecker, I., Lenoir, G., Cote, G., Gagel, R. F., van Amstel, H. K., Lips, C. J., Nishisho, I., Takai, S. I., Marsh, D. J., Robinson, B. G., Frank-Raue, K., Raue, F., Xue, F., Noll, W. W., Romei, C., Pacini, F., Fink, M., Niederle, B., Zedenius, J., Nordenskjold, M., Komminoth, P., Hendy, G. N., Mulligan L. M. and et al. (1996). "The relationship between specific RET proto-oncogene mutations and disease phenotype in multiple endocrine neoplasia type 2. International RET mutation consortium analysis." JAMA **276**: 1575-1579.

Erovic, B. M., Kim, D., Cassol, C., Goldstein, D. P., Irish, J. C., Asa, S. L. and Mete, O. (2012). "Prognostic and predictive markers in medullary thyroid carcinoma." Endocr Pathol **23**: 232-242.

Eulalio, A., Behm-Ansmant, I. and Izaurralde, E. (2007). "P bodies: at the crossroads of post-transcriptional pathways." Nat Rev Mol Cell Biol **8**: 9-22.

Fabian, M. R. and Sonenberg, N. (2012). "The mechanics of miRNA-mediated gene silencing: a look under the hood of miRISC." Nat Struct Mol Biol **19**: 586-593.

Fabian, M. R., Sonenberg, N. and Filipowicz, W. (2010). "Regulation of mRNA translation and stability by microRNAs." Annu Rev Biochem **79**: 351-379.

Filipowicz, W., Bhattacharyya, S. N. and Sonenberg, N. (2008). "Mechanisms of post-transcriptional regulation by microRNAs: are the answers in sight?" Nat Rev Genet **9**: 102-114.

Filipowicz, W., Jaskiewicz, L., Kolb, F. A. and Pillai, R. S. (2005). "Post-transcriptional gene silencing by siRNAs and miRNAs." Curr Opin Struct Biol **15**: 331-341.

Fineberg, S. K., Kosik, K. S. and Davidson, B. L. (2009). "MicroRNAs potentiate neural development." Neuron **64**: 303-309.

Fire, A., Xu, S., Montgomery, M. K., Kostas, S. A., Driver, S. E. and Mello, C. C. (1998). "Potent and specific genetic interference by double-stranded RNA in Caenorhabditis elegans." Nature **391**: 806-811.

Forman, J. J., Legesse-Miller, A. and Coller, H. A. (2008). "A search for conserved sequences in coding regions reveals that the let-7 microRNA targets Dicer within its coding sequence." Proc Natl Acad Sci U S A **105**: 14879-14884.

Franklin, D. S., Godfrey, V. L., Lee, H., Kovalev, G. I., Schoonhoven, R., Chen-Kiang, S., Su, L. and Xiong, Y. (1998). "CDK inhibitors p18(INK4c) and p27(Kip1) mediate two separate pathways to collaboratively suppress pituitary tumorigenesis." Genes Dev **12**: 2899-2911.

Franklin, D. S., Godfrey, V. L., O'Brien, D. A., Deng, C. and Xiong, Y. (2000). "Functional collaboration between different cyclin-dependent kinase inhibitors suppresses tumor growth with distinct tissue specificity." Mol Cell Biol **20**: 6147-6158.

Fritz, A., Walch, A., Piotrowska, K., Rosemann, M., Schaffer, E., Weber, K., Timper, A., Wildner, G., Graw, J., Hofler, H. and Atkinson, M. J. (2002). "Recessive transmission of a multiple endocrine neoplasia syndrome in the rat." Cancer Res **62**: 3048-3051.

Fukuda, T., Yamagata, K., Fujiyama, S., Matsumoto, T., Koshida, I., Yoshimura, K., Mihara, M., Naitou, M., Endoh, H., Nakamura, T., Akimoto, C., Yamamoto, Y., Katagiri, T., Foulds, C., Takezawa, S., Kitagawa, H., Takeyama, K., O'Malley, B. W. and Kato, S. (2007). "DEAD-box RNA helicase subunits of the Drosha complex are required for processing of rRNA and a subset of microRNAs." Nat Cell Biol **9**: 604-611.

Furuta, M., Kozaki, K. I., Tanaka, S., Arii, S., Imoto, I. and Inazawa, J. (2010). "miR-124 and miR-203 are epigenetically silenced tumor-suppressive microRNAs in hepatocellular carcinoma." Carcinogenesis **31**: 766-776.

Garcia, D. M., Baek, D., Shin, C., Bell, G. W., Grimson, A. and Bartel, D. P. (2011). "Weak seed-pairing stability and high target-site abundance decrease the proficiency of lsy-6 and other microRNAs." Nat Struct Mol Biol **18**: 1139-1146.

Garzon, R., Calin, G. A. and Croce, C. M. (2009). "MicroRNAs in Cancer." Annu Rev Med **60**: 167-179.

Geneste, O., Bidaud, C., De Vita, G., Hofstra, R. M., Tartare-Deckert, S., Buys, C. H., Lenoir, G. M., Santoro, M. and Billaud, M. (1999). "Two distinct mutations of the RET receptor causing Hirschsprung's disease impair the binding of signalling effectors to a multifunctional docking site." Hum Mol Genet **8**: 1989-1999.

Ghildiyal, M. and Zamore, P. D. (2009). "Small silencing RNAs: an expanding universe." Nat Rev Genet **10**: 94-108.

Giunti, S., Antonelli, A., Amorosi, A. and Santarpia, L. (2013). "Cellular signaling pathway alterations and potential targeted therapies for medullary thyroid carcinoma." Int J Endocrinol **2013**: 803171.

Gong, J., Li, J., Wang, Y., Liu, C., Jia, H., Jiang, C., Wang, Y., Luo, M., Zhao, H., Dong, L., Song, W., Wang, F., Wang, W., Zhang, J. and Yu, J. (2014). "Characterization of microRNA-29 family expression and investigation of their mechanistic roles in gastric cancer." Carcinogenesis **35**: 497-506.

Gregory, R. I., Yan, K. P., Amuthan, G., Chendrimada, T., Doratotaj, B., Cooch, N. and Shiekhattar, R. (2004). "The Microprocessor complex mediates the genesis of microRNAs." Nature **432**: 235-240.

Grimson, A., Farh, K. K., Johnston, W. K., Garrett-Engele, P., Lim, L. P. and Bartel, D. P. (2007). "MicroRNA targeting specificity in mammals: determinants beyond seed pairing." Mol Cell **27**: 91-105.

Gschwind, A., Fischer, O. M. and Ullrich, A. (2004). "The discovery of receptor tyrosine kinases: targets for cancer therapy." Nat Rev Cancer **4**: 361-370.

Guil, S. and Caceres, J. F. (2007). "The multifunctional RNA-binding protein hnRNP A1 is required for processing of miR-18a." Nat Struct Mol Biol **14**: 591-596.

Guttilla, I. K. and White, B. A. (2009). "Coordinate regulation of FOXO1 by miR-27a, miR-96, and miR-182 in breast cancer cells." J Biol Chem **284**: 23204-23216.

Ha, M. and Kim, V. N (2014). "Regulation of microRNA biogenesis." Nat Rev Mol Cell Biol **15**: 509-524.

Han, Z. B., Yang, Z., Chi, Y., Zhang, L., Wang, Y., Ji, Y., Wang, J., Zhao, H. and Han, Z. C. (2013). "MicroRNA-124 suppresses breast cancer cell growth and motility by targeting CD151." Cell Physiol Biochem **31**: 823-832.

Hanahan, D. and Weinberg, R. A. (2000). "The hallmarks of cancer." Cell **100**: 57-70.

He, L., Thomson, J. M., Hemann, M. T., Hernando-Monge, E., Mu, D., Goodson, S., Powers, S., Cordon-Cardo, C., Lowe, S. W., Hannon, G. J. and Hammond, S. M. (2005). "A microRNA polycistron as a potential human oncogene." Nature **435**: 828-833.

Hennequin, L. F., Stokes, E. S., Thomas, A. P., Johnstone, C., Ple, P. A., Ogilvie, D. J., Dukes, M., Wedge, S. R., Kendrew, J. and Curwen, J. O. (2002). "Novel 4-anilinoquinazolines with C-7 basic side chains: design and structure activity relationship of a series of potent, orally active, VEGF receptor tyrosine kinase inhibitors." J Med Chem **45**: 1300-1312.

Hibio, N., Hino, K., Shimizu, E., Nagata, Y. and Ui-Tei, K. (2012). "Stability of miRNA 5'terminal and seed regions is correlated with experimentally observed miRNA-mediated silencing efficacy." Sci Rep **2**: 996.

Huyck, L., Ampe, C. and Van Troys, M. (2012). "The XTT cell proliferation assay applied to cell layers embedded in three-dimensional matrix." Assay Drug Dev Technol **10**: 382-392.

Ibanez, C. F. (2013). "Structure and physiology of the RET receptor tyrosine kinase." Cold Spring Harb Perspect Biol **5**.

Inui, M., Martello, G. and Piccolo, S. (2010). "MicroRNA control of signal transduction." Nat Rev Mol Cell Biol **11**: 252-263.

Iorio, M. V. and Croce, C. M. (2012). "MicroRNA dysregulation in cancer: diagnostics, monitoring and therapeutics. A comprehensive review." EMBO Mol Med **4**: 143-159.

Ito, Y., Yoshida, H., Nakamura, Y., Tomoda, C., Uruno, T., Takamura, Y., Miya, A., Kobayashi, K., Matsuzuka, F., Kuma, K., Kakudo, K. and Miyauchi, A. (2005). "Expression of Jun activation domain-binding protein 1 and p27 (Kip1) in thyroid medullary carcinoma." Pathology **37**: 216-219.

Iwashita, T., Asai, N., Murakami, H., Matsuyama, M. and Takahashi, M. (1996). "Identification of tyrosine residues that are essential for transforming activity of the ret proto-oncogene with MEN2A or MEN2B mutation." Oncogene **12**: 481-487.

Jeyaseelan, K., Lim, K. Y. and Armugam, A. (2008). "MicroRNA expression in the blood and brain of rats subjected to transient focal ischemia by middle cerebral artery occlusion." Stroke **39**: 959-966.

Jiang, H., Zhang, G., Wu, J. H. and Jiang, C. P. (2014). "Diverse roles of miR-29 in cancer (review)." Oncol Rep **31**: 1509-1516.

Johanson, V., Ahlman, H., Bernhardt, P., Jansson, S., Kolby, L., Persson, F., Stenman, G., Sward, C., Wangberg, B., Stridsberg, M. and Nilsson, O. (2007). "A transplantable human medullary thyroid carcinoma as a model for RET tyrosine kinase-driven tumorigenesis." Endocr Relat Cancer **14**: 433-444.

John, B., Enright, A. J., Aravin, A., Tuschl, T., Sander, C. and Marks, D. S. (2004). "Human MicroRNA targets." PLoS Biol **2**: 1862-1879.

Johnston, D., Hatzis, D. and Sunday, M. E. (1998). "Expression of v-Ha-ras driven by the calcitonin/calcitonin gene-related peptide promoter: a novel transgenic murine model for medullary thyroid carcinoma." Oncogene **16**: 167-177.

Joshi, P. P., Kulkarni, M. V., Yu, B. K., Smith, K. R., Norton, D. L., van Veelen, W., Hoppener, J. W. and Franklin, D. S. (2007). "Simultaneous downregulation of CDK inhibitors p18(Ink4c) and p27(Kip1) is required for MEN2A-RET-mediated mitogenesis." Oncogene **26**: 554-570.

Kaatsch, P., Spix, C., Hentschel, S., Katalinic, A., Luttmann, S., Stegmaier, C., Caspritz, S., Cernaj, J., Ernst, A., Folkerts, J., Hansmann, J. and Kranzhöfer, K. (2013). Krebs in Deutschland 2009/2010 - 9. Ausgabe, 2013, Robert Koch-Institut. **9**.

Kawai, K., Iwashita, T., Murakami, H., Hiraiwa, N., Yoshiki, A., Kusakabe, M., Ono, K., Iida, K., Nakayama, A. and Takahashi, M. (2000). "Tissue-specific carcinogenesis in transgenic mice expressing the RET proto-oncogene with a multiple endocrine neoplasia type 2A mutation." Cancer Res **60**: 5254-5260.

Kawai, S. and Amano, A. (2012). "BRCA1 regulates microRNA biogenesis via the DROSHA microprocessor complex." J Cell Biol **197**: 201-208.

Kedzia, C., Lacroix, L., Ameur, N., Ragot, T., Kelly, P. A., Caillou, B. and Binart, N. (2005). "Medullary thyroid carcinoma arises in the absence of prolactin signaling." Cancer Res **65**: 8497-8503.

Kerbel, R. S. (2008). "Tumor angiogenesis." N Engl J Med **358**: 2039-2049.

Khvorova, A., Reynolds, A. and Jayasena, S. D. (2003). "Functional siRNAs and miRNAs exhibit strand bias." Cell **115**: 209-216.

Kim, V. N., Han, J. and Siomi, M. C. (2009). "Biogenesis of small RNAs in animals." Nat Rev Mol Cell Biol **10**: 126-139.

Kjaer, S., Kurokawa, K., Perrinjaquet, M., Abrescia, C. and Ibanez, C. F. (2006). "Self-association of the transmembrane domain of RET underlies oncogenic activation by MEN2A mutations." Oncogene **25**: 7086-7095.

Klein, C. A. (2008). "Cancer. The metastasis cascade." Science **321**: 1785-1787.

Kloos, R. T., Eng, C., Evans, D. B., Francis, G. L., Gagel, R. F., Gharib, H., Moley, J. F., Pacini, F., Ringel, M. D., Schlumberger, M. and Wells, S. A. Jr. (2009). "Medullary thyroid cancer: management guidelines of the American Thyroid Association." Thyroid **19**: 565-612.

Knight, R. D., Mebus, K., d'Angelo, A., Yokoya, K., Heanue, T., Tübingen 2000 Screen Consortium and Roehl, H. (2011). "Ret signalling integrates a craniofacial muscle module during development." Development **138**: 2015-2024.

Knowles, P. P., Murray-Rust, J., Kjaer, S., Scott, R. P., Hanrahan, S., Santoro, M., Ibanez, C. F. and McDonald, N. Q. (2006). "Structure and chemical inhibition of the RET tyrosine kinase domain." J Biol Chem **281**: 33577-33587.

Kondo, T., Ezzat, S. and Asa, S. L. (2006). "Pathogenetic mechanisms in thyroid follicular-cell neoplasia." Nat Rev Cancer **6**: 292-306.

Koscianska, E., Starega-Roslan, J. and Krzyzosiak, W. J. (2011). "The role of Dicer protein partners in the processing of microRNA precursors." PLoS One **6**: e28548.

Kostoglou-Athanassiou, I., Athanassiou, P., Vecchini, G., Gogou, L. and Kaldrymides, P. (2004). "Mixed medullary-follicular thyroid carcinoma. Report of a case and review of the literature." Horm Res **61**: 300-304.

Kozomara, A. and Griffiths-Jones, S. (2011). "miRBase: integrating microRNA annotation and deep-sequencing data." Nucleic Acids Res **39**: D152-157.

Kraemer, A., Barjaktarovic, Z., Sarioglu, H., Winkler, K., Eckardt-Schupp, F., Tapio, S., Atkinson, M. J. and Moertl, S. (2013). "Cell survival following radiation exposure requires miR-525-3p mediated suppression of ARRB1 and TXN1." PLoS One **8**: e77484.

Kramer, A., Green, J., Pollard, J. Jr. and Tugendreich, S. (2014). "Causal analysis approaches in Ingenuity Pathway Analysis." Bioinformatics **30**: 523-530.

Krek, A., Grun, D., Poy, M. N., Wolf, R., Rosenberg, L., Epstein, E. J., MacMenamin, P., da Piedade, I., Gunsalus, K. C., Stoffel, M. and Rajewsky, N. (2005). "Combinatorial microRNA target predictions." Nat Genet **37**: 495-500.

Kriegel, A. J., Liu, Y., Fang, Y., Ding, X. and Liang, M. (2012). "The miR-29 family: genomics, cell biology, and relevance to renal and cardiovascular injury." Physiol Genomics **44**: 237-244.

Kurzrock, R., Sherman, S. I., Ball, D. W., Forastiere, A. A., Cohen, R. B., Mehra, R., Pfister, D. G., Cohen, E. E., Janisch, L., Nauling, F., Hong, D. S., Ng, C. S., Ye, L., Gagel, R. F., Frye, J., Muller, T., Ratain, M. J. and Salgia, R. (2011). "Activity of XL184 (Cabozantinib), an oral tyrosine kinase inhibitor, in patients with medullary thyroid cancer." J Clin Oncol **29**: 2660-2666.

Lackey, K., Cory, M., Davis, R., Frye, S. V., Harris, P. A., Hunter, R. N., Jung, D. K., McDonald, O. B., McNutt, R. W., Peel, M. R., Rutkowske, R. D., Veal, J. M. and Wood, E. R. (2000). "The discovery of potent cRaf1 kinase inhibitors." Bioorg Med Chem Lett **10**: 223-226.

Lairmore, T. C., Piersall, L. D., DeBenedetti, M. K., Dilley, W. G., Mutch, M. G., Whelan, A. J. and Zehnbauer, B. (2004). "Clinical genetic testing and early surgical intervention in patients with multiple endocrine neoplasia type 1 (MEN 1)." Ann Surg **239**: 637-645.

Lang, Q. and Ling, C. (2012). "MiR-124 suppresses cell proliferation in hepatocellular carcinoma by targeting PIK3CA." Biochem Biophys Res Commun **426**: 247-252.

Laulederkind, S. J., Hayman, G. T., Wang, S. J., Smith, J. R., Lowry, T. F., Nigam, R., Petri, V., de Pons, J., Dwinell, M. R., Shimoyama, M., Munzenmaier, D. H., Worthey, E. A. and Jacob, H. J. (2013). "The Rat Genome Database 2013--data, tools and users." Brief Bioinform **14**: 520-526.

Leboulleux, S., Baudin, E., Travagli, J. P. and Schlumberger, M. (2004). "Medullary thyroid carcinoma." Clin Endocrinol (Oxf) **61**: 299-310.

Lee, E. J., Baek, M., Gusev, Y., Brackett, D. J., Nuovo, G. J. and Schmittgen, T. D. (2008). "Systematic evaluation of microRNA processing patterns in tissues, cell lines, and tumors." RNA **14**: 35-42.

Lee, M. and Pellegata, N. S. (2013). "Multiple endocrine neoplasia syndromes associated with mutation of p27." J Endocrinol Invest **36**: 781-787.

Lee, R. C., Feinbaum, R. L. and Ambros, V. (1993). "The C. elegans heterochronic gene lin-4 encodes small RNAs with antisense complementarity to lin-14." Cell **75**: 843-854.

Lee, Y., Kim, M., Han, J., Yeom, K. H., Lee, S., Baek, S. H. and Kim, V. N. (2004). "MicroRNA genes are transcribed by RNA polymerase II." EMBO J **23**: 4051-4060.

Lee, Y. S. and Dutta, A. (2009). "MicroRNAs in cancer." Annu Rev Pathol **4**: 199-227.

Lemos, M. C. and Thakker, R. V. (2008). "Multiple endocrine neoplasia type 1 (MEN1): analysis of 1336 mutations reported in the first decade following identification of the gene." Hum Mutat **29**: 22-32.

Lena, A. M., Shalom-Feuerstein, R., Rivetti di Val Cervo, P., Aberdam, D., Knight, R. A., Melino, G. and Candi, E. (2008). "miR-203 represses 'stemness' by repressing DeltaNp63." Cell Death Differ **15**: 1187-1195.

Lewis, B. P., Burge, C. B. and Bartel, D. P. (2005). "Conserved seed pairing, often flanked by adenosines, indicates that thousands of human genes are microRNA targets." Cell **120**: 15-20.

Li, X., Mertens-Talcott, S. U., Zhang, S., Kim, K., Ball, J. and Safe, S. (2010). "MicroRNA-27a Indirectly Regulates Estrogen Receptor {alpha} Expression and Hormone Responsiveness in MCF-7 Breast Cancer Cells." Endocrinology **151**: 2462-2473.

Li, Y., Zhang, Z., Liu, X., Huang, T., He, W., Shen, Y., Liu, X., Hong, K. and Cao, Q. (2014). "miR-124 functions as a tumor suppressor in the endometrial carcinoma cell line HEC-1B partly by suppressing STAT3." Mol Cell Biochem **388**: 219-231.

Liao, C., Zhao, M., Song, H., Uchida, K., Yokoyama, K. K. and Li, T. (2000). "Identification of the gene for a novel liver-related putative tumor suppressor at a high-frequency loss of heterozygosity region of chromosome 8p23 in human hepatocellular carcinoma." Hepatology **32**: 721-727.

Libri, V., Miesen, P., van Rij, R. P. and Buck, A. H. (2013). "Regulation of microRNA biogenesis and turnover by animals and their viruses." Cell Mol Life Sci **70**: 3525-3544.

Lim, S. and Kaldis, P. (2013). "Cdks, cyclins and CKIs: roles beyond cell cycle regulation." Development **140**: 3079-3093.

Liu, S. Q., Su, Y. J., Qin, M. B., Mao, Y. B., Huang, J. A. and Tang, G. D. (2013). "Sphingosine kinase 1 promotes tumor progression and confers malignancy phenotypes of colon cancer by regulating the focal adhesion kinase pathway and adhesion molecules." Int J Oncol **42**: 617-626.

Livak, K. J. and Schmittgen, T. D. (2001). "Analysis of relative gene expression data using real-time quantitative PCR and the 2(-Delta Delta C(T)) Method." Methods **25**: 402-408.

Lodish, M. B. and Stratakis, C. A. (2008). "RET oncogene in MEN2, MEN2B, MTC and other forms of thyroid cancer." Expert Rev Anticancer Ther **8**: 625-632.

Lu, J., Getz, G., Miska, E. A., Alvarez-Saavedra, E., Lamb, J., Peck, D., Sweet-Cordero, A., Ebert, B. L., Mak, R. H., Ferrando, A. A., Downing, J. R., Jacks, T., Horvitz, H. R. and Golub, T. R. (2005). "MicroRNA expression profiles classify human cancers." Nature **435**: 834-838.

Lund, E., Guttinger, S., Calado, A., Dahlberg, J. E. and Kutay, U. (2004). "Nuclear export of microRNA precursors." Science **303**: 95-98.

Lyons, J. F., Wilhelm, S., Hibner, B. and Bollag, G. (2001). "Discovery of a novel Raf kinase inhibitor." Endocr Relat Cancer **8**: 219-225.

Lytle, J. R., Yario, T. A. and Steitz, J. A. (2007). "Target mRNAs are repressed as efficiently by microRNA-binding sites in the 5' UTR as in the 3' UTR." Proc Natl Acad Sci U S A **104**: 9667-9672.

Machens, A. and Dralle, H. (2008). "Familial prevalence and age of RET germline mutations: implications for screening." Clin Endocrinol (Oxf) **69**: 81-87.

Machens, A. and Dralle, H. (2009). "Prophylactic thyroidectomy in RET carriers at risk for hereditary medullary thyroid cancer." Thyroid **19**: 551-554.

Machens, A., Lorenz, K. and Dralle, H. (2009). "Individualization of lymph node dissection in RET (rearranged during transfection) carriers at risk for medullary thyroid cancer: value of pretherapeutic calcitonin levels." Ann Surg **250**: 305-310.

Machens, A., Lorenz, K., Sekulla, C., Hoppner, W., Frank-Raue, K., Raue, F. and Dralle, H. (2013). "Molecular epidemiology of multiple endocrine neoplasia 2: implications for RET screening in the new millenium." Eur J Endocrinol **168**: 307-314.

Machens, A., Schaaf, L., Karges, W., Frank-Raue, K., Bartsch, D. K., Rothmund, M., Schneyer, U., Goretzki, P., Raue, F. and Dralle, H. (2007). "Age-related penetrance of endocrine tumours in multiple endocrine neoplasia type 1 (MEN1): a multicentre study of 258 gene carriers." Clin Endocrinol (Oxf) **67**: 613-622.

Maliszewska, A., Leandro-Garcia, L. J., Castelblanco, E., Macia, A., de Cubas, A., Gomez-Lopez, G., Inglada-Perez, L., Alvarez-Escola, C., De la Vega, L., Leton, R., Gomez-Grana, A., Landa, I., Cascon, A., Rodriguez-Antona, C., Borrego, S., Zane, M., Schiavi, F., Merante-Boschin, I., Pelizzo, M. R., Pisano, D. G., Opocher, G., Matias-Guiu, X., Encinas, M. and Robledo, M. (2013). "Differential gene expression of medullary thyroid carcinoma reveals specific markers associated with genetic conditions." Am J Pathol **182**: 350-362.

Malumbres, M. and Barbacid, M. (2005). "Mammalian cyclin-dependent kinases." Trends Biochem Sci **30**: 630-641.

Malumbres, M. and Barbacid, M. (2009). "Cell cycle, CDKs and cancer: a changing paradigm." Nat Rev Cancer **9**: 153-166.

Manie, S., Santoro, M., Fusco, A. and Billaud, M. (2001). "The RET receptor: function in development and dysfunction in congenital malformation." Trends Genet **17**: 580-589.

Margraf, R. L., Crockett, D. K., Krautscheid, P. M., Seamons, R., Calderon, F. R., Wittwer, C. T. and Mao, R. (2009). "Multiple endocrine neoplasia type 2 RET protooncogene database: repository of MEN2-associated RET sequence variation and reference for genotype/phenotype correlations." Hum Mutat **30**: 548-556.

Marinoni, I. and Pellegata, N. S. (2011). "p27kip1: a new multiple endocrine neoplasia gene?" Neuroendocrinology **93**: 19-28.

Marx, S., Spiegel, A. M., Skarulis, M. C., Doppman, J. L., Collins, F. S. and Liotta, L. A. (1998). "Multiple endocrine neoplasia type 1: clinical and genetic topics." Ann Intern Med **129**: 484-494.

Massague, J. (2004). "G1 cell-cycle control and cancer." Nature **432**: 298-306.

Mathonnet, G., Fabian, M. R., Svitkin, Y. V., Parsyan, A., Huck, L., Murata, T., Biffo, S., Merrick, W. C., Darzynkiewicz, E., Pillai, R. S., Filipowicz, W., Duchaine, T. F. and Sonenberg, N. (2007). "MicroRNA inhibition of translation initiation in vitro by targeting the cap-binding complex eIF4F." Science **317**: 1764-1767.

Mayburd, A. L., Martlinez, A., Sackett, D., Liu, H., Shih, J., Tauler, J., Avis, I. and Mulshine, J. L. (2006). "Ingenuity network-assisted transcription profiling: Identification of a new pharmacologic mechanism for MK886." Clin Cancer Res **12**: 1820-1827.

Melo, S. A., Ropero, S., Moutinho, C., Aaltonen, L. A., Yamamoto, H., Calin, G. A., Rossi, S., Fernandez, A. F., Carneiro, F., Oliveira, C., Ferreira, B., Liu, C. G., Villanueva, A., Capella, G., Schwartz, S. Jr., Shiekhattar, R. and Esteller, M. (2009). "A TARBP2 mutation in human cancer impairs microRNA processing and DICER1 function." Nat Genet **41**: 365-370.

Menon, M. P. and Khan, A. (2009). "Micro-RNAs in thyroid neoplasms: molecular, diagnostic and therapeutic implications." J Clin Pathol **62**: 978-985.

Mertens-Talcott, S. U., Chintharlapalli, S., Li, X. and Safe, S. (2007). "The oncogenic microRNA-27a targets genes that regulate specificity protein transcription factors and the G2-M checkpoint in MDA-MB-231 breast cancer cells." Cancer Res **67**: 11001-11011.

Miao, L. J., Huang, S. F., Sun, Z. T., Gao, Z. Y., Zhang, R. X., Liu Y. and Wang, J. (2013). "MiR-449c targets c-Myc and inhibits NSCLC cell progression." FEBS Lett **587**: 1359-1365.

Michiels, F. M., Chappuis, S., Caillou, B., Pasini, A., Talbot, M., Monier, R., Lenoir, G. M., Feunteun, J. and Billaud, M. (1997). "Development of medullary thyroid carcinoma in transgenic mice expressing the RET protooncogene altered by a multiple endocrine neoplasia type 2A mutation." Proc Natl Acad Sci U S A **94**: 3330-3335.

Milan, S. A., Sosa, J. A. and Roman, S. A. (2010). "Current management of medullary thyroid cancer." Minerva Chir **65**: 27-37.

Mitsiades, C. S., Kotoula, V., Poulaki, V., Sozopoulos, E., Negri, J., Charalambous, E., Fanourakis, G., Voutsinas, G., Tseleni-Balafouta, S. and Mitsiades, N. (2006). "Epidermal growth factor receptor as a therapeutic target in human thyroid carcinoma: mutational and functional analysis." J Clin Endocrinol Metab **91**: 3662-3666.

Moerch, U., Nielsen, H. S., Lundsgaard, D. and Oleksiewicz, M. B. (2007). "Flow sorting from organ material by intracellular markers." Cytometry A **71**: 495-500.

Molatore, S., Liyanarachchi, S., Irmler, M., Perren, A., Mannelli, M., Ercolino, T., Beuschlein, F., Jarzab, B., Wloch, J., Ziaja, J., Zoubaa, S., Neff, F., Beckers, J., Hofler, H., Atkinson, M. J. and Pellegata, N. S. (2010). "Pheochromocytoma in rats with multiple endocrine neoplasia (MENX) shares gene expression patterns with human pheochromocytoma." Proc Natl Acad Sci U S A **107**: 18493-18498.

Molatore, S., Neff, F., Wiedemann, T., Lee, M. and Pellegata, N. S. (2011). "Rats heterozygous for the MENX-associated p27 mutation develop a MEN phenotype." Poster presented at: NET Diagnosis and Treatment: A New Era - A New Direction; 2011 Oct 11-13; Minneapolis, Minnesota, USA.

Moley, J. F. (2010). "Medullary thyroid carcinoma: management of lymph node metastases." J Natl Compr Canc Netw **8**: 549-556.

Morabito, A., Piccirillo, M. C., Falasconi, F., De Feo, G., Del Giudice, A., Bryce, J., Di Maio, M., De Maio, E., Normanno, N. and Perrone, F. (2009). "Vandetanib (ZD6474), a dual inhibitor of vascular endothelial growth factor receptor (VEGFR) and epidermal growth factor receptor (EGFR) tyrosine kinases: current status and future directions." Oncologist **14**: 378-390.

Mosmann, T. (1983). "Rapid colorimetric assay for cellular growth and survival: application to proliferation and cytotoxicity assays." J Immunol Methods **65**: 55-63.

Moura, M. M., Cavaco, B. M., Pinto, A. E., Domingues, R., Santos, J. R., Cid, M. O., Bugalho, M. J. and Leite, V. (2009). "Correlation of RET somatic mutations with clinicopathological features in sporadic medullary thyroid carcinomas." Br J Cancer **100**: 1777-1783.

Moura, M. M., Cavaco, B. M., Pinto, A. E. and Leite, V. (2011). "High prevalence of RAS mutations in RET-negative sporadic medullary thyroid carcinomas." J Clin Endocrinol Metab **96**: E863-868.

Mulligan, L. M. (2014). "RET revisited: expanding the oncogenic portfolio." Nat Rev Cancer **14**: 173-186.

Mulligan, L. M., Eng, C., Attie, T., Lyonnet, S., Marsh, D. J., Hyland, V. J., Robinson, B. G., Frilling, A., Verellen-Dumoulin, C., Safar A. and et al. (1994). "Diverse phenotypes associated with exon 10 mutations of the RET proto-oncogene." Hum Mol Genet **3**: 2163-2167.

Murakami, M., Ichihara, M., Sobue, S., Kikuchi, R., Ito, H., Kimura, A., Iwasaki, T., Takagi, A., Kojima, T., Takahashi, M., Suzuki, M., Banno, Y., Nozawa, Y. and Murate, T. (2007). "RET signaling-induced SPHK1 gene expression plays a role in both GDNF-induced differentiation and MEN2-type oncogenesis." J Neurochem **102**: 1585-1594.

Myatt, S. S., Wang, J., Monteiro, L. J., Christian, M., Ho, K. K., Fusi, L., Dina, R. E., Brosens, J. J., Ghaem-Maghami, S. and Lam, E. W. (2010). "Definition of microRNAs that repress expression of the tumor suppressor gene FOXO1 in endometrial cancer." Cancer Res **70**: 367-377.

Nabel, E. G. (2002). "CDKs and CKIs: molecular targets for tissue remodelling." Nat Rev Drug Discov **1**: 587-598.

Nguyen, D. X. and Massague, J. (2007). "Genetic determinants of cancer metastasis." Nat Rev Genet **8**: 341-352.

Nigg, E. A. (1995). "Cyclin-dependent protein kinases: key regulators of the eukaryotic cell cycle." Bioessays **17**: 471-480.

Nikiforova, M. N., Chiosea, S. I. and Nikiforov, Y. E. (2009). "MicroRNA expression profiles in thyroid tumors." Endocr Pathol **20**: 85-91.

Nikiforova, M. N., Tseng, G. C., Steward, D., Diorio, D. and Nikiforov, Y. E. (2008). "MicroRNA expression profiling of thyroid tumors: biological significance and diagnostic utility." J Clin Endocrinol Metab **93**: 1600-1608.

Nilsen, T. W., Grayzel, J. and Prensky, W. (1997). "Dendritic nucleic acid structures." J Theor Biol **187**: 273-284.

Nishikawa, R., Goto, Y., Kojima, S., Enokida, H., Chiyomaru, T., Kinoshita, T., Sakamoto, S., Fuse, M., Nakagawa, M., Naya, Y., Ichikawa T. and Seki, N. (2014). "Tumor-suppressive microRNA-29s inhibit cancer cell migration and invasion via targeting LAMC1 in prostate cancer." Int J Oncol **45**: 401-410.

Oliveros, J. C. (2007). "VENNY. An interactive tool for comparing lists with Venn Diagrams.", from http://bioinfogp.cnb.csic.es/tools/venny/index.html.

Pai, B., Siripornmongcolchai, T., Berentsen, B., Pakzad, A., Vieuille, C., Pallesen, S., Pajak, M., Simpson, T. I., Armstrong, J. D., Wibrand, K. and Bramham, C. R. (2014). "NMDA receptor-dependent regulation of miRNA expression and association with Argonaute during LTP in vivo." Front Cell Neurosci **7**: 285.

Pan, J., Tao, Y. F., Zhou, Z., Cao, B. R., Wu, S. Y., Zhang, Y. L., Hu, S. Y., Zhao, W. L., Wang, J., Lou, G. L., Li, Z., Feng, X. and Ni, J. (2011). "An novel role of sphingosine kinase-1 (SPHK1) in the invasion and metastasis of esophageal carcinoma." J Transl Med **9**: 157.

Papagiannakopoulos, T. and Kosik, K. S. (2008). "MicroRNAs: regulators of oncogenesis and stemness." BMC Med **6**: 15.

Parker, R. and Song, H. (2004). "The enzymes and control of eukaryotic mRNA turnover." Nat Struct Mol Biol **11**: 121-127.

Paroo, Z., Ye, X., Chen, S. and Liu, Q. (2009). "Phosphorylation of the human microRNA-generating complex mediates MAPK/Erk signaling." Cell **139**: 112-122.

Pellegata, N. S. (2012). "MENX and MEN4." Clinics (Sao Paulo) **67 Suppl 1**: 13-18.

Pellegata, N. S., Quintanilla-Martinez, L., Siggelkow, H., Samson, E., Bink, K., Hofler, H., Fend, F., Graw, J. and Atkinson, M. J. (2006). "Germ-line mutations in p27Kip1 cause a multiple endocrine neoplasia syndrome in rats and humans." Proc Natl Acad Sci U S A **103**: 15558-15563.

Pestell, R. G. (2013). "New roles of cyclin D1." Am J Pathol **183**: 3-9.

Pfaffl, M. W. (2001). "A new mathematical model for relative quantification in real-time RT-PCR." Nucleic Acids Res **29**: e45.

Pillai, R. S., Bhattacharyya, S. N., Artus, C. G., Zoller, T., Cougot, N., Basyuk, E., Bertrand, E. and Filipowicz, W. (2005). "Inhibition of translational initiation by Let-7 MicroRNA in human cells." Science **309**: 1573-1576.

Plaisier, C. L., Pan, M. and Baliga, N. S. (2012). "A miRNA-regulatory network explains how dysregulated miRNAs perturb oncogenic processes across diverse cancers." Genome Res **22**: 2302-2314.

Png, K. J., Yoshida, M., Zhang, X. H., Shu, W., Lee, H., Rimner, A., Chan, T. A., Comen, E., Andrade, V. P., Kim, S. W., King, T. A., Hudis, C. A., Norton, L., Hicks, J., Massague, J. and Tavazoie, S. F. (2011). "MicroRNA-335 inhibits tumor reinitiation and is silenced through genetic and epigenetic mechanisms in human breast cancer." Genes Dev **25**: 226-231.

Qin, B. and Cheng, K. (2010). "Silencing of the IKKepsilon gene by siRNA inhibits invasiveness and growth of breast cancer cells." Breast Cancer Res **12**: R74.

Qiu, C., Yu, M., Shan, L. and Snyderwine, E. G. (2003). "Allelic imbalance and altered expression of genes in chromosome 2q11-2q16 from rat mammary gland carcinomas induced by 2-amino-1-methyl-6-phenylimidazo[4,5-b]pyridine." Oncogene **22**: 1253-1260.

R Development Core Team (2008). R: A Language and Environment for Statistical Computing, R Foundation for Statistical Computing, Vienna, Austria.

Rainer, J., Sanchez-Cabo, F., Stocker, G., Sturn, A. and Trajanoski, Z. (2006). "CARMAweb: comprehensive R- and bioconductor-based web service for microarray data analysis." Nucleic Acids Res **34**: W498-503.

Raue, F. and Frank-Raue, K. (2009). "Genotype-phenotype relationship in multiple endocrine neoplasia type 2. Implications for clinical management." Hormones (Athens) **8**: 23-28.

Recchi, C. and Seabra, M. C. (2012). "Novel functions for Rab GTPases in multiple aspects of tumour progression." Biochem Soc Trans **40**: 1398-1403.

Rodriguez, A., Griffiths-Jones, S., Ashurst, J. L. and Bradley, A. (2004). "Identification of mammalian microRNA host genes and transcription units." Genome Res **14**: 1902-1910.

Rodriguez-Antona, C., Pallares, J., Montero-Conde, C., Inglada-Perez, L., Castelblanco, E., Landa, I., Leskela, S., Leandro-Garcia, L. J., Lopez-Jimenez, E., Leton, R., Cascon, A., Lerma, E., Martin, M. C., Carralero, M. C., Mauricio, D., Cigudosa, J. C., Matias-Guiu, X. and Robledo, M. (2010). "Overexpression and activation of EGFR and VEGFR2 in medullary thyroid carcinomas is related to metastasis." Endocr Relat Cancer **17**: 7-16.

Romei, C., Pardi, E., Cetani, F. and Elisei, R. (2012). "Genetic and clinical features of multiple endocrine neoplasia types 1 and 2." J Oncol **2012**: 705036.

Ruiz-Llorente, S., Montero-Conde, C., Milne, R. L., Moya, C. M., Cebrian, A., Leton, R., Cascon, A., Mercadillo, F., Landa, I., Borrego, S., Perez de Nanclares, G., Alvarez-Escola, C., Diaz-Perez, J. A., Carracedo, A., Urioste, M., Gonzalez-Neira, A., Benitez, J., Santisteban, P., Dopazo, J., Ponder, B. A., Robledo, M. and the Medullary Thyroid Carcinoma Clinical Group (2007). "Association study of 69 genes in the ret pathway identifies low-penetrance loci in sporadic medullary thyroid carcinoma." Cancer Res **67**: 9561-9567.

Santarpia, L. and Bottai, G. (2013). "Inhibition of RET activated pathways: novel strategies for therapeutic intervention in human cancers." Curr Pharm Des **19**: 864-882.

Santarpia, L., Calin, G. A., Adam, L., Ye, L., Fusco, A., Giunti, S., Thaller, C., Paladini, L., Zhang, X., Jimenez, C., Trimarchi, F., El-Naggar, A. K. and Gagel, R. F. (2013). "A miRNA signature associated with human metastatic medullary thyroid carcinoma." Endocr Relat Cancer **20**: 809-823.

Santarpia, L., Ye, L. and Gagel, R. F. (2009). "Beyond RET: potential therapeutic approaches for advanced and metastatic medullary thyroid carcinoma." J Intern Med **266**: 99-113.

Santoro, M., Melillo, R. M., Carlomagno, F., Vecchio, G. and Fusco, A. (2004). "Minireview: RET: normal and abnormal functions." Endocrinology **145**: 5448-5451.

Santoro, M., Melillo, R. M., Carlomagno, F., Visconti, R., De Vita, G., Salvatore, G., Lupoli, G., Fusco, A. and Vecchio, G. (1998). "Molecular biology of the MEN2 gene." J Intern Med **243**: 505-508.

Sanuki, R., Onishi, A., Koike, C., Muramatsu, R., Watanabe, S., Muranishi, Y., Irie, S., Uneo, S., Koyasu, T., Matsui, R., Cherasse, Y., Urade, Y., Watanabe, D., Kondo, M., Yamashita, T. and Furukawa, T. (2011). "miR-124a is required for hippocampal axogenesis and retinal cone survival through Lhx2 suppression." Nat Neurosci **14**: 1125-1134.

Scarola, M., Schoeftner, S., Schneider, C. and Benetti, R. (2010). "miR-335 directly targets Rb1 (pRb/p105) in a proximal connection to p53-dependent stress response." Cancer Res **70**: 6925-6933.

Schlessinger, J. and Lemmon, M. A. (2003). "SH2 and PTB domains in tyrosine kinase signaling." Sci STKE **2003**: RE12.

Schlumberger, M., Carlomagno, F., Baudin, E., Bidart, J. M. and Santoro, M. (2008). "New therapeutic approaches to treat medullary thyroid carcinoma." Nat Clin Pract Endocrinol Metab **4**: 22-32.

Schwarz, D. S., Hutvagner, G., Du, T., Xu, Z., Aronin, N. and Zamore, P. D. (2003). "Asymmetry in the assembly of the RNAi enzyme complex." Cell **115**: 199-208.

Sheaff, R. J., Groudine, M., Gordon, M., Roberts J. M. and Clurman, B. E. (1997). "Cyclin E-CDK2 is a regulator of p27Kip1." Genes Dev **11**: 1464-1478.

Sherr, C. J. (1994). "G1 phase progression: cycling on cue." Cell **79**: 551-555.

Sherr, C. J. and Roberts, J. M. (1995). "Inhibitors of mammalian G1 cyclin-dependent kinases." Genes Dev **9**: 1149-1163.

Shimizu, K., Goldfarb, M., Perucho, M. and Wigler, M. (1983). "Isolation and preliminary characterization of the transforming gene of a human neuroblastoma cell line." Proc Natl Acad Sci U S A **80**: 383-387.

Shu, M., Zheng, X., Wu, S., Lu, H., Leng, T., Zhu, W., Zhou, Y., Ou, Y., Lin, X., Lin, Y., Xu, D. and Yan, G. (2011). "Targeting oncogenic miR-335 inhibits growth and invasion of malignant astrocytoma cells." Mol Cancer **10**: 59.

Siomi, H. and Siomi, M. C. (2010). "Posttranscriptional regulation of microRNA biogenesis in animals." Mol Cell **38**: 323-332.

Smith, C. M., Finger, J. H., Kadin, J. A., Richardson, J. E. and Ringwald, M. (2014). "The gene expression database for mouse development (GXD): Putting developmental expression information at your fingertips." Dev Dyn **243**: 1176–1118.

Smith-Hicks, C. L., Sizer, K. C., Powers, J. F., Tischler, A. S. and Costantini, F. (2000). "C-cell hyperplasia, pheochromocytoma and sympathoadrenal malformation in a mouse model of multiple endocrine neoplasia type 2B." EMBO J **19**: 612-622.

Sonkoly, E., Loven, J., Xu, N., Meisgen, F., Wei, T., Brodin, P., Jaks, V., Kasper, M., Shimokawa, T., Harada, M., Heilborn, J., Hedblad, M. A., Hippe, A., Grander, D., Homey, B., Zaphiropoulos, P. G., Arsenian-Henriksson, M., Stahle, M. and Pivarcsi, A. (2012). "MicroRNA-203 functions as a tumor suppressor in basal cell carcinoma." Oncogenesis **1**: e3.

Spitzweg, C., Baker, C. H., Bergert, E. R., O'Connor, M. K. and Morris, J. C. (2007). "Image-guided radioiodide therapy of medullary thyroid cancer after carcinoembryonic antigen promoter-targeted sodium iodide symporter gene expression." Hum Gene Ther **18**: 916-924.

Stears, R. L., Getts, R. C. and Gullans, S. R. (2000). "A novel, sensitive detection system for high-density microarrays using dendrimer technology." Physiol Genomics **3**: 93-99.

Suzuki, H. I., Yamagata, K., Sugimoto, K., Iwamoto, T., Kato, S. and Miyazono, K. (2009). "Modulation of microRNA processing by p53." Nature **460**: 529-533.

Sweetser, D. A., Froelick, G. J., Matsumoto, A. M., Kafer, K. E., Marck, B., Palmiter, R. D. and Kapur, R. P. (1999). "Ganglioneuromas and renal anomalies are induced by activated RET(MEN2B) in transgenic mice." Oncogene **18**: 877-886.

Tavazoie, S. F., Alarcon, C., Oskarsson, T., Padua, D., Wang, Q., Bos, P. D., Gerald, W. L. and Massague, J. (2008). "Endogenous human microRNAs that suppress breast cancer metastasis." Nature **451**: 147-152.

Thakker, R. V., Newey, P. J., Walls, G. V., Bilezikian, J., Dralle, H., Ebeling, P. R., Melmed, S., Sakurai, A., Tonelli, F. and Brandi, M. L. (2012). "Clinical practice guidelines for multiple endocrine neoplasia type 1 (MEN1)." J Clin Endocrinol Metab **97**: 2990-3011.

Thiery, J. P. (2002). "Epithelial-mesenchymal transitions in tumour progression." Nat Rev Cancer **2**: 442-454.

Thomas, L., Lai, S. Y., Dong, W., Feng, L., Dadu, R., Regone, R. M. and Cabanillas, M. E. (2014). "Sorafenib in metastatic thyroid cancer: a systematic review." Oncologist **19**: 251-258.

Thomson, J. M., Newman, M., Parker, J. S., Morin-Kensicki, E. M., Wright, T. and Hammond, S. M. (2006). "Extensive post-transcriptional regulation of microRNAs and its implications for cancer." Genes Dev **20**: 2202-2207.

Toetsch, S., Olwell, P., Prina-Mello, A. and Volkov, Y. (2009). "The evolution of chemotaxis assays from static models to physiologically relevant platforms." Integr Biol (Camb) **1**: 170-181.

Tolia, N. H. and Joshua-Tor, L. (2007). "Slicer and the argonautes." Nat Chem Biol **3**: 36-43.

Tome, M., Lopez-Romero, P., Albo, C., Sepulveda, J. C., Fernandez-Gutierrez, B., Dopazo, A., Bernad, A. and Gonzalez, M. A. (2011). "miR-335 orchestrates cell proliferation, migration and differentiation in human mesenchymal stem cells." Cell Death Differ **18**: 985-995.

Utiger, R. D. (2005). "The multiplicity of thyroid nodules and carcinomas." N Engl J Med **352**: 2376-2378.

van Veelen, W., Klompmaker, R., Gloerich, M., van Gasteren, C. J., Kalkhoven, E., Berger, R., Lips, C. J., Medema, R. H., Hoppener, J. W. and Acton, D. S. (2009). "P18 is a tumor suppressor gene involved in human medullary thyroid carcinoma and pheochromocytoma development." Int J Cancer **124**: 339-345.

van Veelen, W., van Gasteren, C. J., Acton, D. S., Franklin, D. S., Berger, R., Lips, C. J. and Hoppener, J. W. (2008). "Synergistic effect of oncogenic RET and loss of p18 on medullary thyroid carcinoma development." Cancer Res **68**: 1329-1337.

Verges, B., Boureille, F., Goudet, P., Murat, A., Beckers, A., Sassolas, G., Cougard, P., Chambe, B., Montvernay, C. and Calender, A. (2002). "Pituitary disease in MEN type 1 (MEN1): data from the France-Belgium MEN1 multicenter study." J Clin Endocrinol Metab **87**: 457-465.

Vriens, M. R., Suh, I., Moses, W. and Kebebew, E. (2009). "Clinical features and genetic predisposition to hereditary nonmedullary thyroid cancer." Thyroid **19**: 1343-1349.

Wang, B., Yanez, A. and Novina, C. D. (2008). "MicroRNA-repressed mRNAs contain 40S but not 60S components." Proc Natl Acad Sci U S A **105**: 5343-5348.

Wang, C., Ren, R., Hu, H., Tan, C., Han, M., Wang, X. and Zheng, Y. (2014). "MiR-182 is up-regulated and targeting Cebpa in hepatocellular carcinoma." Chin J Cancer Res **26**: 17-29.

Wang, H., Zhao, Y., Zhang, C., Li, M., Jiang, C. and Li, Y. (2014). "Rab27a was identified as a prognostic biomaker by mRNA profiling, correlated with malignant progression and subtype preference in gliomas." PLoS One **9**: e89782.

Wells, S. A. Jr., Pacini, F., Robinson, B. G. and Santoro, M. (2013). "Multiple endocrine neoplasia type 2 and familial medullary thyroid carcinoma: an update." J Clin Endocrinol Metab **98**: 3149-3164.

Wells, S. A. Jr. and Santoro, M. (2009). "Targeting the RET pathway in thyroid cancer." Clin Cancer Res **15**: 7119-7123.

Wennerberg, K., Rossman, K. L. and Der, C. J. (2005). "The Ras superfamily at a glance." J Cell Sci **118**: 843-846.

Wilczynska, A. and Bushell, M. (2015). "The complexity of miRNA-mediated repression." Cell Death Differ **22**: 22-33.

Winter, J., Jung, S., Keller, S., Gregory, R. I. and Diederichs, S. (2009). "Many roads to maturity: microRNA biogenesis pathways and their regulation." Nat Cell Biol **11**: 228-234.

Witkos, T. M., Koscianska, E. and Krzyzosiak, W. J. (2011). "Practical Aspects of microRNA Target Prediction." Curr Mol Med **11**: 93-109.

Wu, M., Piccini, M., Koh, C. Y., Lam, K. S. and Singh, A. K. (2013). "Single cell microRNA analysis using microfluidic flow cytometry." PLoS One **8**: e55044.

Xie, L., Zhang, Z., Tan, Z., He, R., Zeng, X., Xie, Y., Li, S., Tang, G., Tang, H. and He, X. (2014). "microRNA-124 inhibits proliferation and induces apoptosis by directly repressing EZH2 in gastric cancer." Mol Cell Biochem **392**: 153-159.

Xu, X., Li, S., Lin, Y., Chen, H., Hu, Z., Mao, Y., Xu, X., Wu, J., Zhu, Y., Zheng, X., Luo, J. and Xie, L. (2013). "MicroRNA-124-3p inhibits cell migration and invasion in bladder cancer cells by targeting ROCK1." J Transl Med **11**: 276.

Yakes, F. M., Chen, J., Tan, J., Yamaguchi, K., Shi, Y., Yu, P., Qian, F., Chu, F., Bentzien, F., Cancilla, B., Orf, J., You, A., Laird, A. D., Engst, S., Lee, L., Lesch, J., Chou, Y. C. and Joly, A. H. (2011). "Cabozantinib (XL184), a novel MET and VEGFR2 inhibitor, simultaneously suppresses metastasis, angiogenesis, and tumor growth." Mol Cancer Ther **10**: 2298-2308.

Yamagata, K., Fujiyama, S., Ito, S., Ueda, T., Murata, T., Naitou, M., Takeyama, K., Minami, Y., O'Malley, B. W. and Kato, S. (2009). "Maturation of microRNA is hormonally regulated by a nuclear receptor." Mol Cell **36**: 340-347.

Yang, Y. and Hua, X. (2007). "In search of tumor suppressing functions of menin." Mol Cell Endocrinol **265-266**: 34-41.

Yi, R., Qin, Y., Macara, I. G. and Cullen, B. R. (2003). "Exportin-5 mediates the nuclear export of pre-microRNAs and short hairpin RNAs." Genes Dev **17**: 3011-3016.

Young, N., Pearl, D. K. and Van Brocklyn, J. R. (2009). "Sphingosine-1-phosphate regulates glioblastoma cell invasiveness through the urokinase plasminogen activator system and CCN1/Cyr61." Mol Cancer Res **7**: 23-32.

Zbuk, K. M. and Eng, C. (2007). "Cancer phenomics: RET and PTEN as illustrative models." Nat Rev Cancer **7**: 35-45.

Zdanowicz, A., Thermann, R., Kowalska, J., Jemielity, J., Duncan, K., Preiss, T., Darzynkiewicz E. and Hentze, M. W. (2009). "Drosophila miR2 primarily targets the m7GpppN cap structure for translational repression." Mol Cell **35**: 881-888.

Zeytinoglu, F. N., Gagel, R. F., Tashjian, A. H. Jr., Hammer R. A. and Leeman, S. E. (1980). "Characterization of neurotensin production by a line of rat medullary thyroid carcinoma cells." Proc Natl Acad Sci U S A **77**: 3741-3745.

Ziebold, U., Lee, E. Y., Bronson R. T. and Lees, J. A. (2003). "E2F3 loss has opposing effects on different pRB-deficient tumors, resulting in suppression of pituitary tumors but metastasis of medullary thyroid carcinomas." Mol Cell Biol **23**: 6542-6552.

8 Acknowledgements

First and foremost I want to thank my doctoral thesis supervisor Prof Dr Jochen Graw for giving me the opportunity to carry out my dissertation under his guidance. I would like to express my gratitude for his supervision and the critical reading this work. In addition, I would also like to thank Prof Dr Gabrielle Multhoff for evaluation and examination of my thesis.

In particular, I want to emphasise my gratitude to Dr Natalia S. Pellegata for initiating the MTC project, her continuous guidance, sincerity support and help during the entire course of this project. I am very thankful for the insights, advice and the critical comments concerning my thesis.

Furthermore, I want to thank Dr Martin Irmler for conducting the miRNA array experiments and the statistical and bioinformatical analysis of the obtained expression profiles. I want to express my warmest thanks to him for the strong support and help, especially on short notice.

The work with Dr Frauke Neff was very productive, I want to thank her for the histopathological evaluation of thyroid gland tissues used in this study. I am very grateful for all suggestions, support and encouragement that has made this work easier.

In addition, I would like to thank Prof Dr Christine Spitzweg for the close collaboration and the access to MTC tumour tissues. Furthermore, I want to thank Christine for providing me with patient data and valuable insights from a clinical point of view. Through the cooperation with Dr Thomas Negele and Sergio Pereira de Almeida Toledo I had access to MTC tumour tissues. I would like to express my gratitude to both for the collaboration and contribution to the project and my work.

I would like to take this opportunity to thank Dr Simone Mörtl and Klaudia Winkler for providing me with the pmiRGLO constructs and teaching me how to determine miRNA targets *in vitro* in a pleasant work environment.

I also want to express my thanks to Eleonore Samson, Elke Pulz, David Mörzl and all colleagues from the Institute of Pathology for skilled technical support, friendly atmosphere, helpful discussions and for all the advise and suggestions during my work. In addition, I want to thank especially Sara Molatore and Tobias Wiedemann for the guidance, help and the work environment with friends.

Finally, I want to express my thanks to my parents, Lorena, her family and my family for love, patience, their support and believing in me during the whole of my life